ZINC SIGNALING IN NEURONAL TOLERANCE

by

Mandar Anil Aras

B.S. Neuroscience and Economics, University of Pittsburgh, 2004

Submitted to the Graduate Faculty of

School of Medicine in partial fulfillment

of the requirements for the degree of

Doctor of Philosophy

University of Pittsburgh

2009

UNIVERSITY OF PITTSBURGH

School of Medicine

This dissertation was presented

by

Mandar Anil Aras

It was defended on

August 24, 2009

and approved by

John P. Horn, Ph.D., Professor, Department of Neurobiology, Committee Chair

Kathryn M. Albers, Ph.D., Professor, Department of Medicine

Donald B. DeFranco, Ph.D., Professor, Department of Pharmacology and Chemical Biology

Bruce R. Pitt, Ph.D., Professor, Department of Environmental and Occupational Heath

C.William Shuttleworth, Ph.D., Associate Professor, Outside Examiner

Thesis Advisor: Elias Aizenman, Professor, Department of Neurobiology

ZINC SIGNALING IN NEURONAL TOLERANCE

Mandar Anil Aras, PhD

University of Pittsburgh, 2009

Sub-lethal preconditioning stimuli can confer neuronal tolerance by triggering the activation of endogenous survival pathways that limit or resist subsequent injury. Recent evidence has demonstrated that neuroprotection is paradoxically dependent on the sub-lethal activation of cell death mediators. As intracellular Zn^{2+} accumulation has been closely associated with neuronal cell death pathways, I tested the hypothesis that neuronal tolerance is also dependent on sub-lethal Zn^{2+} signals. I found that preconditioning triggered an immediate transient rise in neuronal free Zn^{2+}, while lethal excitotoxicity led to a delayed accumulation of the metal. The sub-lethal rise in Zn^{2+} was necessary and sufficient in attenuating subsequent Zn^{2+}-dependent toxicity in preconditioned neurons. Chelating Zn^{2+} during the preconditioning stimulus restored the lethal excitotoxic accumulation in neuronal Zn^{2+} and abolished neuronal tolerance. These data suggested that preconditioning-induced Zn^{2+} could trigger mechanisms for preventing subsequent Zn^{2+}-dependent cell death. Indeed, preconditioning triggered protein kinase C (PKC)-dependent Zn^{2+}-regulated gene expression in neurons. Examination of the mechanism involved in modulating Zn^{2+}-regulated gene expression revealed a surprisingly early role for PKC in directly modifying the intracellular source of Zn^{2+}. A conserved PKC phosphorylation site was identified at serine 32 of the metal binding protein metallothionein, which was important in modulating Zn^{2+} regulated gene expression and ultimately conferring neuronal tolerance. In addition to modulating gene expression, Zn^{2+} signals may also be important in mediating the

acute cellular response to stress. Here, I found a critical role for the transient Zn^{2+} rise in modulating changes in voltage-gated potassium channel activity and localization following ischemia. Together, these data strongly suggest that a transient rise in neuronal free Zn^{2+} is an important early signal in conferring neuronal tolerance and in mediating acute cellular adaptive responses to stress. Thus, Zn^{2+} is a previously unrecognized, highly regulated signaling component in the initiation of survival pathways in neurons.

TABLE OF CONTENTS

LIST OF FIGURES

SUPPLEMENTARY FIGURES

PREFACE

This dissertation would not have been completed without the support and guidance of some very important people. I would like to thank my thesis committee members for offering new perspectives and very helpful suggestions on my experiments. I would especially like to thank Dr. John Horn for serving as a committee chair for all of my graduate school milestones. I would also like to thank Dr. Karl Kandler for his generosity in allowing me access to his laboratory equipment as well as providing very helpful technical expertise. I would like to thank past and present members of the Aizenman lab, especially Karen Hartnett, Patrick Redman, Megan Knoch, Kai He, and Mia Jefferson. You all have been very helpful in lab, but more importantly, have become my good friends and made everyday in lab so enjoyable. Most importantly, I would like to thank my thesis advisor Dr. Elias Aizenman. Elias has been a constant source of motivation, direction, and encouragement throughout my graduate training. It is certainly rare to find an advisor that truly cherishes the role of a mentor as much as Elias does. Not only is Elias a brilliant scientist and fantastic mentor, but he has become one of my very good friends. Thank you so much for a wonderful graduate school experience. Finally, I would like to thank my parents, Anil and Smita, and my brother, Mayur. Whatever successes I have achieved in my early career have been because of your unconditional love and support.

1.0 GENERAL INTRODUCTION

1.1 THESIS OVERVIEW

Zinc has been referred to as the "calcium of the 21st century", reflecting its diverse roles in normal cell physiology and, in turn, its deregulation as a contributor to cellular pathological changes (Frederickson et al., 2005). Relatively abundant in the mammalian brain, Zn^{2+} plays a critical role as a structural component of numerous proteins and transcription factors, and has recently emerged as a neuromodulator and intracellular signaling factor (Frederickson and Bush, 2001; Yamasaki et al., 2007). The concentration of intracellular free, or "chelatable" Zn^{2+}, is maintained in the picomolar range under normal conditions due to exquisite regulation by metal binding proteins, a family of Zn^{2+} efflux transporters, and compartmentalization into organelles (Frederickson, 1989; Sensi et al., 1997). However, an accumulation of free Zn^{2+}, likely mediated by liberation of the metal from intracellular stores (Aizenman et al., 2000b) along with translocation from presynaptic vesicles (Koh et al., 1996), plays an important role in ischemic neurodegeneration (Weiss et al., 2000).

Neuronal tolerance to lethal ischemic cell death can be conferred by sub-lethal preconditioning stimuli, which activate endogenous survival pathways that limit or resist subsequent lethal injury (Kitagawa et al., 1990). Interestingly, increasing evidence suggests that

preconditioning stimuli induce the sub-lethal activation of cell death factors that trigger survival pathways, which can prevent lethal injurious signaling (O'Duffy et al., 2007). In light of this idea, I hypothesized that a sub-lethal rise in neuronal free Zn^{2+} would activate endogenous protective mechanisms to prevent subsequent Zn^{2+}-dependent injury. In this dissertation, I establish a novel role for Zn^{2+} as an important, early signal in the initiation of survival pathways critical to neuronal tolerance. The results from these studies offer insights into endogenous mechanisms that protect neurons in the face of lethal cellular injury.

1.2 THE SIGNIFICANCE OF STROKE

Stroke is the second leading cause of death worldwide and the third leading cause of death in the United States, accounting for about 10% of all deaths (Rothwell, 2001). However, mortality data do not capture the true burden of stroke, as there are more than 3.5 million survivors of stroke in the US alone (Lo et al., 2003). In fact, most strokes are not fatal, but instead result in severe limitations with activities of daily living as well as serious long-term disability, such as dementia, depression, epilepsy, falls, and fractures (Rothwell, 2001; Lo et al., 2003). Strokes occur due to an occlusion or hemorrhage of blood vessels supplying the brain. Ischemic strokes, caused by a loss of blood flow to an area of the brain due to an occluded vessel, occur more commonly than hemorrhagic strokes, which are due to vessel rupture (Lo et al., 2003). Regardless of etiology, strokes ultimately result in neuronal dysfunction and death, manifesting in a spectrum of neurological deficits that reflect the location of the compromised brain area. Although a large body of research has implicated several molecular cascades as possible neuroprotective therapeutic targets, the translation of experimental results into clinical practice

remains challenging and, thus far, largely unsuccessful. Studies aimed at understanding endogenous molecular mechanisms of neuronal protection may provide novel therapeutic targets and intervention strategies for stroke.

1.3 EXCITOTOXICITY MODELS ISCHEMIC NEURONAL DEATH

The cellular and molecular mechanisms of stroke pathophysiology are centered around three fundamental overlapping pathways of neuronal cell death: excitotoxicity, oxidative and nitrosative stress, and apoptosis (Lo et al., 2003). Of these, excitotoxicity, a term first coined by Olney referring to neuronal injury elicited by glutamate and structurally-related excitatory amino acids (Olney, 1986), has received much attention over the past 25 years. Excitotoxic neuronal cell death consists of two components: a reversible early component mediated by an influx of extracellular Na^+ and Cl^- causing marked neuronal swelling, and a delayed component mediated by the influx of Ca^{2+} (Choi, 1987) predominantly through ionotropic N-methyl-D-aspartate (NMDA) receptors (Simon et al., 1984; Goldberg et al., 1987). This delayed rise in cellular Ca^{2+} can mediate neurotoxicity by impairing mitochondrial function, producing reactive oxygen species (ROS) and other free radicals, and activating destructive lipases and proteases (Choi, 1988; Kristian and Siesjo, 1998).

Although several voltage-gated and ligand-gated ion channels may contribute to the influx of Ca^{2+}, the NMDA receptor is particularly important in mediating acute ischemic injury (Simon et al., 1984; Choi, 1988). This is illustrated by the finding that: i) in experimental models of stroke, extracellular glutamate levels rise in the microdialysate and blockade of

NMDA receptors can reduce infarct size (McDonald et al., 1987), ii) NMDA receptor antagonists are neuroprotective in temperature controlled animal models of focal ischemia (Yang et al., 1994), and iii) knockout mice deficient in NMDA receptor subunits showed decreased infarct size after focal cerebral ischemia (Morikawa et al., 1998). As such, in the present studies, acute exposure of NMDA is used to model ischemia-mediated neuronal death in cultured neurons (Choi, 1990). It is noteworthy, however, that NMDA receptor antagonists have failed in a large number of stroke clinical trials due to their severe toxic side effects and their inability to significantly reduce stroke morbidity (Muir, 2006). Thus, complete understanding of the signaling pathways involved in the ischemic pathophysiology may uncover novel alternative therapeutic interventions. Deregulation of other ions may be equally, if not more, important than Ca^{2+} in mediating neuronal death following ischemic injury.

1.4 ROLE OF ZINC IN ISCHEMIC NEURONAL DEATH

1.4.1 Physiological roles for Zn^{2+}

Zinc is the second most prevalent trace element in the body and is very abundant in the brain (overall content of ~150μM) with highest concentrations in forebrain regions including the hippocampus, amygdala, and cortex (Choi and Koh, 1998; Weiss et al., 2000). Since its discovery in brain almost 55 years ago (Maske, 1955), Zn^{2+} has been shown to play critical roles in protein structure, enzymatic activity, and gene regulation (Choi and Koh, 1998; Frederickson et al., 2005). Zn^{2+} can associate with over 300 enzymes, where it can interact strongly with electronegative sulfur, nitrogen, and oxygen moieties in multiple coordination geometries,

serving catalytic and structural roles in maintaining active peptide conformations (Choi and Koh, 1998). In addition to metalloenzymes, Zn^{2+} is most known for its ability to bind and stabilize proteins involved in gene regulation in domains called zinc fingers, zinc clusters, and zinc twists (Vallee et al., 1991). Because of the critical role Zn^{2+} plays in protein structure and function, it is not surprising that chronic dietary Zn^{2+} deficiency manifests in multi-systemic dysfunction including growth failure, skin changes, delayed wound healing, immune system impairment, neurosensory disorders, and lack of sexual development (Prasad, 1995).

Besides the structure and function of proteins, brain Zn^{2+} may also be important in modulation of neuronal activity (Frederickson et al., 2005). Approximately 10% of neuronal Zn^{2+} is selectively stored in presynaptic vesicles of certain glutamatergic neuronal terminals by the neuronal specific zinc transporter 3 (ZnT3). Because of this, much attention has been given to determining whether synaptic Zn^{2+} release is activity dependent (Paoletti et al., 2009). The most convincing evidence for activity-dependent Zn^{2+} release was provided by Qian and Nobles, who used a membrane-impermeant form of the Zn^{2+}-selective indicator FluoZin-3 to show extracellular Zn^{2+} in mossy-fiber synapses of wild-type, but not ZnT-3 knock-out mice following individual action potentials (Qian and Noebels, 2005, 2006). Zn^{2+} released from presynaptic neurons has several potential post-synaptic targets. Zn^{2+} is a potent inhibitor of NMDA receptors (Vogt et al., 2000; Li et al., 2001a; Li et al., 2001b; Kim et al., 2002; Qian and Noebels, 2005) and GABA receptor subtypes (Westbrook and Mayer, 1987; Hosie et al., 2003). Zn^{2+} can potentiate glycine receptors at submicromolar concentrations and inhibit them at submillimolar concentrations (Bloomenthal et al., 1994; Laube et al., 1995). In addition to modulating ionotropic pathways, synaptic Zn^{2+} has also been reported to transactivate receptor

tyrosine kinase b (TrkB; Huang et al., 2008b) and regulate metabotropic activity through the activation of a recently described "Zn^{2+} receptor" (Besser et al., 2009). However, since the exact amplitude and time course of synaptic Zn^{2+} remain unclear (Kay, 2003), the functional importance of vesicular Zn^{2+} is yet to be fully established.

Perhaps a more relevant role of physiologic Zn^{2+} is its emergence as an intracellular signal. Yamasaki and colleagues recently found evidence for intracellular Zn^{2+} release in mast cells within minutes of extracellular stimulation of the high affinity immunoglobulin E receptor 1 (FcεR1), a phenomenon they called a "zinc wave" (Yamasaki et al., 2007). Rapid Ca^{2+} influx and mitogen-activated protein/extracellular signal-regulated kinase (MEK) activity were required for the Zn^{2+} rise, although neither the Ca^{2+} ionophore ionomycin nor a MEK activator was sufficient in eliciting a Zn^{2+} wave (Yamasaki et al., 2007). A likely role for such intracellular Zn^{2+} signals is the modulation of protein phosphorylation. While increased cellular Zn^{2+} can activate many kinase pathways including p70 S6 kinase (Kim et al., 2000), extracellular signal-regulated kinase (Park and Koh, 1999; Kim et al., 2006), and p38 (McLaughlin et al., 2001; Bossy-Wetzel et al., 2004), the reports indicate a target upstream in the signaling cascade rather than direct effect of Zn^{2+} on these kinases. Furthermore, activation of Zn^{2+}-dependent kinase cascades was examined in the context of large exogenous Zn^{2+} exposure or cellular toxicity. On the other hand, physiologically relevant nanomolar concentrations of Zn^{2+} have been shown to inhibit protein tyrosine phosphatase (PTP) activity (Maret et al., 1999; Haase and Maret, 2003, 2005). Interestingly, inhibition assays in these studies were performed with a truncated form of the phosphatase containing only the catalytic domain, suggesting that the inhibitory action of Zn^{2+} is through direct interaction with this highly conserved domain of PTPs (Haase and Maret,

2003; Alonso et al., 2004). Thus, a major physiological role for Zn^{2+} may be in the modulation of cell signaling cascades, especially those involving protein phosphorylation.

1.4.2 Regulation of neuronal Zn^{2+}

Despite relatively high Zn^{2+} content in the brain, the extracellular Zn^{2+} concentration is normally below 500 nM and the intracellular "free" Zn^{2+} is generally less than 1 nM (Weiss et al., 2000). Intracellular free Zn^{2+} is tightly regulated though the opposing actions of the solute-linked carrier 39 (SLC39) family (also known as Zrt- and Irt-like proteins or Zips; Eide, 2004) and the SLC30 family (also known as ZnTs; Palmiter and Huang, 2004). Zip and ZnT proteins appear to have opposing roles in Zn^{2+} homeostasis, as Zips increase cytoplasmic Zn^{2+}, while ZnTs promote Zn^{2+} efflux from the cytoplasm into intracellular compartments or across the plasma membrane (Liuzzi and Cousins, 2004). Mechanisms and energetics of transport by these proteins are not well characterized, but are believed to be mediated by facilitated diffusion, secondary active transport, or symporters (Liuzzi and Cousins, 2004).

Of the 14 Zip family members (Eide, 2003), Zip1 mRNA has been found in almost all tissues (Dufner-Beattie et al., 2003) including in neuronal cell bodies and white matter tracts of rat brain (Belloni-Olivi et al., 2009). Zip4 mRNA was also found in the brain but was restricted to choroid plexus and brain capillaries (Belloni-Olivi et al., 2009), and may suggest that the brain can respond to changes in dietary Zn^{2+}. Although the functions of brain Zips have not been carefully studied in the brain, Zip1 and Zip4 mediate Zn^{2+} uptake across the plasma membrane in prostate cells and in intestinal luminal cells, respectively (Gaither and Eide, 2001; Franklin et al., 2003; Dufner-Beattie et al., 2004).

Opposing the actions of Zips are the nine members of the mammalian ZnT family (Palmiter and Huang, 2004). ZnT1 is a ubiquitous member of the SLC30 family found on the plasma membrane of neurons (Tsuda et al., 1997) and glia (Sekler et al., 2002; Nolte et al., 2004). ZnT1 was discovered by Palmiter and Findley for its ability to confer Zn^{2+} resistance to highly Zn^{2+} sensitive baby hamster kidney (BHK) cells (Palmiter and Findley, 1995). ZnT1 overexpression in these cells increased radioactive ^{65}Zn efflux across the plasma membrane and reduced the cytoplasmic concentration of Zn^{2+}, supporting an export function for the protein (Palmiter and Findley, 1995). Recent evidence suggests that in addition to exporting Zn^{2+}, neuronal ZnT1 may confer resistance to Zn^{2+} toxicity by also regulating routes of Zn^{2+} entry, such as through voltage-gated Ca^{2+} channels (Ohana et al., 2006). However, a direct interaction between ZnT1 and Ca^{2+} channels has yet to be demonstrated.

Expression of ZnT1 has been shown in several brain regions, including cerebellum, cerebral cortex, and olfactory bulb, corresponding to areas containing synaptic Zn^{2+} and, thus, requiring significant Zn^{2+} homeostasis (Sekler et al., 2002). The first physiologically relevant role for neuronal ZnT1 came from a report that showed increased ZnT1 expression in degenerating hippocampal neurons following Zn^{2+}-dependent ischemic injury in the gerbil (Tsuda et al., 1997). Similar to lethal injury, sub-lethal Zn^{2+} exposure has been reported to induce ZnT1 expression in astrocytes (Nolte et al., 2004). Thus, the upregulation of ZnT1 may be an important adaptive response to cellular injury. The remaining ZnT family members are localized to intracellular membranes, where they play limited tissue-specific functions in Zn^{2+} sequestration (Liuzzi and Cousins, 2004). Of these, the most extensively studied ZnT is neuronal ZnT3, which transports Zn^{2+} into synaptic vesicles of certain glutamatergic neurons

(Wenzel et al., 1997). Immunohistochemical analysis of ZnT3 expression revealed a staining pattern identical to that produced by Timm staining for vesicular Zn^{2+} (Palmiter et al., 1996; Wenzel et al., 1997). Timm staining, first described in 1958 as a "sulfide-silver procedure" (Timm, 1958) and optimized for visualizing Zn^{2+} (Danscher, 1984; Danscher et al., 1997), is the process of silver-amplifying sulfide-loaded tissue by autometallography, allowing for visualization of zinc-sulfide crystal lattices. ZnT3 immunoreactivity is evident on membranes of Zn^{2+}-rich Timm stained synaptic vesicles (Wenzel et al., 1997). ZnT3 knock-out (ZnT3-KO) mice express no histochemically reactive (vesicular) Zn^{2+} (Cole et al., 1999). Despite completely lacking vesicular Zn^{2+}, ZnT3-KO mice do not have impaired spatial learning, memory, or sensorimotor functions (Cole et al., 2001), but may be more susceptible to kainate-induced seizures (Lee et al., 2000; Lee et al., 2003). Thus, while a significant role of vesicular Zn^{2+} has not yet been established, the ZnT3-KO mouse will be an invaluable tool in designing new experiments to uncover previously unexplored mechanisms in synaptic Zn^{2+} signaling.

Metallothioneins also play a major role in regulating intracellular Zn^{2+} homeostasis by binding, releasing, and distributing Zn^{2+}. Metallothioneins are a family of non-enzymatic, cysteine-rich, metal-binding polypeptides (61-68 amino acids) found throughout mammalian tissues (Aschner, 1996; Haq et al., 2003; Penkowa, 2006). MTs are well-known for their metal-binding properties as they are structurally composed of two globular metal-binding domains (α and β) containing a total of 20 cysteine residues, allowing them to bind up to seven Zn^{2+} or Cd^{2+} ions or up to 12 Cu^{2+} ions (Haq et al., 2003). These cysteine residues in MTs occur in unique Cys-X-Cys, Cys-X-Y-Cys, and Cys-Cys motifs, where X and Y represent non-cysteine amino acids (Kagi and Schaffer, 1988). Interestingly, analysis of the association of Zn^{2+} with the

apoprotein thionein revealed three classes of binding affinities that vary by several orders of magnitude. Four Zn^{2+} ions were bound tightly (log K_d = 11.8), making the thionein a strong chelating agent; one Zn^{2+} was relatively weakly bound (log K_d = 7.7), making metallothionein a Zn^{2+} donor; and the remaining two Zn^{2+} ions were with intermediately bound (log K_d ~ 10) (Krezel and Maret, 2007). This suggests that MT molecules are not saturated with seven Zn^{2+} ions under normal physiological conditions and can actively participate in cellular Zn^{2+} buffering and distribution (Krezel and Maret, 2007). Thus, MT is a dynamic protein with species containing varying amounts of Zn^{2+} due to the constant transfer of Zn^{2+} to thioneins and other metalloenzymes (Yang et al., 2001; Krezel and Maret, 2007). Further, because of the unique Zn^{2+} coordination environment of MT, the redox environment of the cell may ultimately dictate cellular Zn^{2+} availability (discussed further in Section 1.4.6; Maret and Vallee, 1998).

Three major MT isoforms are expressed in the adult mammalian central nervous system. The precise cellular localization of MT I, II, and III is still a matter of debate due to the lack of isoform-specific antibodies leading to conflicting results between *in vivo* and *in vitro* studies and between mRNA and protein expression assays (Hidalgo et al., 2001). The general consensus, however, is that the MT I and MT II are the predominant astrocytic isoforms (where they are expressed over seven-fold higher than in neurons; Hidalgo et al., 1994; Kramer et al., 1996b; Kramer et al., 1996a; Suzuki et al., 2000), while MT III is predominantly expressed in neurons (Masters et al., 1994; Hidalgo et al., 2001). Interestingly, MT III was first identified in pursuit of putative mechanisms underlying Alzheimer's disease neuropathology. Abundant MT III expression, which was then identified as growth inhibitory factor (GIF) due to its ability to inhibit neurotrophic factors and neurite outgrowth, was found in normal brain astrocytes, but not

in Alzheimer's disease brains (Uchida et al., 1991). However, since then, the association between MT III and Alzheimer's disease has not fully developed (Erickson et al., 1994; Carrasco et al., 2006). Instead, MTs are thought to play a major role in heavy metal detoxification and Zn^{2+} homeostasis, as previously discussed. Interestingly, expression of MT I and II is highly inducible in response to a range of stimuli in addition to Zn^{2+} and Cd^{2+}, including hormones, cytokines, oxidative agents, inflammation, and ischemia (Bremner et al., 1987; Sato and Bremner, 1993; Vasak and Hasler, 2000; Trendelenburg et al., 2002). Because of this, MTs have been implicated in mediating a more general cellular response to injury (West et al., 2008). Exciting recent reports have shown that following brain injury, astrocytes are able to secrete MT into the extracellular space, which is internalized by neurons promoting cell survival (Ambjorn et al., 2008; Chung et al., 2008; West et al., 2008). Thus, MTs play diverse roles in regulating cellular Zn^{2+} homeostasis, heavy metal detoxification, and intercellular response to injury.

1.4.3 Zn^{2+}-regulated gene expression

A major role for physiologic Zn^{2+} is the regulation of the proteins that control the intracellular concentration of the metal. The inducible metallothionein isoforms, MT I and MT II, are regulated in a coordinated manner through the activation of gene transcription (Penkowa, 2006). The promoter regions of MT I/II genes contain several *cis*-acting DNA elements, including metal, glucocorticoid, anti-oxidant, and interleukin-6/signal transducers and activator of transcription (STAT) responsive elements (MREs, GREs, AREs, and IL-6 RE) that can bind *trans*-acting transcription factors involved in the regulation of both constitutive and inducible MT expression (Haq et al., 2003; Penkowa, 2006). Metal response element transcription factor 1 (MTF-1) is the predominant gene regulatory protein mediating constitutive as well as metal- and

oxidative stress-induced MT I/II expression (Heuchel et al., 1994; Dalton et al., 1996). MTF-1 is a 72.5 kDa, ubiquitous zinc-finger transcription factor in the Cys_2His_2 family that binds to DNA sequence motifs, known as metal response elements (MREs), at the consensus site TGCRCNC (Stuart et al., 1984). MRE sequences are present in five, non-identical copies (MREa-MREe) in the 5' flanking region of the MT I/II gene (Larochelle et al., 2001a). MTF-1 mediated MRE activation sufficiently upregulates MT I/II in response to Zn^{2+} or Cd^{2+} (Stuart et al., 1984; Stuart et al., 1985), oxidative stress (Dalton et al., 1994), and hypoxia (Murphy et al., 1999). Following Zn^{2+}, acute hypoxia, or oxidative stress induced by H_2O_2 or tert-butylhydroquinone, MTF-1 translocates from the cytoplasm to the nucleus and acquires tight DNA-binding ability (Dalton et al., 1996; Dalton et al., 1997; Andrews, 2000; Smirnova et al., 2000). However, following exposure to other heavy metals, most notably Cd^{2+}, the DNA-binding ability of MTF-1 is inhibited in cell-free DNA binding assays, despite induction of MTF-1-dependent MT gene transcription *in vivo* (Heuchel et al., 1994; Palmiter, 1994; Bittel et al., 1998; Murata et al., 1999; Zhang et al., 2001). This paradox was solved by demonstrating that transcriptional activation following Cd^{2+} requires Zn^{2+}-saturated metallothionein (Zhang et al., 2003). Cd^{2+}, which binds to metallothioneins with higher affinity than Zn^{2+}, can displace Zn^{2+} from the metal-binding protein, making Zn^{2+} available for MTF-1 activation (Zhang et al., 2003). Activation of gene transcription also requires the occupancy of the Zn^{2+} fingers with Zn^{2+} (Westin and Schaffner, 1988) and the interaction among three distinct transcriptional activation domains in the C-terminal region of MTF-1 (Radtke et al., 1995). While most of the evidence characterizing Zn^{2+}-regulated gene expression has been performed studying MT gene activation, changes in ZnT1 expression can also be induced by Zn^{2+} or Cd^{2+} (Andrews, 2000). Constitutive and metal-induced activation of the ZnT1 gene also required MTF-1 (Langmade et al., 2000). On the other

hand, while the organization of the promoter regions of all MT genes is conserved, the MT III gene was found to contain a 'silencing element' in the 5' flanking regions upstream from the first cluster of putative MREs (Watabe et al., 1997; Chapman et al., 1999), eliminating Zn^{2+}-regulation. Closer inspection of this silencing element of the rat MT III promoter revealed that it contained a quadruplicate CTG sequence approxiametely 400 base-pairs upstream of the translation start site (Chapman et al., 1999). CTG-repeat elements have been shown to act as repressors on a number of heterologous promoters independent of its orientation and proximity to the gene, and thus may account for the silencing effect on the promoter region of the MT III gene (Chapman et al., 1999). Overall, these studies suggest that Zn^{2+} regulated, MTF-1/MRE-mediated gene expression plays an important role in coordinating the expression of proteins involved in intracellular Zn^{2+} homeostasis. In this dissertation, I show that Zn^{2+} regulated gene expression can be stimulated by sub-lethal ischemia in neurons and thus may be an important endogenous mechanism conferring tolerance to subsequent Zn^{2+}-dependent injury.

1.4.4 PKC modulation of Zn^{2+}-regulated gene expression

Zn^{2+} regulated gene expression has been shown to be dependent on a number of kinase cascades, especially protein kinase C (PKC; LaRochelle et al., 2001b; Adams et al., 2002; Saydam et al., 2002). PKC is a family of serine/threonine kinases, which consists of at least 10 isozymes (Newton, 2001). These isozymes have been classified into three groups according to their structure and cofactor regulation. Conventional PKCs (α, β1, β2, and γ) are directly activated by calcium or diacylglycerol (DAG); novel PKCs (δ, ε, σ, φ, and μ) are independent of calcium but responsive to DAG; and atypical PKCs are independent of calcium and DAG but require membrane phospholipids for activation (Newton, 2001). Interestingly, PKC is also a Zn^{2+}-

metalloenzyme, containing four Zn^{2+} atoms bound to two cysteine-rich repeats in the regulatory domain of the N-terminus (Quest et al., 1992). Nanomolar concentrations of Zn^{2+} activated PKC, and the cell-permeant Zn^{2+} chelator *N,N,N',N'*-tetrakis (2-pyridalmethyl)ethylenediamine (TPEN) inhibited PKC activation (Csermely et al., 1988b, a). Furthermore, oxidation of the Zn^{2+}-binding cysteine residues led to release of PKC-bound Zn^{2+}, which was sufficient in activating the enzyme (Knapp and Klann, 2000). Oxidative release of PKC-bound Zn^{2+} has been shown to cause a substantial increase in intracellular free Zn^{2+} in cardiomyocytes (Korichneva, 2005). Thus, Zn^{2+} may play a critical regulatory role in PKC activity. In turn, PKC may also play an important role in the regulation of intracellular Zn^{2+} concentration. Activators of PKC are sufficient stimulants of Zn^{2+}-regulated gene expression (Imbra and Karin, 1987; Garrett et al., 1992), while PKC inhibitors can interfere with metal-induced MRE activation (Yu et al., 1997a). Despite evidence suggesting that PKC activity can modulate of Zn^{2+}-regulated gene expression, the mechanism of action of the kinase in this process is unclear (LaRochelle et al., 2001a; Adams et al., 2002; Saydam et al., 2002; Jiang et al., 2004). It has been shown that MTF-1 is constitutively phosphorylated at serine and tyrosine residues and that metal exposure increases its level of phosphorylation by a mechanism involving PKC (LaRochelle et al., 2001a; Saydam et al., 2002). Treatment with kinase inhibitors decreased MTF-1/MRE-mediated gene transcription (LaRochelle et al., 2001a), and inhibition of dephosphorylation resulted in elevated constitutive and induced MT expression (Chen et al., 2001). However, studies have shown that although MTF-1 can be phosphorylated in unstimulated cells, metal exposure does not increase its phosphorylation state or its ability to bind DNA (Jiang et al., 2004). Further, kinase inhibition does not affect metal-induced MTF-1 nuclear translocation, MTF-1 DNA binding, or the formation of a stable MTF-1-chromatin complex (Larochelle et al., 2001a; Jiang et al., 2004).

Thus, modulation of Zn^{2+}-regulated gene expression by signaling kinases may be cell-type specific, and may not target MTF-1 directly (Jiang et al., 2004). It is certainly possible that modulation of Zn^{2+}-regulated gene expression by PKC may not be mediated by post-translational modification of MTF-1. In this dissertation, I identify MT as a previously unrecognized target for PKC phosphorylation, and examine its effect on neuronal Zn^{2+}-regulated gene expression.

1.4.5 Zn^{2+} translocation in ischemic cell death

As the intracellular concentration of Zn^{2+} is kept in the picomolar range through the actions of several regulatory processes mentioned in earlier sections, an increase of free intracellular Zn^{2+} in neurons can have deleterious consequences. During the height of the debate regarding the exact roles for Ca^{2+}, glutamate, and excitotoxicity in mediating neuronal death following ischemia, Zn^{2+} emerged as another cation important in ischemia pathophysiology. Using TSQ (N-[6-methoxy-8-quinolyl]-P-toluenesulfonamide) and acid fuschin to simultaneously stain the presence of Zn^{2+} and degenerating neurons, respectively, Tonder and colleagues were first to suggest a translocation of Zn^{2+} from mossy fibers terminals to degenerating dentate hilar neurons 2-24 hrs following 20 min of cerebral ischemia (Tonder et al., 1990). This observation, coupled with reports suggesting that the amount of Zn^{2+} stored in synaptic vesicles (~300 μM) was sufficient in killing neurons (Yokoyama et al., 1986; Frederickson et al., 1988), led to the Zn^{2+} translocation hypothesis. This hypothesis proposes that the extracellular release of vesicular Zn^{2+} and its uptake by postsynaptic neurons is responsible for the toxic accumulation of neuronal Zn^{2+} following ischemia (Frederickson et al., 1989; Choi and Koh, 1998; Lee et al., 1999). More direct evidence came from Koh and colleagues who showed that intraventricular injection of the membrane-impermeant Zn^{2+} chelator, ethylenediaminetetraacetic acid (EDTA) saturated with

Ca^{2+} (CaEDTA), blocked the accumulation of neuronal Zn^{2+} and prevented neuronal death following transient global cerebral ischemia (Koh et al., 1996). While Zn^{2+} was known to be toxic to neurons when applied exogenously (Choi et al., 1988; Weiss et al., 1993; Koh and Choi, 1994), these reports were first to implicate endogenous accumulation of Zn^{2+} in ischemic neuronal death.

Extracellular Zn^{2+} can lead to toxic intracellular Zn^{2+} accumulations by entering through voltage-sensitive Ca^{2+} channels (VSCC; Weiss et al., 1993), NMDA channels (Koh and Choi, 1994), or Ca^{2+}-permeable a-amino-3-hydroxy-5-methyl-4-isoxazole propionic acid (AMPA) / kainate channels (Ca^{2+}-A/K; Yin and Weiss, 1995; Yin et al., 1998). Of these, Ca^{2+}-A/K channels exhibit the highest Zn^{2+} permeability (Sensi et al., 1999) and may be the primary route of Zn^{2+} entry following ischemia (Yin et al., 2002). In hippocampal slices, ischemia-induced Zn^{2+} accumulation and subsequent neurodegeneration can be attenuated with a Ca^{2+}-A/K channel inhibitor but not NMDA or VSCC channel antagonists (Yin et al., 2002). Hippocampal pyramidal neurons, which are especially sensitive to ischemic injury, express Ca^{2+}-A/K channels on distal dendritic branches (Lerma et al., 1994; Yin et al., 1999; Ogoshi and Weiss, 2003). Unlike all other heterotetrameric AMPA receptors, Ca^{2+}-A/K channels lack the GluR2 subunit (Dingledine et al., 1999; Kwak and Weiss, 2006). GluR2 subunits contain an arginine (R) in its pore-forming domain due to RNA editing of a genomically encrypted glutamine (Q) codon (Sommer et al., 1991). The arginine is functionally dominant because it dictates gating kinetics, channel conductance, channel assembly and importantly, Ca^{2+} permeability (Burnashev et al., 1992; Geiger et al., 1995; Greger et al., 2003). Edited GluR2(R) subunits form Ca^{2+}-impermeable channels, whereas unedited GluR2(Q) channels are Ca^{2+} permeable (Geiger et al.,

1995; Jonas and Burnashev, 1995). Generation of mice with unedited GluR2(Q) produced fulmitant seizures and death by three weeks of age (Brusa et al., 1995). Interestingly, GluR2 expression can be modulated by ischemic injury, as ischemia has been shown to induce GluR2 down-regulation (Gorter et al., 1997; Opitz et al., 2000) and disrupt Q/R editing (Peng et al., 2006). This modulation of GluR2 subunits render AMPA channels Ca^{2+} permeable, allowing entry of toxic Ca^{2+} and Zn^{2+} during ischemia (Pellegrini-Giampietro et al., 1992; Gorter et al., 1997; Opitz et al., 2000; Sensi and Jeng, 2004). Thus, regulation of Ca^{2+}-A/K channel composition may play a critical role in ischemic injury.

Regulation of Ca^{2+}-A/K channel composition following ischemic injury may involve Zn^{2+}. In an *in vivo* model of ischemia, application of CaEDTA 30 minutes prior to global ischemia attenuated the ischemic downregulation of GluR2, the delayed rise in neuronal Zn^{2+}, and neuronal death (Calderone et al., 2004). Ischemic downregulation of GluR2 may occur by Zn^{2+}-dependent expression of the nine Zn^{2+}-finger transcription factor restrictive element-1 silencing transcription factor (REST-1), which suppresses neuronal-specific targets including GluR2 (Calderone et al., 2003; Calderone et al., 2004). Application of CaEDTA 48-60 hours following global ischemia, presumably after GluR2-lacking A/K channels are already expressed, only attenuated the late rise in neuronal Zn^{2+} and cell death (Calderone et al., 2004). These data suggest that Zn^{2+} entry through Ca^{2+}-A/K channels contributes to the accumulation of the metal following ischemia.

1.4.6 Intracellular sources for ischemic Zn^{2+}

Several key observations have shown that Zn^{2+} translocation cannot fully account for the accumulation of free Zn^{2+} following ischemia. Zn^{2+} accumulation in degenerating neurons following global ischemia is observed in areas that are not highly innervated by glutamate- and Zn^{2+}-releasing fibers, such as thalamic neurons (Koh et al., 1996). Thus, intracellular sources of Zn^{2+} must play a major role in lethal Zn^{2+} accumulation in these brain regions. More importantly, if presynaptic Zn^{2+} was the only source of toxic Zn^{2+} that contributed to ischemic injury, then animals without presynapic Zn^{2+} would not be susceptible to Zn^{2+}-dependent toxicity. Mice lacking the zinc transporter ZnT3 show no histochemically reactive Zn^{2+} in presynaptic vesicles, but still undergo significant Zn^{2+} accumulation in degenerating CA1 and CA3 neurons following kainate-induced seizures (Lee et al., 2000). These data suggest that lethal neuronal injury can induce intracellular Zn^{2+} accumulation and neurodegeneration in the absence of presynaptic vesicular Zn^{2+}. While CaEDTA nearly completely abolished the Zn^{2+} accumulation and neuronal cell death, suggesting an extracellular source of Zn^{2+}, CaEDTA has been since shown to deplete intracellular Zn^{2+} compartments, including synaptic vesicles (Frederickson et al., 2002). The membrane-impermeant Zn^{2+} chelator CaEDTA may chelate and trap extracellular Zn^{2+}, giving rise to a steep Zn^{2+} gradient across the plasma membrane resulting in "pulling" of free Zn^{2+} from the neuronal cytoplasm. Taken together, these reports suggest that accumulation of intracellular Zn^{2+} following neuronal injury may not be solely dependent on translocation of the metal from presynaptic neurons.

As Zn^{2+} accumulation can occur in the absence of vesicular Zn^{2+}, liberation of Zn^{2+} from intracellular stores may be a significant mechanism of cell injury, especially in brain regions

with little or no synaptic Zn^{2+}. Vallee and colleagues suggest that Zn^{2+} binding and release in cells are dynamic processes that are dependent on the redox status of the cell (Jacob et al., 1998; Jiang et al., 1998). Of the Zn^{2+} metalloproteins, only those with Zn^{2+}/sulfur coordination environments are susceptible to oxidative mobilization of Zn^{2+} during excitotoxicity (Maret, 1995). These coordination environments allow for tight binding of Zn^{2+} and for the mobilization of redox-inert Zn^{2+} (Berg and Shi, 1996) by biological oxidants. Of the thiol-Zn^{2+} metalloproteins in neurons, MT III is a likely source of injury-induced mobilized Zn^{2+}. Despite binding Zn^{2+} with high thermodynamic stability (K_d = 1.4 X 10^{-13} M for human MT, pH 7.0; Maret and Vallee, 1998), the redox potential for MT is very negative (-366 mV), causing even mild cellular oxidants to release Zn^{2+} from the metal-binding protein (Maret and Vallee, 1998). Consistent with this, exposure of neurons to oxidative stress promotes the release of Zn^{2+} from intracellular stores, an event critical to initiation of neuronal apoptosis (Aizenman et al., 2000b). Further, nitric oxide (NO) and subsequent peroxynitrite ($ONOO^-$) formation, two powerful cellular oxidants contributing to ischemic "nitrosative stress" (Lo et al., 2003), also liberate neuronal Zn^{2+} from intracellular stores triggering neurodegeneration (Cuajungco and Lees, 1998; Bossy-Wetzel et al., 2004; Zhang et al., 2004). NO has been shown to more readily release Zn^{2+} from MT III than other MT isoforms due to the unique presence of consensus motifs for catalytic nitrosylation and the preferential reactivity of S-nitrosothiols with MT III through transnitrosylation, allowing direct transfer of NO between sulfhydryl groups that result in sequential release of Zn^{2+} ions (Chen et al., 2002). Thus, liberation of Zn^{2+} from intracellular stores, especially neuronal MT III, may be a significant source of the Zn^{2+} rise following ischemia. In this dissertation, I provide evidence supporting a major role for metallothionein as the primary source and sink for free Zn^{2+} in neurons.

1.4.7 Zn^{2+}-dependent signaling in ischemia

Accumulation of neuronal Zn^{2+}, likely mediated by a combination of Zn^{2+} translocation from presynaptic vesicles and Zn^{2+} liberation from intracellular stores, can trigger subsequent neurodegenerative signaling following ischemia. Zn^{2+}-induced cell death involves several serial and parallel signaling events, has features of both apoptosis and necrosis (Kim et al., 1999b), and is likely mediated by oxidative and nitrosative stress (Kim et al., 1999a; Noh et al., 1999; Kim et al., 2002; Sensi et al., 2002). The diversity of cell death signaling attributed to Zn^{2+} may depend on the intensity of Zn^{2+} exposure, as brief exposure to high concentrations of Zn^{2+} lead to signs of necrotic, caspase-independent cell death, while longer exposures to lower Zn^{2+} concentrations trigger apoptotic, caspase-dependent cascades (Kim et al., 1999a; Kim et al., 1999b; Lobner et al., 2000).

In addition to concentration-dependent signaling, accumulation of Zn^{2+} following ischemia may trigger divergent signaling mechanisms along multiple temporal profiles. While a delayed rise in neuronal Zn^{2+} in degenerating neurons following ischemia has been well described (Koh et al., 1996; Park et al., 2000), recent reports suggest that an early Zn^{2+} rise following ischemia onset also contributes to ischemic injury (Stork and Li, 2006; Medvedeva et al., 2009). In hippocampal neurons loaded with both Zn^{2+} and Ca^{2+} indicators, an accumulation of neuronal Zn^{2+} within the first minutes following ischemia was detected before, and shown to contribute to, Ca^{2+} deregulation (Medvedeva et al., 2009). Interestingly, previously utilized Ca^{2+} probes actually bind Zn^{2+} with higher affinity, and what was previously attributed to Ca^{2+} deregulation may be in fact due to Zn^{2+} (Stork and Li, 2006). Two important reports (Stork and Li, 2006; Medvedeva et al., 2009) used oxygen-glucose deprivation in hippocampal slices to

model ischemia, but neither examined the source of the early Zn^{2+} rise, leaving the possibility that areas of brain deficient in Ca^{2+}-A/K channels or vesicular Zn^{2+} may not undergo an early ischemic Zn^{2+} rise. Nevertheless, this early Zn^{2+} accumulation in ischemic neurons may trigger neurodegenerative signaling previously attributed to Ca^{2+}.

Mechanisms involved in Zn^{2+}-dependent ischemic neuronal death are incompletely understood, and may resemble the complexity in Ca^{2+}-mediated cell death pathways. However, central to Zn^{2+}-dependent neuronal cell death are roles for mitochondria and oxidative stress. Exogenously-applied Zn^{2+} can be taken up by mitochondria (Manev et al., 1997; Sensi et al., 2000) leading to changes in mitochondrial potential ($\Delta\Psi_m$), release of reactive oxygen species and pro-apoptotic proteins, and induction of mitochondrial swelling (Sensi et al., 1999; Jiang et al., 2001; Dineley et al., 2005). These effects on mitochondria could also be produced following oxidant-induced liberation of intracellular Zn^{2+} (Sensi et al., 2003; Bossy-Wetzel et al., 2004). *In vivo*, Zn^{2+} chelation by CaEDTA prior to global ischemia attenuates the activity of large multi-conductance mitochondrial channels, prevents the cytosolic accumulation of mitochondrial proapoptotic proteins, and ultimately decreases the apoptotic cell death execution protein, caspase-3 (Calderone et al., 2004; Bonanni et al., 2006). Mitochondria are widely implicated in oxidative- and nitrosative-stress mediated neuronal injury, as deficits in the electron transport chain are linked to ROS generation (Adam-Vizi, 2005, but see Brennan et al., 2009). Zn^{2+} exposure leads to increased levels of superoxides and lipoperoxides (markers for oxidative injury) and the resultant neurotoxicity is attenuated by antioxidants (Kim et al., 1999a; Kim et al., 1999b). However, under these conditions, the source of ROS is likely to be mediated by PKC dependent, nicotinamide adenine dinucleotide phosphate (NADPH) oxidase activation

(Noh et al., 1999; Noh and Koh, 2000; Brennan et al., 2009). Aside from mitochondria and oxidative stress, other Zn^{2+}-dependent cell death signaling events have also been described, including regulation of Zn^{2+}-dependent transcription factors (Park and Koh, 1999), induction of p75 neurotrophin receptor-mediated pathways (Park et al., 2000), and activation of kinases (Noh et al., 1999; McLaughlin et al., 2001; Du et al., 2002; Bossy-Wetzel et al., 2004) and poly-ADP-ribose polymerase (PARP-1) (Sheline et al., 2003). Thus, Zn^{2+}-dependent neurodegeneration may be mediated by several diverging and redundant cellular processes that only have begun to be elucidated.

1.5 PRECONDITIONING OFFERS INSIGHT INTO STROKE NEUROPROTECTION

Preconditioning refers to the activation of endogenous adaptive processes by sub-lethal stimuli that can increase cellular tolerance to subsequent, lethal injury (Obrenovitch, 2008). Tolerance to lethal ischemic injury was first described by preconditioning cardiac myocytes with brief sub-lethal ischemic episodes (Murry et al., 1986). This phenomenon was subsequently shown to also be present in the brain (Kitagawa et al., 1990). Preconditioning triggers an adaptive cellular response that is characterized by specific time frames of tolerance induced relative to preconditioning stimulus and subsequent lethal ischemia. Acute tolerance is short-lasting (~1 hr) and is mediated by post-translational protein modifications. In contrast, delayed tolerance can be detected 24 hr following preconditioning and can last for days, requiring gene expression and protein synthesis (Lo et al., 2003; Obrenovitch, 2008).

Activation of several transcription factors have been shown to mediate neuronal tolerance, including activating protein 1 (AP1), cyclic AMP responsive element-binding protein (CREB), nuclear-factor κB (NF-κB), and the redox regulated transcriptional activator SP1 (Blondeau et al., 2001; Ryu et al., 2003; Meller et al., 2005). However, the most evidence for a role in mediating neuronal tolerance has been found for the hypoxia-inducible factor (HIF) isoforms (Bergeron et al., 2000; Bernaudin et al., 2002b). HIF is a heterodimer consisting of α and β protein subunits. Under normal conditions, the HIF1α isoform is targeted for degradation by an oxygen-sensitive prolyl hydroxylase, which allows for the interaction between HIF1α and ubquitin ligase (Gidday, 2006). Hypoxia inactivates the hydroxylase enzyme, stabilizing HIF1α and allowing it to enter the nucleus, where it can dimerize with HIF1β and promote transcription of genes that enhance tolerance (Bergeron et al., 2000). Hypoxia can also activate HIF1α transcription, further promoting the activation of HIF-sensitive genes (Semenza, 2001). HIF target genes that may play a role in neuronal tolerance are those related to angiogenesis, such as vascular endothelial growth factor (VEGF), and blood and iron metabolism, such as erythropoietin (Sharp and Bernaudin, 2004). In addition to these genes, studies using oligonucleotide-based DNA microarrays have described general families of genes that are particularly affected by preconditioning, including genes related to cell metabolism, immune response, ion channel activity, and blood coagulation (Stenzel-Poore et al., 2004). Thus, despite the multitude of stimuli, transducers, and effectors involved in various models of tolerance, the overall implication of neuronal preconditioning is the development of a genetically reprogrammed, primed brain that can effectively limit cellular injury after ischemia.

Preconditioning may represent the most powerful mechanism described to date for limiting infarct size other than timely reperfusion. Preconditioning-induced tolerance has been demonstrated clinically in retrospective case-controlled studies that showed that patients with transient ischemic attacks (TIAs) have decreased morbidity following stroke (Weih et al., 1999). Understanding the molecular mechanisms involved in the preconditioning-induced neuroprotection may help develop novel therapeutic strategies not only for limiting morbidity following stroke, but also following high-risk surgical procedures that involve the potential for hemodynamic compromise (Dirnagl et al., 2009). In this dissertation, I present evidence suggesting that a transient Zn^{2+} rise may be a previously unexplored early signaling event critical for the development of delayed neuronal tolerance.

1.6 NEURONAL TOLERANCE IS CONFERRED BY CELL DEATH MEDIATORS

A variety of stress stimuli known to cause ischemic brain injury, when exposed at sub-lethal levels have been reported to trigger neuronal tolerance, including ischemia, hypoxia, metabolic inhibitors, excitotoxins, and inflammatory cytokines (Gidday, 2006). Generally, a particular stress stimulus can either be too weak to elicit any response, sufficient to precondition neurons and confer tolerance, or too robust and therefore lethal (Dirnagl et al., 2003). Similarly, the intensity or duration of conserved cellular mediators may be critical in determining cell fate. Indeed, recent evidence suggests that pro-survival mechanisms conferring neuroprotection in ischemic preconditioning may involve sub-lethal activation of cell death pathways. For example, antioxidants and protease inhibitors, which limit cell death following lethal stimuli, can paradoxically increase vulnerability to subsequent lethal injury when administered during the

preconditioning period (McLaughlin et al., 2003). Thus, the ultimate fate of neurons may not depend on which molecules are activated following a particular insult, but rather the extent and duration of their activity. Below, I highlight several examples of such mediators that are particularly relevant to my dissertation work.

1.6.1 Caspase-3

Cysteine aspartic acid-specific proteases (caspases) are a family of proteolytic enzymes that cleave hundreds of targeted proteins during apoptosis including structural proteins, DNA repair enzymes, and cleavage-activated kinases (Taylor et al., 2008). The family is divided into initiators (such as caspase-8), which can auto-activate and cause the proteolysis of other caspases, and effectors (such as caspases-3, -6 and -7), which are activated by other caspases and carry out substrate proteolysis and cell death (Taylor et al., 2008). Activation of caspases eventually leads to, or is accompanied by, cellular changes of apoptosis, including membrane blebbing, DNA fragmentation, chromatin condensation, and formation of apoptotic bodies (Kerr et al., 1972). Caspase activation has been shown to play an important role in ischemic neurodegeneration as genetic or pharmacological inhibition of caspases is neuroprotective in experimental stroke (Endres et al., 1998; Le et al., 2002). Caspase-3 mRNA, protein, and cleavage products can be detected in animal models of stroke at varying time points following insult depending on the extent of ischemia and reperfusion injury (Asahi et al., 1997; Namura et al., 1998). Caspase-3 inhibition prior to, or following, cerebral ischemia markedly reduced neuronal injury due to ischemia and reperfusion injury (Fink et al., 1998). Thus, caspase-3 plays a significant role in ischemic neuronal death.

Surprisingly, caspase-3 has also been implicated in neuronal tolerance. Our laboratory was first to show that preconditioning led to caspase cleavage *in vivo* and that caspase-3 activity was required for neuronal tolerance *in vitro* (McLaughlin et al., 2003). Pro-caspase cleavage and caspase enzymatic activity reach maximum levels six hours following a preconditioning stimulus and are dependent on ROS generation and K_{ATP} channel opening (Garnier et al., 2003; McLaughlin et al., 2003). Although widespread caspase-3 activation characterizes many cell death processes, the relatively modest preconditioning-induced caspase-3 activation is held in check by sequestration with caspase-binding proteins including the constitutively active heat shock protein 70 (HSP70) homologue HSC70 (McLaughlin et al., 2003) and the pro-survival inhibitor-of-apoptosis (IAP) family member cIAP (Tanaka et al., 2004). The depletion of the free pool of HSC70 leads to increased synthesis of HSP70, which is observed 24 hours following preconditioning and is able to buffer lethal caspase-3 generation (McLaughlin et al., 2003). Importantly, inhibiting the activation of caspase-3 or the upregulation of HSP70 attenuates the neuroprotective effect of preconditioning (McLaughlin et al., 2003).

Aside from upregulating survival proteins in preconditioned neurons, caspase-3 has also been shown to target poly(ADP-ribose) polymerase-1 (PARP-1; Szabo and Dawson, 1998; Garnier et al., 2003; Lee et al., 2008). PARP-1, which accounts for >80% of nuclear PARP activity (Heller et al., 1995; D'Amours et al., 1999), facilitates DNA repair by mediating the enzymatic transfer of ADP-ribose groups from NAD^+ to form branched ADP-ribose polymers on acceptor proteins in the vicinity of DNA strand breaks or kinks. However, extensive PARP-1 activation, which occurs in ischemia (Virag and Szabo, 2002), depletes NAD and ATP, leading to cellular energy failure and cell death (Ha and Snyder, 1999). Caspase-3 can irreversibly

cleave the catalytic site of PARP-1 from its DNA binding domain, effectively inactivating the polymerase (Lazebnik et al., 1994; Le et al., 2002). Accordingly, preconditioning stimulates caspase-dependent PARP-1 cleavage, attenuating PARP-1 activity, and protecting neurons from subsequent PARP-1 mediated cell death (Garnier et al., 2003). Caspase inhibition during preconditioning blocked PARP-1 cleavage and severely diminished the neuronal tolerance (Garnier et al., 2003). Thus, the killer protease caspase-3, when activated to sub-lethal levels, is a critical mediator of neuroprotection in preconditioned neurons. Although the preconditioning-induced caspase activation and some of its downstream targets have been characterized, little is known about proximal signaling events that contribute to sub-lethal caspase activation. A recent report showed that preconditioning mouse cortical cultures with sub-lethal Zn^{2+} activated caspase-3-dependent PARP-1 cleavage and HSP70 upregulation (Lee et al., 2008). Not surprisingly, caspase-3 and HSP70 induction were required for conferring tolerance to subsequent excitotoxic and Zn^{2+}-dependent toxicity (Lee et al., 2008). Most importantly, however, Lee and colleagues showed a sub-lethal accumulation of neuronal Zn^{2+} following preconditioning *in vivo*, which was necessary for ischemic tolerance (Lee et al., 2008). Despite these findings, the mechanism underlying the rise in free Zn^{2+} in preconditioned neurons was not explained. In this dissertation, I concentrate on upstream Zn^{2+}-dependent signaling pathways involved in initaing tolerance by examining the source of the Zn^{2+} rise in preconditioned neurons and investigating preconditioning-induced Zn^{2+}-regulated gene expression.

1.6.2 Protein kinase C (PKC)

As mentioned above, PKC is a family of serine/threonine kinases shown to play a role in Zn^{2+}-dependent cell death signaling (Noh et al., 1999; Newton, 2001). Zn^{2+} overload toxicity triggers

a PKC-dependent activation of NADPH oxidase, which generates ROS, resulting in cell death (Noh and Koh, 2000). On the other hand, PKC plays a central role in the signal transduction pathway following a preconditioning stimulus in multiple models of rapid and delayed, cardiac and neuronal tolerance (Bright and Mochly-Rosen, 2005). The seemingly opposing actions of PKC may be mediated by different isoforms. For example, in neurons δPKC has been implicated in mediating oxidative stress, apoptosis, and inflammation following cerebral ischemic injury (Koponen et al., 2000; Brodie and Blumberg, 2003), while εPKC has been identified as a critical isoform responsible for neuroprotection (Raval et al., 2003). Although PKC signaling clearly mediates neuroprotection in preconditioned neurons, the mechanistic details of its activation and its molecular targets remain unclear. Diverse signaling mechanisms involving extracellular adenosine, mitogen-activated protein kinases (MAPK), mitochondrial proteins, and ROS have all been hypothesized to play a role as PKC activators or targets in preconditioned neurons (Bright and Mochly-Rosen, 2005). In this dissertation, I provide evidence suggesting that PKC plays a novel early role in the post-translational modification of metallothionein, facilitating intracellular Zn^{2+} release, and driving neuroprotection.

1.6.3 Potassium channels

The enhancement of voltage-gated K^+ channel activity, producing K^+ efflux, is a critical step in many apoptotic programs (Yu, 2003; Bortner and Cidlowski, 2007). Apoptotic K^+ current enhancement leads to a decrease in the concentration of this cation in the cytoplasm (Yu et al., 1999), which may serve as a permissive apoptotic signal (Bortner and Cidlowski, 1999, 2007), as pro-apoptotic factors are activated most efficiently at reduced K^+ concentrations (Hughes and Cidlowski, 1999). In our laboratory, Kv2.1 was identified as the critical mediator of K^+ efflux

during neuronal apoptosis (Pal et al., 2003). Kv2.1 is the major component of delayed-rectifying K^+ current in cortical neurons (Murakoshi and Trimmer, 1999), and exists in large, highly phosphorylated clusters on the somatic surface and proximal dendrites of cortical neurons (Scannevin et al., 1996). Stimulation of a caspase-dependent neuronal apoptotic cascade by oxidative injury triggers the liberation of intracellular Zn^{2+}, leading to p38 MAPK-dependent phosphorylation and insertion of new Kv2.1-encoded channels (McLaughlin et al., 2001; Pal et al., 2006; Redman et al., 2007).

As lethal K^+ efflux is a component of apoptotic cell death, a sub-lethal modulation of voltage-gated K channel activity may mediate tolerance. Ischemia leads to profound changes in neuronal excitability, manifesting as an early phase of cellular hyperpolarization and depression of neural activity followed by a second phase of dramatic enhancement of excitability (Krnjevic, 2008). Changes in metabolic state or intracellular Ca^{2+} concentration following ischemia can modulate a variety of K^+ channels, including K_{ATP} channels, Ca^{2+}-activated BK channels, and delayed rectifier voltage-dependent K^+ channels (Runden-Pran et al., 2002; Ballanyi, 2004; Misonou et al., 2005). Recent evidence has shown that sub-lethal ischemic injury is associated with a protein-phosphatase 2B (PP2B or calcineurin)-dependent dephosphorylation of existing Kv2.1 channels, which is accompanied by a dispersal of somatodendritic Kv2.1 clusters and hyperpolarizing shifts in voltage-dependency (Misonou et al., 2005). The latter has been proposed to limit neuronal excitability and thus prevent widespread excitotoxic cell death (Surmeier and Foehring, 2004). Thus, the modulation of Kv2.1 following mild ischemia may be an important adaptive response to cellular injury. In this dissertation, I provide evidence that

Kv2.1 modulation following sub-lethal ischemia requires neuronal free Zn^{2+} providing a novel target of Zn^{2+} in a neuroprotective pathway.

1.7 THESIS GOALS

The overall goal of this thesis was to establish the role of Zn^{2+} in endogenous neuroprotective signaling mechanisms involved in neuronal tolerance. Accumulating evidence suggests the sub-lethal activation of cell death mediators can paradoxically activate endogenous protective pathways in neurons. Several downstream signaling events including caspase-3 activation, PARP-1 cleavage, and HSP70 upregulation have been identified. However, upstream signaling events that initiate neuroprotective signaling cascades in preconditioned neurons remain unclear. Zn^{2+} has been shown to play a critical role in ischemic neuronal cell death, but has recently emerged as a potentially important intracellular messenger. Thus, I hypothesized that a sub-lethal increase in neuronal free Zn^{2+} is required for conferring neuronal tolerance in preconditioned cells. My first goal was to characterize the increase in free Zn^{2+} in preconditioned neurons and to determine whether this Zn^{2+} rise contributed to attenuating subsequent Zn^{2+}-dependent toxicity. The results from these studies are presented in Chapter 2. PKC has been shown to be an important signaling agent in both Zn^{2+}-regulated gene expression as well as in neuronal tolerance. Accordingly, I examined the role of PKC in mediating Zn^{2+}-regulated gene expression in preconditioned neurons. Results from these studies suggested a very early role for PKC in facilitating Zn^{2+} liberation from intracellular stores. Based on these data, I examined whether PKC could directly modulate MT in promoting a Zn^{2+} rise in

preconditioned neurons. These data are also presented in Chapter 2. This chapter represents the contents of a manuscript that was recently published (Aras et al., 2009).

Kv2.1 encoded K^+ channels are modulated following sub-lethal ischemic injury and are thought to be important in limiting neuronal excitability following ischemia. Because a toxic Zn^{2+} rise triggers Kv2.1 modulation in lethal neuronal injury, I hypothesized that a sub-lethal increase in free neuronal Zn^{2+} may mediate Kv2.1 modulation in neuroprotection. The results from these experiments are presented in Chapter 3. This chapter represents the contents of a recently submitted manuscript. The findings of my thesis work suggest that sub-lethal accumulation of free Zn^{2+} plays important roles in diverse pathways involved in protecting neurons from lethal ischemic injury (Figure 1). With this dissertation, I detail this novel neuroprotective role for Zn^{2+} and examine a previously unexplored mechanism of triggering Zn^{2+}-regulated gene expression by PKC-dependent modulation of the metallothionein/Zn^{2+} interaction. In addition, I have included a related published study in Appendix B describing the critical role of apoptosis signal-regulating kinase-1 (ASK-1) in the Kv2.1 mediated K^+ current enhancement following oxidant-induced injury (Aras and Aizenman, 2005). Appendix C contains a published paper in detailing the variety of methods used to assess neuronal viability in primary neuronal cultures (Aras et al., 2008).

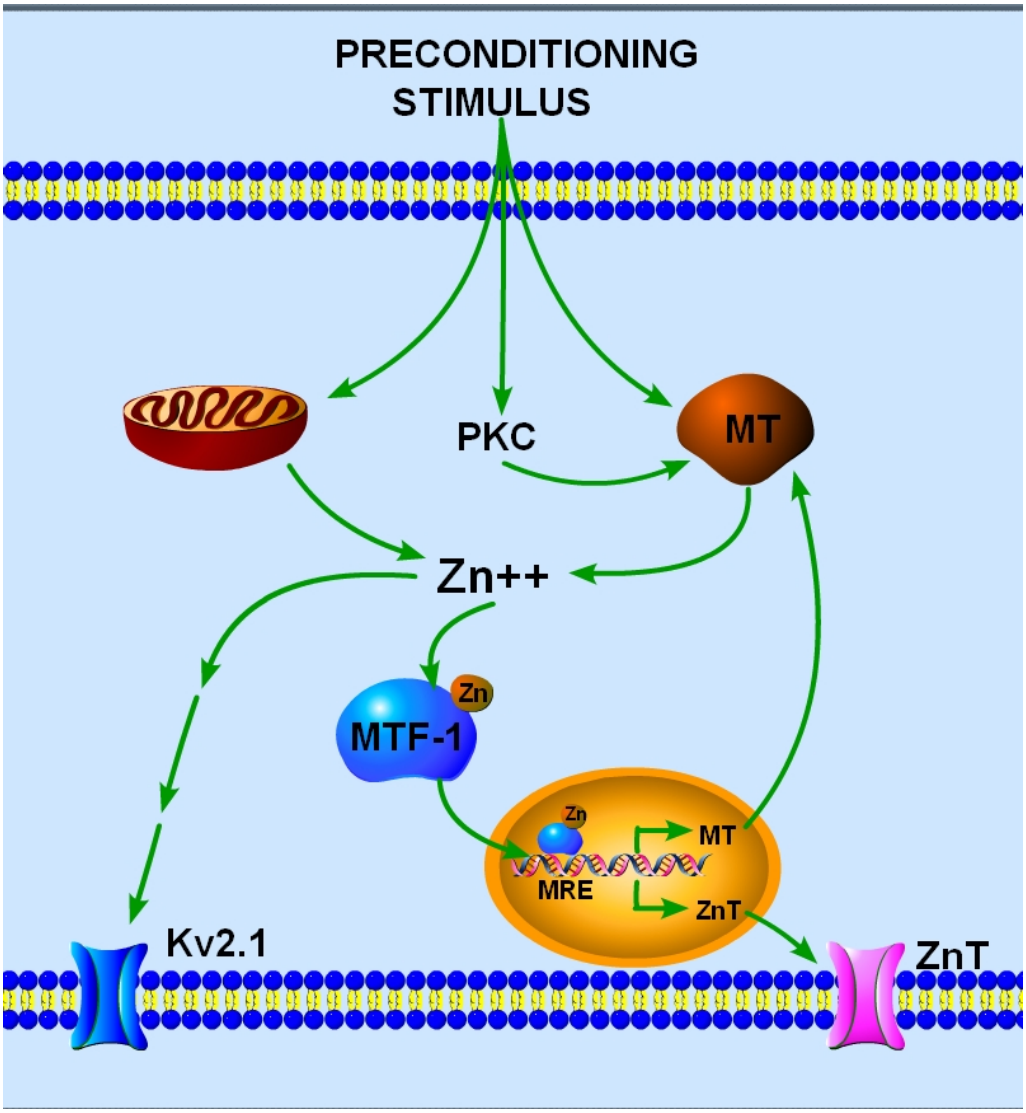

Figure 1 - Model of zinc-induced neuronal tolerance

Figure 1. Schematic diagram representing a proposed model in which a sub-lethal Zn^{2+} rise following preconditioning leads to the activation of Zn^{2+}-regulated gene expression and the modulation of Kv2.1 channel properties. The accumulation of free Zn^{2+} is facilitated by PKC-dependent phosphorylation of MT. The transient Zn^{2+} rise in preconditioned neurons may upregulate endogenous Zn^{2+} buffers, preventing subsequent lethal Zn^{2+}-dependent cell death.

2.0 PKC REGULATION OF NEURONAL ZINC SIGNALING MEDIATES SURVIVAL DURING PRECONDITIONING

2.1 ABSTRACT

Sub-lethal activation of cell death processes initiate pro-survival signaling cascades. As intracellular Zn^{2+} liberation mediates many neuronal death pathways, we tested whether a sub-lethal increase in free Zn^{2+} could also trigger neuroprotection. Neuronal free Zn^{2+} transiently increased following preconditioning and, importantly, this Zn^{2+} rise was both necessary and sufficient for conferring excitotoxic tolerance. Lethal exposure to NMDA led to a delayed increase in Zn^{2+} that contributed significantly to excitotoxicity in non-preconditioned neurons, but not in tolerant neurons, unless preconditioning-induced free Zn^{2+} was chelated. Thus, preconditioning may trigger the expression of Zn^{2+}-regulating processes, which, in turn, prevent subsequent Zn^{2+}-mediated toxicity. Indeed, preconditioning increased Zn^{2+}-regulated gene expression in neurons. Examination of the molecular signaling mechanism leading to this early Zn^{2+} signal revealed a critical role for protein kinase C (PKC) activity in the Zn^{2+} rise, suggesting that PKC may act directly on the intracellular source of neuronal Zn^{2+}. As such, we identified a conserved PKC phosphorylation site at serine-32 (S32) of metallothionein (MT) that was important in modulating Zn^{2+}-regulated gene expression and conferring excitotoxic tolerance. Importantly, we observed increased serine phosphorylation in immunopurified MT1, but not in

mutant MT1(S32A), when incubated with catalytically active PKC. These results indicate that neuronal Zn^{2+} serves as an important, highly regulated signaling component responsible for the initiation of a neuroprotective pathway.

2.2 INTRODUCTION

The mammalian brain contains relatively high concentrations of Zn^{2+} (~150μM; Weiss et al., 2000), reflecting its critical role not only as a structural component of numerous proteins and transcription factors but also as a neuromodulator and intracellular signaling messenger (Frederickson and Bush, 2001; Yamasaki et al., 2007). Most cellular Zn^{2+} is tightly bound to metal-binding proteins, limiting the amount of chelatable, "free" Zn^{2+} in the cytoplasm under physiological conditions (Outten and O'Halloran, 2001; Krezel and Maret, 2006). Nonetheless, the liberation of neuronal Zn^{2+} from intracellular stores, mediated by oxidative and nitrative stress, can readily trigger cell death signaling (Aizenman et al., 2000b; Bossy-Wetzel et al., 2004; Zhang et al., 2004). Neurotoxicity initiated by endogenous Zn^{2+} liberation is mediated by the generation of reactive oxygen species (ROS; McLaughlin et al., 2001; Bossy-Wetzel et al., 2004; Dineley et al., 2008), the release of cytochrome c and apoptosis-inducing factor from mitochondria (Sensi et al., 2003), and phosphorylation of mitogen-activated protein kinases (MAPK; McLaughlin et al., 2001; Du et al., 2002; Bossy-Wetzel et al., 2004).

A sub-lethal, preconditioning stimulus can activate endogenous pathways that limit or resist subsequent lethal injury in the brain (Kitagawa et al., 1990; for recent review, see Gidday, 2006). While the mechanisms conferring neuronal tolerance have yet to be fully defined,

increasing evidence suggests that preconditioning stimuli induce the sub-lethal activation of cell death factors that trigger endogenous survival pathways, which, in turn, prevent subsequent lethal signaling (Gidday, 2006). For example, ischemic preconditioning leads to sub-lethal activation of caspase-3 both *in vivo* and *in vitro* (Garnier et al., 2003; McLaughlin et al., 2003; Tanaka et al., 2004; Lee et al., 2008). Importantly, caspase activation is required for the establishment of tolerance to lethal stimuli (McLaughlin et al., 2003). Analogous roles in the establishment of neuronal tolerance have also been described for other signaling molecules linked to cell death including poly (ADP-ribose) polymerase-1 (PARP-1), p38 mitogen-activated protein kinase (MAPK), and protein kinase C (PKC; Garnier et al., 2003; Nishimura et al., 2003; Raval et al., 2003; Lee et al., 2008).

Here, we establish endogenous intracellular Zn^{2+} as a necessary and sufficient early signal in an *in vitro* model of excitotoxic tolerance (see also Lee et al., 2008). A preconditioning-induced increase in neuronal Zn^{2+} was critical in rendering neurons resistant to lethal excitotoxic insults that would otherwise induce Zn^{2+}-mediated toxicity. Examination of a potential Zn^{2+}-mediated neuroprotective pathway revealed that the major source of preconditioning-induced Zn^{2+} is metallothionein (MT) and that the Zn^{2+} signal emanating from the metal binding protein can be directly modulated by PKC phosphorylation. The results presented here strongly suggest that neuronal free Zn^{2+} serves as an upstream signaling component responsible for the initiation of pro-survival pathways that ultimately confer excitotoxic tolerance.

2.3 MATERIALS AND METHODS

Materials. Reagents were obtained from Sigma (St. Louis, MO) unless otherwise noted. Tissue culture supplies were purchased from Invitrogen (Carlsbad, CA), except for heat-inactivated and iron-supplemented bovine calf serum (Hyclone, Logan, UT). *Renilla* luciferase reporter gene (pRL-TK) and Dual-Glo luciferase assay system were purchased from Promega (Madison, WI). The MRE-luciferase construct (pLuc-MCS/4MREa) was kindly provided by Dr. David Giedroc (Indiana University, Bloomington, IN; Chen et al., 2004). Isoform-specific constitutively active PKC plasmids were kindly provided by Dr. Jae-Won Soh (Inha University, Incheon, South Korea; Soh et al., 1999).

Rat primary cortical culture and transfection. All experiments were performed in cortical cultures prepared from embryonic day 16 Sprague-Dawley rats (Charles River Laboratories, Wilmington, MA) as previously described (Hartnett et al., 1997). Cultures were utilized at 18–22 days in vitro (DIV). For transfection, neurons were treated for 5 hours with 2μL Lipofectamine 2000 (Invitrogen, Carlsbad, CA), 100μL OptiMEM (GIBCO, Grand Island, NY), and 1.5μg DNA per well in 500μL 2% serum-containing media.

Preconditioning and assessment of neuronal viability. An *in vitro* model of ischemic preconditioning was previously developed in our laboratory (Aizenman et al., 2000a; McLaughlin et al., 2003). Briefly, cortical cultures were treated with 3mM potassium cyanide (KCN) in a glucose-free balanced salt solution (150mM NaCl, 2.8mM KCl, 1mM $CaCl_2$, 10mM HEPES, pH 7.2) for 90min at 37^{o}C. Twenty-four hours later, neurons were exposed to 100μM

N-methyl-D-aspartate (NMDA) and 10μM glycine for 60 min prepared in phenol red-free MEM, supplemented with 25mM HEPES and 0.01% BSA. Neuronal viability was determined 18-24 hours following NMDA treatment with a lactate dehydrogenase (LDH) release assay (TOX-7 in vitro toxicology assay kit; Sigma) and/or by cell counting, with essentially similar results (Koh and Choi, 1987; Aras et al., 2008).

Neuronal viability in transfected neurons was assessed using a luciferase reporter assay (Aras et al., 2008). Twenty-four to forty-eight hours following transfection of a luciferase reporter plasmid (pUHC13-3) and any other plasmids of interest, neurons were treated with control and experimental conditions and assayed for luciferase-mediated luminescence using a SteadyLite luciferase assay system (PerkinElmer, Waltham, MA). Following 10-minute incubation in the luciferase reagent, luminescence was measured using a 96-well microplate reader (Wallac 1420, PerkinElmer Life Sciences, Waltham, MA). Cell viability is proportional to luciferase activity.

Intraneuronal Zn^{2+} imaging. To assess the relative magnitude of intracellular free Zn^{2+} in neurons, we utilized the Zn^{2+}-sensitive fluorescent probe, FluoZin-3 AM (Molecular Probes, Eugene, OR). FluoZin-3 AM is a cell-permeant, non-ratiometric fluorescent dye that responds robustly to physiological changes in cellular free Zn^{2+} and is highly selective for this metal (Devinney et al., 2005). Following treatment with chemical ischemia or an excitotoxic stimulus, neurons were loaded with FluoZin-3 (30min; 5μM prepared in buffered solution containing 144mM NaCl, 3mM KCl, 10mM HEPES, 5.5mM glucose, 5mg/mL bovine serum albumin; pH 7.3). The culture-containing glass coverslips were then immediately transferred to a recording

chamber (Warner, Hamden, CT) mounted on an inverted epifluorescence microscope superfused with phenol red-free MEM, supplemented with 25mM HEPES and 0.01% BSA. Images were acquired by exciting the fluorescent dye with 490 nm light every 10 seconds for 5 minutes using a computer controlled monochromator (Polychrome II, TILL photonics, Martinsried, Germany) and CCD camera (IMAGO, TILL photonics). Following acquisition of baseline metal levels (for approximately 100s), any neuronal free Zn^{2+} was chelated by superfusing cells with the membrane-permeant Zn^{2+} chelator *N,N,N',N'*-tetrakis (2-pyridalmethyl) ethylenediamine (TPEN, 20μM). The magnitude of the Zn^{2+} fluorescence for all neuronal cell bodies in a single field (n = 5–20 neurons) was determined by subtracting the fluorescence signal after TPEN perfusion from the initial baseline signal (ΔF_{TPEN}). With this method, larger ΔF_{TPEN} values correspond to higher amounts of pre-existing free intracellular Zn^{2+} in cells (Knoch et al., 2008).

Luciferase reporter assay. Cortical neurons were co-transfected with the metal response element (MRE)-firefly luciferase reporter (pLuc-MCS/4MREa) and *Renilla* luciferase reporter (pRL-TK) using Lipofectamine 2000 (Invitrogen, Carlsbad, CA) as previously described (Hara and Aizenman, 2004). The MRE-luciferase construct contains four tandem repeats of the endogenous MREa sequence (GGCTTTTGCACTCGTCCCGGCT) from the human metallothionein-IIA (hMT-IIA) gene upstream of a basal promoter that drives transcription of firefly luciferase (Chen et al., 2004). In transfected neurons, activation of MRE by Zn^{2+} drives the transcription of the firefly luciferase gene, increasing enzymatic luciferase activity. *Renilla* luciferase, driven by the constitutively active herpes simplex virus thymidine kinase (HSV-TK) promoter, is a non-inducible reporter used to standardize transfection efficiency. Neurons were treated 24 - 48 hours following transfection. Following treatment, neurons were extensively

washed and placed in a humidified 37^{o}C incubator for 5-24 hours until luciferase activity was measured.

Generation of MT3 targeted short hairpin RNA (shRNA) expression plasmid. RNA interference (RNAi) technology was used to knock-down endogenous MT3 in neurons. A MT3-shRNA targeting plasmid was constructed by inserting targeting oligonucleotides into the pSuppressorNeo plasmid (Imgenex; San Diego, CA). Inserted clones express RNAs under the U6 promoter in transfected mammalian cells as fold-back stem-loop structures that are processed into siRNA (Dykxhoorn et al., 2003). The synthetic oligonucleotides (sense, tcgagcctgctcggacaaatgcaattcaagattgcatttgtccgagcaggttttt; antisense, ctagaaaaacctgctcggacaaatgca atcttgaattgcatttgtccgagcaggc) were used for the preparation of the MT3-shRNA fragment. A MT1-shRNA construct was prepared using a similar strategy (sense, tcgagaactgcaaatgcacctccttcaagaggaggtgcatttgcagttcttttt; antisense, ctagaaaaagaactgcaaatgcacctc ctcttgaaggaggtgcatttgcagttc).

To confirm the specificity of the MT3-shRNA plasmid, we generated MT3 and MT1 expression vectors, each coupled to a different fluorescent probe. The MT3 and MT1 expression plasmids were constructed by first amplifying the MT3 and MT1 full-length cDNAs from rat brain and liver cDNAs, respectively. Specific primers for MT3 (sense primer, agaagcttgccaccatggaccctgagacctgccc; antisense primer, gaggatcctggcagcagctgcatttct) and MT1 (sense, agaagcttgccaccatggaccccaactgctcctg; antisense, gaggatccgcacagcacgtgcacttgtc) were used for the amplification. Second, the MT3 and MT1 cDNAs obtained were inserted into the *Hind* III/*BamH* I sites of the pEGFP-N1 and the pDsRed2-N1 vectors, respectively, in frame. The

final constructs encoded fusion proteins that fluoresced green for MT3 and red for MT1. Third, Chinese hamster ovary (CHO) cells were used as an expression system to verify the specificity of the constructs in epifluorescence and immunoblotting experiments (Supplementary Figure 1).

Site-directed mutagenesis. Mutagenesis of the MT1-DsRed cDNA was performed with a QuikChange XL kit (Stratagene, La Jolla, CA) according to the manufacturer's directions. Primers containing the desired mutation, serine on residue 32 to alanine (S32A) or aspartic acid (S32D), were obtained from Integrated DNA Technologies (Coralville, IA). The specific primers for MT1(S32A) used in the amplification were as follows: sense primer, aaatgcacctcctgcaagaaggcctgctgctcctgctgccccgtg; antisense primer, cacggggcagcaggagcagcaggcctt gcaggaggtgcattt. The specific primers for MT1(S32D) used in amplification were as follows: sense primer, aaatgcacctcctgcaagaaggactgctgctcctgctgccccgtg; antisense primer, cacggggcagcaggagcagcagtccttcttgcagcaggtgcattt. Mutations in MT1-DsRed were confirmed by sequencing. These constructs were used in neuronal transfection experiments where they were co-expressed with luciferase reporters.

Cell-free kinase assay. Wild-type MT1- and mutant MT1(S32A)-expressed protein from transfected CHO cells was immunoprecipitated by incubating cell lysates with an anti-metallothionein rabbit polyclonal antibody (1μg antibody per 1mL of cell lysate; Santa Cruz Biotechnology, Santa Cruz, CA) followed by a Protein A/G PLUS-Agarose immunoprecipitation reagent (Santa Cruz). The immunoprecipitated substrate was incubated in 15μl of kinase buffer (25mM Hepes, pH 8.0/2mM DTT/0.1mM vanadate), 15μl of Mg/ATP (50mM $MgCl_2$ and 50μM ATP), and 20ng of activated PKC catalytic subunit (Calbiochem, San Diego, CA) at 30^{o}C for 1

hour. Reactions containing kinase buffer alone, kinase buffer plus Mg/ATP, and 100nM Ro318220 were used as controls. The reaction was stopped with sample preparation buffer (62.5mM Tris-HCl, pH 6.8/25% glycerol/2% SDS/0.01% bromophenol blue/5% β-mecaptoethanol) and incubated at 95^{o}C for 5 min before SDS/PAGE and immunoblotting. Immunoblotting was performed with a phospho-Serine (PKC substrate-specific) antibody (Cell Signaling Technology, Beverly, MA, cat #2261; 1:1000) and the metallothionein rabbit polyclonal antibody (1:1000).

Data analysis. Data are expressed as mean ± SEM. Statistical analysis was performed using Student's *t* test or ANOVA with post hoc comparisons, as indicated in figure legends. An α of $p<0.05$ was considered statistically significant.

2.4 RESULTS

Inhibitors of energy metabolism, including KCN, can be coupled with glucose-free conditions to model ischemia (Aizenman et al., 2000a; Garnier et al., 2003; McLaughlin et al., 2003). Sub-lethal KCN exposure has been shown to induce excitotoxic tolerance in cortical neurons (McLaughlin et al., 2003). This *in vitro* preconditioning paradigm, which is used in the present study, expresses the hallmark features of delayed neuronal tolerance including requisite protein synthesis, involvement of mitochondrial K_{ATP} channels, and production of ROS (McLaughlin et al. 2003).

2.4.1 Preconditioning induces a transient increase in neuronal free Zn^{2+}.

The cell-permeant, non-ratiometric, Zn^{2+}-sensitive fluorescent probe, FluoZin-3 was used to determine whether sub-lethal chemical ischemia increases neuronal free Zn^{2+}. Cortical neurons were treated with increasing concentrations of KCN in glucose-free conditions for 90 minutes and immediately loaded with FluoZin-3 (5μM, 30 minutes). Neuronal TPEN-sensitive Zn^{2+} fluorescence (ΔF_{TPEN}) increased in a dose-dependent manner immediately following sub-lethal chemical ischemia (Figure 2a). Importantly, the concentration of KCN that has been shown to be a successful preconditioning stimulus (3mM; McLaughlin et al. 2003) resulted in a statistically significant increase in ΔF_{TPEN} when compared to vehicle-treated cells (Figure 2a). This increase in neuronal free Zn^{2+} following preconditioning was transient, as it diminished to intermediate levels 4 hours post-preconditioning (not shown) and returned to baseline levels 24 hours following preconditioning (e.g., see Figure 3c). However, the kinetic characteristics of the

preconditioning-induced Zn^{2+} rise are not representative of the "zinc wave" phenomenon as recently reported for mast cells (Yamasaki et al., 2007).

2.4.2 Excitotoxicity increases free Zn^{2+} in non-preconditioned neurons.

We investigated whether intracellular Zn^{2+} increased following NMDA exposure in *non-preconditioned* neurons and evaluated the contribution of this metal to NMDA-mediated toxicity. FluoZin-3 fluorescence was measured at various time points following treatment of neurons with an excitotoxic insult (100μM NMDA plus 10μM glycine, 60 minutes). NMDA treatment led to a delayed increase in ΔF_{TPEN}, reaching significant levels 6 hours following the excitotoxic insult (Figure 2b). To determine whether this delayed increase in neuronal free Zn^{2+} is critical for excitotoxic cell death, neuronal free Zn^{2+} was chelated with 1μM TPEN during and 24 hours following exposure to increasing concentrations of NMDA (plus 10μM glycine) in non-preconditioned neurons. We found that co- and post-treatment with 1μM TPEN significantly attenuated NMDA-induced toxicity (Figure 2c). We confirmed that this concentration of TPEN is non-toxic to neurons (not shown), as higher concentrations of TPEN can lead to neuronal toxicity (Ahn et al., 1998). We also confirmed that pre-treatment with TPEN alone for 24 hours prior to NMDA exposure does not subsequently affect NMDA-induced toxicity (Figure 4a), or the NMDA-induced increase in Zn^{2+} (Figure 3c). As an additional method for chelating intracellular Zn^{2+}, cortical neurons were transfected with the metal-binding protein, metallothionein-3 (MT3), and subsequently exposed to 30μM NMDA (plus 10μM glycine). Overexpression of MT3 serves as a sink for free Zn^{2+} in neurons (e.g., see Figure 7a), and like TPEN, would be expected to effectively chelate NMDA-induced free Zn^{2+}. We found that

transfected neurons overexpressing MT3 had significantly reduced toxicity following NMDA compared to vector-expressing neurons (Figure 2c, inset). These results indicate that the delayed increase in neuronal Zn^{2+} following NMDA contributes substantially to excitotoxicity, confirming previous reports (Bossy-Wetzel et al., 2004).

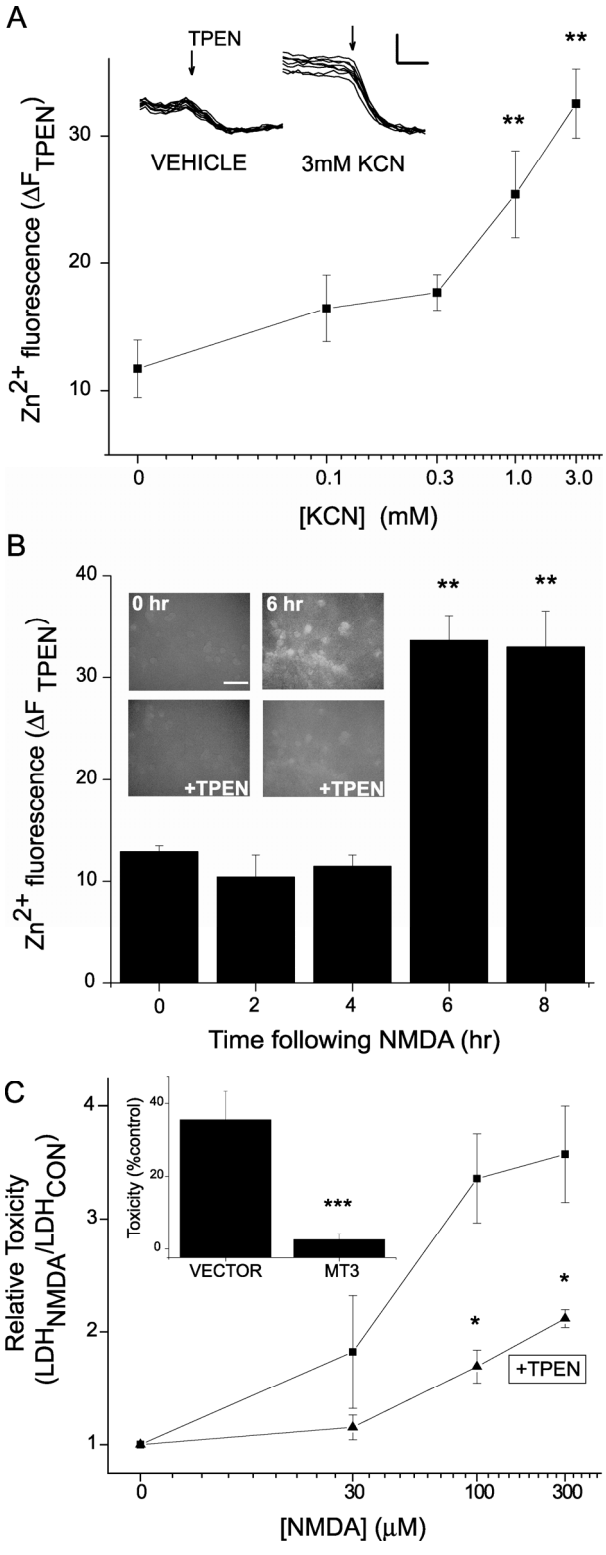

Figure 2 - Preconditioning and excitotoxicity increase neuronal zinc

Figure 2. (A) Inset, representative fluorescence traces of several vehicle and 3mM KCN-treated neurons in a single coverslip. Each trace reflects the level of intracellular free Zn^{2+} in a single neuron. Arrow depicts the beginning of superfusion with 20μM TPEN to chelate Zn^{2+} and quench florescence. Calibration: 10 arbitrary fluorescence units, 60 seconds. Plot shows TPEN-sensitive Zn^{2+} fluorescence, expressed as ΔF_{TPEN}, which was determined by subtracting the fluorescence signal after TPEN superfusion from the baseline signal. Data represent the mean (± s.e.m.) ΔF_{TPEN} measurements from 5-10 coverslips, each containing 5-10 neurons (**$p<0.01$ compared to 0mM KCN group; one-way ANOVA-Dunnett). (B) Cortical neurons were exposed to 100μM NMDA (with 10μM glycine) for 60 minutes and allowed to recover for various times prior to FluoZin-3 loading. Inset, examples of fluorescent images of cortical neurons loaded with 5μM FluoZin either immediately (left panels) or 6 hours (right panels) following NMDA. Images show FluoZin fluorescence from a representative field before (top panels) and after (bottom panels) 20μM TPEN superfusion. Scale: 100μm. Plot shows ΔF_{TPEN} (mean ± s.e.m.) measurements from 5-10 coverslips, each containing 5-10 neurons (**$p<0.01$ compared to 0 hr time point, one-way ANOVA-Dunnett). (C) Neurons were treated with vehicle (squares) or 1μM TPEN (triangles) during and 24-hours following exposure of non-preconditioned neurons to increasing concentrations of NMDA (plus 10μM glycine). Neuronal viability was determined with LDH release, measured 24 hours following NMDA exposure. Data are expressed as mean (± s.e.m) relative toxicity from 4 independent experiments performed in triplicate (*$p<0.05$ compared to corresponding 0μM TPEN group; paired two-tailed t-test). Inset, neurons expressing either vector or MT3 (0.5μg/well) along with a firefly luciferase reporter (pUHC13-3; 1.0μg/well) were treated with 30μM NMDA with 10μM glycine (10min) twenty-four hours following transfection. Twenty-four hours following treatment,

luciferase activity (viability; mean ± s.e.m) was measured from 4 independent experiments performed in quadruplicate (***$p<0.001$ Repeated measures ANOVA-Bonferroni Multiple Comparisons Test).

2.4.3 Preconditioning-induced Zn^{2+} elevation attenuates subsequent excitotoxicity-induced Zn^{2+} rise.

Previous work in our laboratory has shown that sub-lethal activation of cell death mediators initiates endogenous neuroprotective cascades that can buffer subsequent lethal levels of the same factor (McLaughlin et al. 2003). Since preconditioning induces a sub-lethal increase in Zn^{2+}, it is possible that preconditioned neurons may be tolerant to a subsequent NMDA-mediated elevation in Zn^{2+}. To test this, ΔF_{TPEN} was measured from preconditioned and non-preconditioned neurons six hours following exposure to NMDA (Figure 3a). Remarkably, the NMDA-induced delayed increase in neuronal Zn^{2+} was completely abolished in preconditioned neurons (Figure 3b, c). To determine whether the preconditioning-induced free Zn^{2+} is required for the diminished NMDA-induced Zn^{2+}, 1μM TPEN was added during and 24 hours following preconditioning. Following extensive washing to remove TPEN from the bathing medium, neurons were subsequently exposed to NMDA and assayed for the delayed increase in Zn^{2+} (Figure 3a). We found that chelating preconditioning-induced free Zn^{2+} restores the excitotoxic delayed increase in neuronal Zn^{2+} (Figure 3c). We verified that TPEN treatment without preconditioning had no effect on subsequent NMDA-induced Zn^{2+} elevation (Figure 3c). These results suggest that the preconditioning-induced transient increase in neuronal Zn^{2+} triggers the expression of Zn^{2+}-regulating processes, which, in turn, prevent or dampen subsequent increases in Zn^{2+} and Zn^{2+}-mediated toxicity following NMDA.

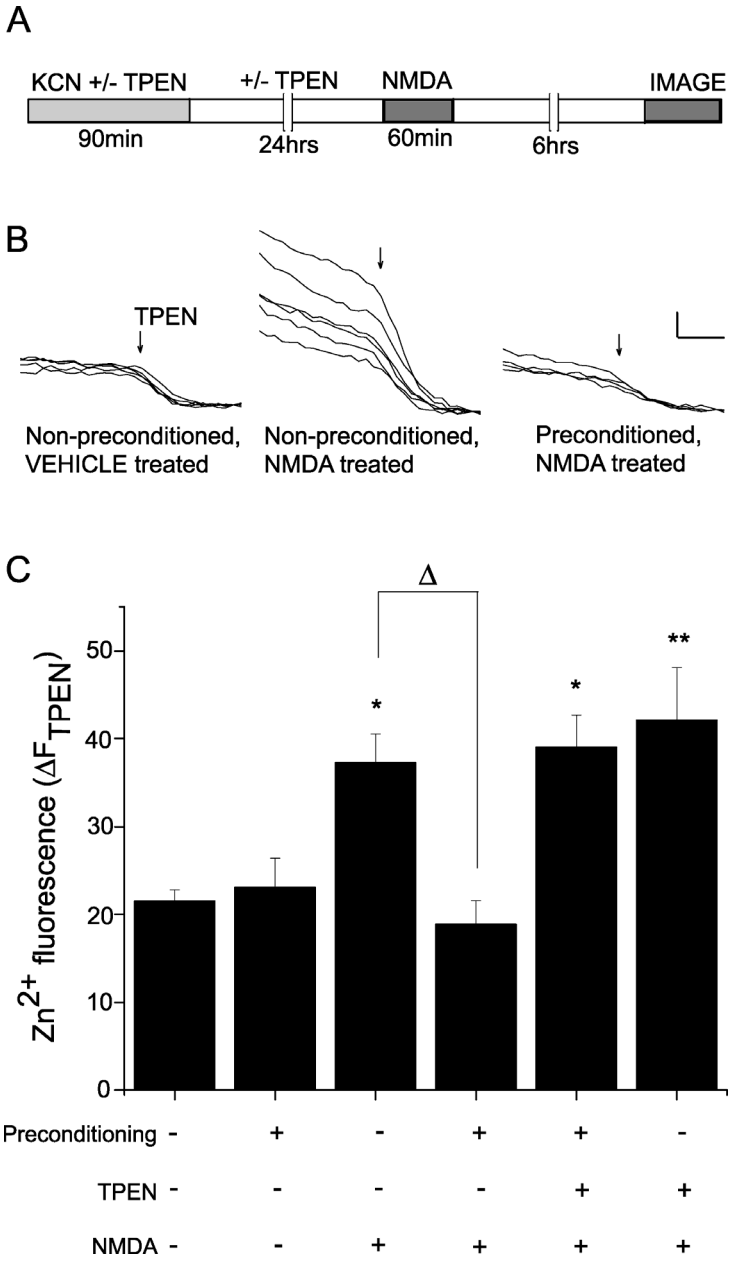

Figure 3 - Excitotoxic zinc rise is attenuated by preconditioning-induced increase in neuronal zinc

Figure 3. (A) Diagram representing experimental protocol designed to measure the effect of the preconditioning-induced increase in Zn^{2+} on the NMDA-induced Zn^{2+} rise. (B) Representative FluoZin fluorescence traces of a single coverslip containing non-preconditioned neurons exposed to vehicle, non-preconditioned neurons exposed to 100μM NMDA (with 10μM glycine, 60min), and 3mM KCN preconditioned neurons exposed to NMDA. Each trace reflects the level of intracellular Zn^{2+} in a single neuron. Arrow depicts the beginning of superfusion with 20μM TPEN to quench Zn^{2+} fluorescence. Calibration: 10 arbitrary fluorescence units, 60 seconds. (C) Preconditioned (3mM KCN, 90 minutes) and non-preconditioned neurons were exposed to 100μM NMDA (with 10μM glycine) for 60 minutes. FluoZin fluorescence was measured from neurons 6 hours following NMDA. In TPEN-treated groups, 1μM TPEN was present during and 24 hours following preconditioning, but not during or after NMDA exposure. ΔF_{TPEN} (mean ± s.e.m.) was measured from 5-10 coverslips in each group, each containing 5-10 neurons (*$p<0.05$, **$p<0.01$ compared to non-preconditioned, non-NMDA treated group; $^{\Delta}p<0.05$; one-way ANOVA-Tukey).

2.4.4 Zn^{2+} is necessary and sufficient for excitotoxic tolerance.

If chelating Zn^{2+} during preconditioning restores the NMDA-induced lethal increase in Zn^{2+}, then Zn^{2+} chelation during preconditioning would also be expected to attenuate excitotoxic tolerance. To test this, cortical neurons were treated with 1μM TPEN 30 minutes prior to, during, and 24 hours following preconditioning. Neurons were subsequently exposed to NMDA and assayed for cell viability 18-20 hours following excitotoxic exposure. In the absence of TPEN, preconditioning with chemical ischemia significantly reduced NMDA-induced toxicity (Figure 4a; McLaughlin et al. 2003). In contrast, chelation of preconditioning-induced free Zn^{2+} restored the vulnerability of neurons to NMDA (Figure 4a). TPEN treatment alone (without preconditioning) had no effect on subsequent NMDA-induced toxicity (Figure 4a). Therefore, these data suggest that excitotoxic tolerance is critically dependent on the preconditioning-induced transient increase in neuronal Zn^{2+}.

Next, to confirm the Zn^{2+}-selectivity of the TPEN results above, we investigated whether Zn^{2+} exposure alone was sufficient to induce excitotoxic tolerance. Cortical neurons were preconditioned with 30μM Zn^{2+} in the presence of 300nM pyrithione, which selectively transports extracellular Zn^{2+} into cells. Immediately following 18-24 hour incubation with Zn^{2+} and pyrithione, neurons were exposed to 30μM NMDA plus 10μM glycine for 30 minutes. Cell viability was determined 24 hours following NMDA insult. We found that 30μM Zn^{2+} with 300nM pyrithione afforded significant neuroprotection against NMDA toxicity (Figure 4b, c), to a similar degree as KCN preconditioning (e.g., see Figure 4a, inset). In general, however, we found that exogenous Zn^{2+} administration was not an ideal preconditioning agent due to intrinsic

Zn^{2+} neurotoxicity (Choi and Koh, 1998). Lower concentrations of Zn^{2+} (3, 10, and 20μM), or 30μM Zn^{2+} without pyrithione, failed to induce tolerance, while higher concentrations of Zn^{2+} (100μM) or pyrithione (1μM, along with Zn^{2+}) were themselves neurotoxic. Further, although 30 minute exposure of neurons to 30μM NMDA led to significant toxicity (e.g., see Figure 4b, c), no tested combination of Zn^{2+} and pyrithione afforded significant neuroprotection from a 60 minute exposure to 100μM NMDA.

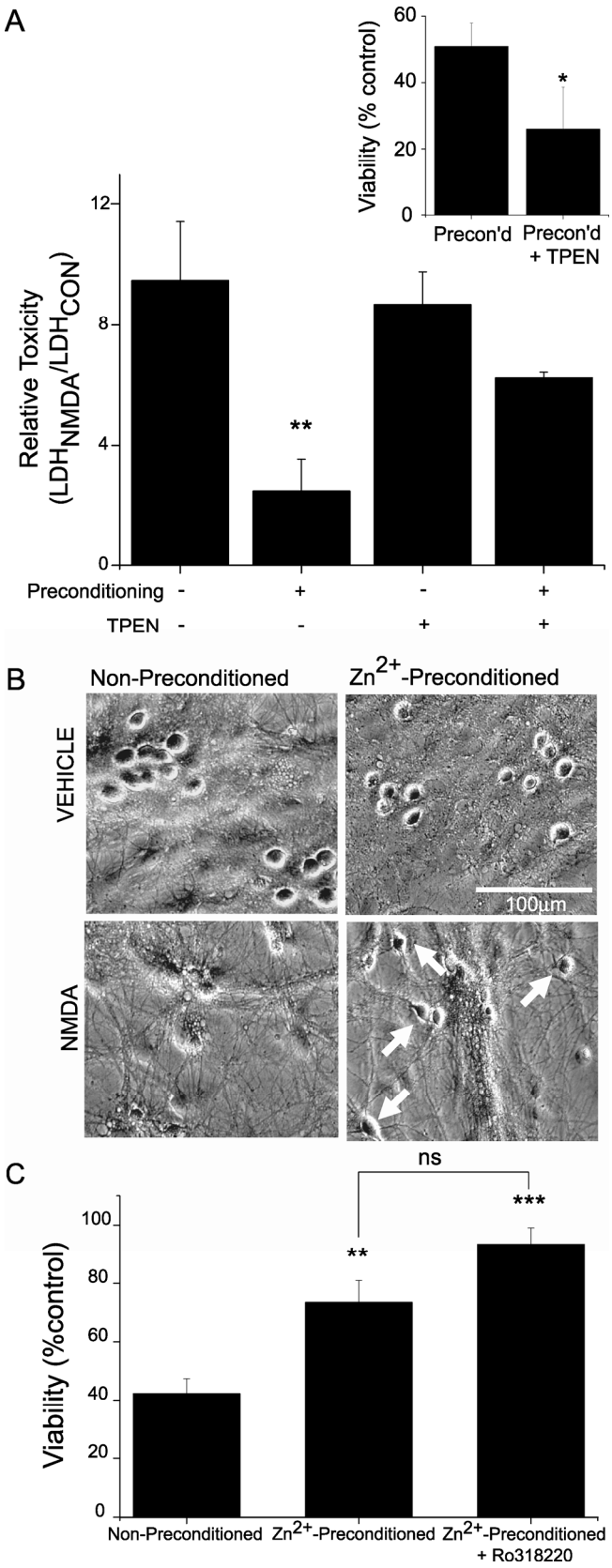

Figure 4 - Zinc is necessary and sufficient for excitotoxic tolerance

Figure 4. (A) LDH release was measured following 100μM NMDA (plus 10μM glycine, 60min) exposure in 3mM KCN preconditioned and non-preconditioned neurons treated in the presence or absence of 1μM TPEN. Main plot shows relative toxicity (mean ± s.d.) in a representative experiment (performed in quadruplicate; **$p<0.01$ compared to non-preconditioned, vehicle treated group; one-way ANOVA-Dunnett), while inset shows pooled viability data normalized to its corresponding control (n=5 independent experiments in triplicate or quadruplicate; *$p<0.05$; Paired, two-tailed t-test). (B) Cortical neurons were preconditioned with 30μM Zn^{2+} in the presence of 300nM pyrithione or 300nM pyrithione alone (non-preconditioned) for 18-24 hours prior to exposure to 30μM NMDA (plus 10μM glycine) or vehicle (10μM glycine alone). Phase-contrast images were obtained 24 hours following NMDA exposure. White arrows point to the presence of phase-bright, viable neurons in Zn^{2+}-precondioned cultures following NMDA exposure. (C) Cortical neurons were preconditioned with 300nM pyrithione alone (non-preconditioned), 30μM Zn^{2+} in the presence of 300nM pyrithione, or 30μM Zn^{2+}/300nM pyrithione in the presence of 1μM Ro318220 for 18-24 hours prior to exposure to 30μM NMDA (plus 10μM glycine) or vehicle (10μM glycine alone). Quantification of neuronal viability was determined by counting phase-bright live neurons in 10 random, high-power (200X) fields. Cell counts were performed 24-hours following NMDA exposure and expressed as percent viability (mean ± s.e.m.; n=4-9 independent experiments, each performed in triplicate; **$p<0.01$, ***$p<0.001$, significantly different from non-preconditioned condition; ANOVA/Tukey).

2.4.5 PKC modulates the intraneuronal Zn^{2+} signal.

Preconditioning triggers a transient increase in neuronal Zn^{2+} that is required for the attenuation of a subsequent, NMDA-induced lethal Zn^{2+} rise. Thus, it is conceivable that the preconditioning-induced Zn^{2+} rise triggers a neuroprotective mechanism that involves the activation of Zn^{2+} regulatory elements that prevent subsequent Zn^{2+} toxicity. An increase in intracellular free Zn^{2+} activates the metal response element transcription factor-1 (MTF-1), which translocates to the nucleus and activates a conserved metal response element (MRE), located on the promoter regions of Zn^{2+}-regulated genes (Andrews, 2001). Thus, a MRE-luciferase reporter construct (Chen et al., 2004; Hara and Aizenman, 2004) was utilized not only to monitor the level of free Zn^{2+} in transfected neurons, but also to determine whether the Zn^{2+} rise was sufficient to trigger Zn^{2+}-regulated gene expression. While PKC has been previously implicated in Zn^{2+}-regulated gene expression, all prior work had been performed in non-neuronal cell lines (LaRochelle et al., 2001b; Adams et al., 2002; Saydam et al., 2002; Jiang et al., 2004). Thus, we first confirmed that PKC plays a similar role in neurons. Cortical neurons were co-transfected with the MRE-firefly luciferase (pLuc-MCS/4MREa) and *Renilla* luciferase (pRL-TK) reporters. Twenty-four hours following transfection, neurons were treated with one of two PKC inhibitors, Ro318220 and Gö6976, during metal exposure (20μM Cd^{2+} + 50 μM NMDA/10μM glycine, 10 minutes; Hara & Aizenman 2004). In this treatment paradigm, Cd^{2+} permeates through the NMDA receptor (Ascher and Nowak, 1988), and strongly promotes MTF-1/MRE activation indirectly by displacing Zn^{2+} from MT (Zhang et al., 2003). We found that both PKC inhibitors blocked Zn^{2+}-regulated gene expression in a concentration-dependent manner (Figure 5a). Next, constitutively active forms of PKC were used to determine whether

PKC activity could enhance metal-induced MRE activation in neurons. The constitutively active PKC constructs encode a truncated protein in which the catalytic domain of PKC is preserved and the regulatory N-terminal domain is deleted (Soh et al., 1999). Forty-eight hours following transfection, neurons expressing a vector plasmid, constitutively active PKCβ1, or constitutively active PKCγ , along with the MRE-firefly and *Renilla* luciferase reporters were exposed to vehicle or Cd^{2+} and assayed for MRE activation. We found enhanced basal and metal-induced MRE activation in neurons expressing constitutively active PKC isoforms compared to vector expressing neurons (Figure 5b). Collectively, these data strongly implicate PKC activity in modulating the intracellular free Zn^{2+} signal and Zn^{2+}-regulated gene expression in neurons.

To determine whether PKC plays a role in preconditioning-induced Zn^{2+}-regulated gene expression, neurons expressing the two luciferase reporter genes were exposed to KCN in the presence or absence of 1μM Ro318220. Ro318220 is a cell-permeable, competitive, and relatively selective inhibitor of PKC. We first observed that preconditioning led to a significant activation of the MRE, similar to the positive control, 100μM Zn^{2+} (Figure 5c, left). PKC inhibition during preconditioning significantly attenuated Zn^{2+}-regulated MRE activation (Figure 5c, left) to a similar degree as during metal exposure (compare Figure 5c left to 5a). To confirm the PKC selectivity of Ro318220, neurons expressing the MRE firefly and *Renilla* luciferase reporters were stimulated with KCN preconditioning in the presence of 1μM H-89. H-89 is a cell-permeable, selective, and potent inhibitor of PKA. We found that, in contrast to Ro318220, H-89 had no effect on preconditioning-induced MRE activation (Figure 5c, left). These data suggest that a signaling cascade involving PKC is necessary for Zn^{2+}-dependent gene expression in preconditioned neurons.

PKC plays a central role in the signal transduction pathway in multiple models of neuronal tolerance (Raval et al., 2003; Bright and Mochly-Rosen, 2005; Dave et al., 2008). To confirm that PKC plays a critical role in excitotoxic tolerance in our model, cortical neurons were exposed to 1μM Ro318220 30 minutes prior to, during, and 24-hours following preconditioning. Cell viability was determined 24 hours following excitotoxic NMDA exposure. Indeed, PKC inhibition during preconditioning significantly blocked excitotoxic tolerance (Figure 5c, right). Thus, PKC plays a major role in preconditioning-induced Zn^{2+}-regulated gene expression and is required for excitotoxic tolerance.

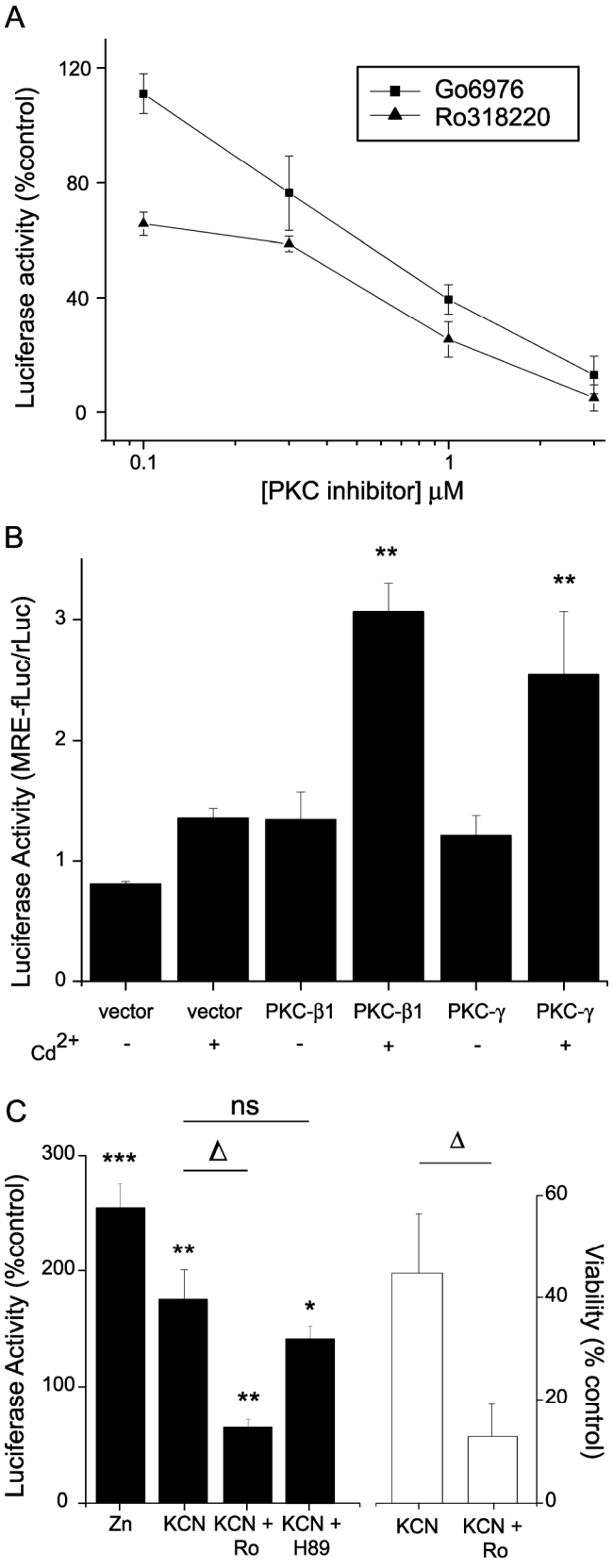

Figure 5 - Critical role of PKC in zinc-regulated gene expression in neurons

Figure 5. (A) MRE-firefly (fLuc; 1μg/well) and Renilla luciferase (rLuc; 0.5μg/well) - expressing neurons were stimulated with 20μM Cd^{2+} plus 50μM NMDA and 10μM glycine (10min) or vehicle in the presence or absence of increasing concentrations of the PKC inhibitors, Gö6976 and Ro318220. Relative MRE-fLuc/rLuc values (mean ± s.e.m., n=4-7 independent experiments in quadruplicates) were normalized to the control response in the absence of any PKC inhibitor (100%). (B) Neurons were transfected with MRE-firefly (0.375 μg/well) and Renilla luciferase (0.375μg/well) expressing plasmids in conjunction with plasmids encoding vector alone, constitutively active PKC-β1, or constitutively active PKC-γ (0.75μg/well). Forty-eight hours later, neurons were stimulated with 3μM Cd^{2+} plus 50μM NMDA and 10μM glycine (10min) or vehicle. Luciferase activity (MRE-fLuc/rLuc; mean ± s.e.m) was measured in 3-6 independent experiments performed in quadruplicate (**$p<0.01$ compared to vector-expressing neurons stimulated by Cd^{2+}). (C) Left (filled bars), neurons expressing the MRE-firefly (1μg/well) and Renilla luciferase (0.5μg/well) reporters were stimulated with 100μM Zn^{2+} (10min), KCN preconditioning (3mM, 90 min), or KCN in the presence of either 1μM Ro318220 or 1μM H-89, and subsequently assayed for luciferase activity 24 hours following treatment. Relative MRE-fLuc/rLuc values (mean ± s.e.m., n=4-11 independent experiments in triplicate) were normalized to the response in corresponding control neurons (*$p<0.05$, **$p<0.01$, ***$p<0.001$ compared to 100%; one-sample two-tailed t-test; $^{\Delta}p<0.05$ one-way ANOVA-Tukey). Right (open bars), neuronal viability was determined with LDH release following NMDA exposure in preconditioned neurons in the absence or presence or 1μM Ro318220. Data from 4 independent experiments performed in triplicate are expressed as viability (± s.e.m.) normalized to corresponding control condition ($^{\Delta}p<0.05$; paired, two-tailed t-test).

2.4.6 Preconditioning-induced Zn^{2+} rise is downstream of PKC activity.

Next, we examined the temporal relationship between Zn^{2+} liberation and PKC activation in preconditioned neurons. Previous reports have shown that acute exposure of a high concentration of exogenous Zn^{2+} can activate neuronal PKC (Noh et al., 1999). Zn^{2+}-overload neurotoxicity involves a PKC-dependent activation of NADPH-oxidase, which contributes to intracellular ROS generation (Noh and Koh, 2000). In other work, Knapp and Klann (2000) reported that mild oxidant-induced Zn^{2+} released directly from the Zn^{2+} finger motif of the cysteine-rich region of PKC is sufficient to trigger the activation of the kinase, suggesting that PKC activation and Zn^{2+} release occur almost simultaneously. Thus, the precise temporal relationship between PKC and Zn^{2+} remains unclear and may be stimulus-dependent. Here, KCN-induced Zn^{2+} accumulation was measured in neurons that were preconditioned in the presence of the PKC inhibitor Ro318220. Again, to confirm the selectivity of Ro318220 for PKC, H-89 was also used in these experiments. Surprisingly, co-treatment with Ro318220 during preconditioning completely blocked the increase in neuronal Zn^{2+} (Figure 6), suggesting that PKC activity occurs upstream of the Zn^{2+} rise in preconditioned neurons. To confirm this, we examined the requirement of PKC in the Zn^{2+}-induced preconditioning model. If intracellular Zn^{2+} is indeed downstream of PKC activity in the neuroprotective cascade, then PKC activity would not be required for Zn^{2+}-induced preconditioning. Neurons were preconditioned with 30μM Zn^{2+}/300nM pyrithione in the presence of Ro318220, and subsequently exposed to lethal NDMA. We found that neuroprotection was maintained in the presence of PKC inhibition (Figure 4c). Thus, in the Zn^{2+}-induced preconditioning model, application of exogenous Zn^{2+} can bypass PKC and directly trigger the neuroprotective cascade, confirming the temporal relationship of PKC activity prior to Zn^{2+} signaling in preconditioning.

2.4.7 Intracellular Zn^{2+} is likely the primary source of the preconditioning-induced Zn^{2+} rise.

In addition to liberation of neuronal Zn^{2+} from intracellular stores, synaptic release of vesicular Zn^{2+} and its translocation to postsynaptic neurons may contribute to neuronal injury following ischemia (Frederickson et al., 1989; Suh et al., 2000; but see Lee et al., 2000; Kay, 2003). We approached this issue two ways: 1) by targeting the main route of extracellular Zn^{2+} entry during ischemia, namely Ca^{2+}-permeable AMPA/kainate (Ca-A/K) channels (Sensi et al., 1999; Yin et al., 2002; Noh et al., 2005) with the competitive AMPA/kainate channel antagonist 6-cyano-7-nitroquinoxaline-2,3-dione (CNQX); and 2) by chelating extracellular Zn^{2+} using a cell-impermeant Zn^{2+} chelator, tricine (N-[Tris(hydroxymethyl)methyl]glycine; Paoletti et al., 2009). Intracellular Zn^{2+} was measured in neurons preconditioned in the presence CNQX (10μM), or tricine (1mM). We found that co-treatment with CNQX or tricine during preconditioning had little effect on the increase in neuronal Zn^{2+} (Figure 6), suggesting that the major source of preconditioning-induced Zn^{2+} is not extracellular. It must be noted, however, that the use of a higher affinity extracellular Zn^{2+} chelator (1mM CaEDTA) substantially decreased both baseline and preconditioning-induced intracellular Zn^{2+} levels (data not shown). As such, other sources of Zn^{2+} may be at play in this process, although CaEDTA has been reported to eliminate intracellular Zn^{2+} signals (Lee et al., 2000; Frederickson et al., 2002).

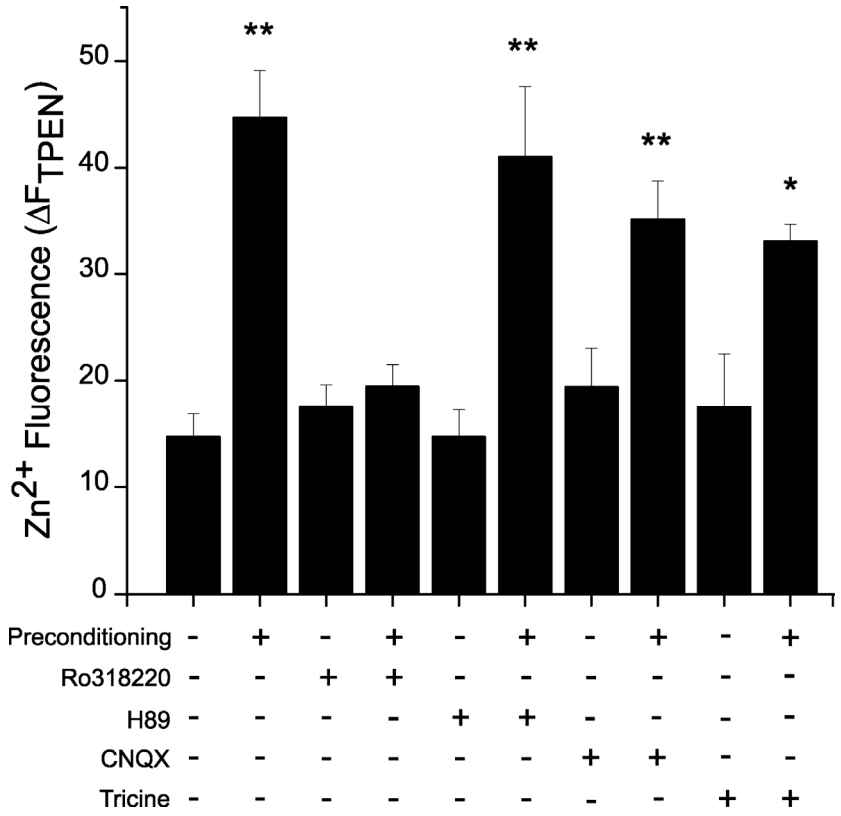

Figure 6 - Preconditioning-induced PKC activation is upstream of zinc release

Figure 6. Cortical neurons were preconditioned (3mM KCN, 90min) in the presence or absence of 3μM Ro318220, 1μM H-89, 10μM CNQX, or 1mM tricine immediately before FluoZin-3 loading. ΔF_{TPEN} (mean ± s.e.m.) was measured from 4-18 coverslips, each containing 10-20 neurons (*$p<0.05$, **$p<0.01$ compared to non-preconditioned vehicle-treated neurons, one-way ANOVA-Tukey).

2.4.8 PKC alters the MT / Zn^{2+} interaction.

Finally, we examined a possible site of action for PKC in Zn^{2+}-regulated gene expression in cortical neurons. Our results suggest that PKC acts upstream of preconditioning-induced Zn^{2+} release and may directly target an intracellular source of the liberated Zn^{2+} signal. A likely source of such labile Zn^{2+} in neurons is MT3, which is the predominant MT isoform in neurons (Aschner, 1996; Aschner et al., 1997; Palmiter, 1998; Hidalgo et al., 2001). When MT3 expression is reduced using a MT3-specific targeting plasmid that generates RNAi (MT3-shRNA; Supplementary Figure 1), MRE activation was enhanced, suggesting that under normal conditions, a fraction of MT3 is devoid of Zn^{2+} and can serve as a sink for intracellular free Zn^{2+} (Figure 7a). Knock-down of MT1, which is not normally significantly expressed in neurons, had no effect on neuronal MRE activity (Figure 7a). In contrast, neurons overexpressing MT3 or MT1 have excess Zn^{2+}-binding capacity, resulting in reduced levels of free Zn^{2+} released to trigger MRE activation (Figure 7a). Thus, MT3 may be a substantial source of labile Zn^{2+} in cortical neurons *in vitro*, and could potentially be one of the sites of PKC action during preconditioning.

Scansite (http://scansite.mit.edu), a computer program that predicts protein phosphorylation sites (Obenauer et al., 2003) was used to search for potential PKC phosphorylation target motifs on MT. All MT isoforms examined, regardless of species, contained a highly conserved, putative PKC phosphorylation site (serine 32 for MT1/2, serine 33 for MT3). In order to determine the role of this conserved site in Zn^{2+}-regulated gene expression, site-directed mutagenesis was used to create mutant forms of MT, in which the amino acid of the putative PKC phosphorylation site, serine (S), was substituted for either a non-

phosphorylatable alanine (A) or a phospho-mimicking charged aspartic acid (D) residue. Since neurons predominantly express MT3, cells were transfected with the MT3-shRNA targeting vector to reduce background provided by this isoform. In MT3-depleted neurons, overexpression of MT1 can restore the Zn^{2+}-binding capacity of cells, thus permitting substitution of the endogenous protein (Figure 7a). Using this approach, MRE activation was measured in MT3-depleted neurons expressing either wild-type MT1, a non-phosphorylatable mutant, MT1(S32A), or a phospho-mimicking mutant, MT1(S32D). Forty-eight hours following transfection, Zn^{2+}-regulated gene expression was stimulated with 100μM Zn^{2+} for 10 minutes. Twenty-four hours following this treatment, Zn^{2+}-induced MRE activation was significantly diminished in MT3-depleted, MT1(S32A)-expressing neurons, while significantly enhanced in MT3-depleted, MT1(S32D)-expressing neurons compared to MT3-depleted, wild-type MT1-expressing neurons (Figure 7b). These data suggest that neurons expressing a mutant MT, in which the putative PKC phosphorylation site is replaced with either a non-phosphorylatable residue or a phospho-mimicking charged residue, have altered efficiency in binding free Zn^{2+}, resulting in modulation of Zn^{2+}-regulated gene expression.

In order to determine whether PKC could directly phosphorylate MT, we performed a cell-free assay in which recombinantly expressed, immunoprecipitated wild-type MT1 was used as a substrate for active PKC (Figure 7b, inset). We found that wild-type MT1 exposed to active PKC produced increased phospho-serine immunoreactivity. This increase in the phospho-specific signal was abolished when the assay was performed in the presence of a PKC inhibitor (not shown). Similar experiments were performed with the mutant MT1(S32A) protein yielding

no change in phospho-serine immunoreactivity. Thus, active PKC can directly induce selective phosphorylation of MT1 at residue S32.

During preconditioning, PKC may influence Zn^{2+}-regulated gene expression by targeting MT at S32 and modulating the MT/Zn^{2+} interaction, ultimately leading to altered levels of neuroprotection. To test this, MT3-depleted neurons expressing either wild-type MT1 or MT1(S32A) along with a luciferase reporter plasmid were preconditioned with KCN. Twenty-four hours following preconditioning, neurons were exposed to NMDA excitotoxicity and subsequently assayed for viability. We found that KCN preconditioning was less efficient in conferring excitotoxic tolerance to MT3-depleted, MT1(S32A)-expressing neurons compared to MT3-depleted, wild-type MT1-expressing neurons (Figure 7c). Collectively, these data strongly suggest that PKC can directly phosphorylate MT and influence the MT/Zn^{2+} interaction, resulting in modulation of neuronal free Zn^{2+} and Zn^{2+}-regulated gene expression critical for preconditioning-induced tolerance.

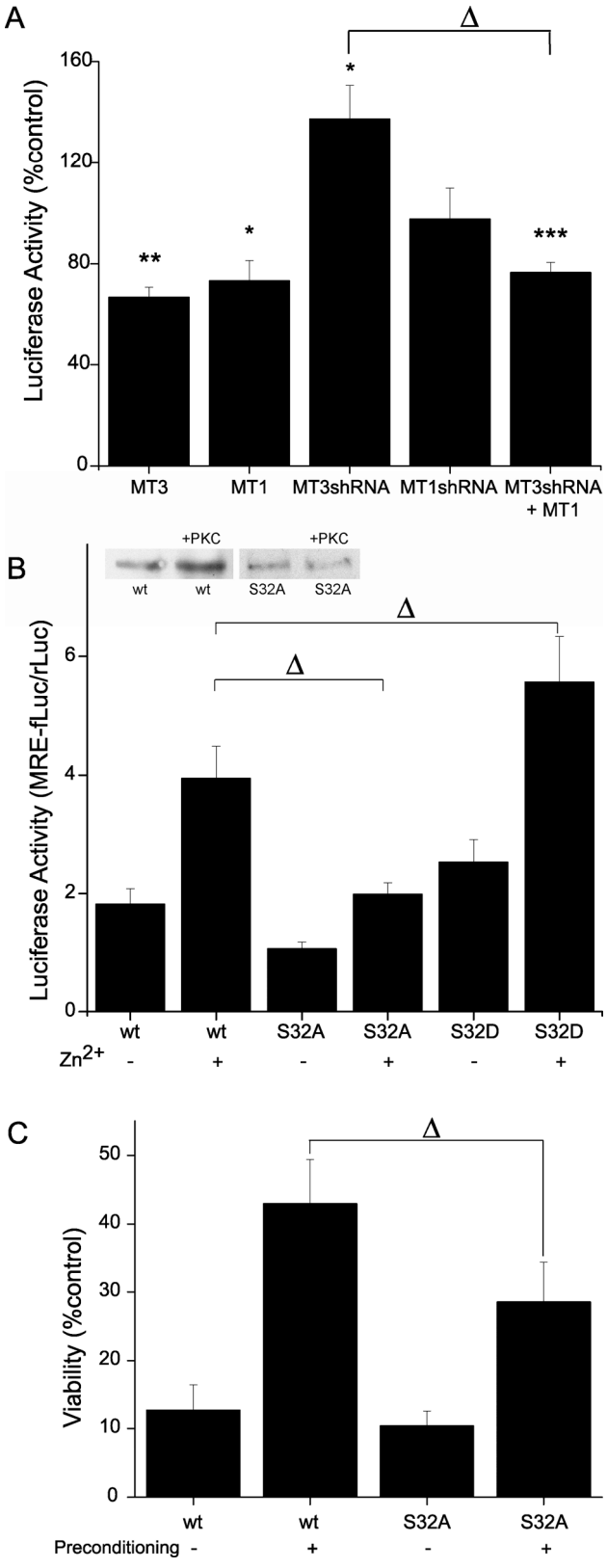

Figure 7 - PKC alters the MT/zinc interaction

Figure 7. (A) Neurons were transfected with MRE-firefly (0.5μg/well) and Renilla luciferase (0.5μg/well) expressing plasmids in conjunction with a plasmid encoding vector, MT3, MT1, the MT3-shRNA targeting vector, the MT1-shRNA targeting vector, or the MT3-shRNA targeting vector with MT1 (0.5 μg/well). Forty-eight hours later, neurons were stimulated with 20μM Cd^{2+} plus 50μM NMDA/10μM glycine or vehicle and assayed for luciferase expression. Relative MRE-fLuc/rLuc values (mean ± s.e.m., n=3-11 independent experiments in quadruplicate) were normalized to the response in corresponding vehicle-treated groups and then to the response in vector-expressing neurons (*$p<0.05$, **$p<0.01$, ***$p<0.001$ compared to 100%; One-sample two-tailed t-test.; $^{\Delta}p<0.05$ one-way ANOVA-Tukey). (B) Neurons were transfected with MRE-firefly (0.375μg/well) and Renilla (0.375μg/well) luciferase reporters in addition to the MT3-shRNA targeting vector (0.375μg/well) and either a wild-type MT1, a mutant MT1(S32A) plasmid, or a mutant MT1(S32D) plasmid (0.375μg/well). Forty-eight hours following transfection, neurons were stimulated by 100μM Zn^{2+} and assayed for luciferase activity. Luciferase activity (mean ± s.e.m.) was measured from 3-11 independent experiments performed in quadruplicate ($^{\Delta}p<0.05$; repeated measures ANOVA-Bonferroni Multiple Comparisons Test). Inset, wild-type MT1 and mutant MT1(S32A) proteins were immunoprecipitated from CHO cell lysates with a metallothionein rabbit polyclonal antibody (1μg antibody per 1mL of cell lysate) and reacted with 15μl of kinase buffer (25mM Hepes, pH 8.0/2mM DTT/0.1mM vanadate), 15μl of Mg/ATP (50mM $MgCl_2$ and 50μM ATP), and 20ng of activated PKC catalytic subunit at 30°C for 1 hour. Immunoblots were probed with the phospho-Serine (PKC substrate-specific) antibody (1:1000). Representative immunoblot of 4 independent experiments is shown. (C) Neurons were transfected with a firefly luciferase reporter (pUHC13-3; 0.5μg/well) in conjunction with the MT3shRNA targeting vector (0.5μg/well) and either wild-

type MT1 or the mutant MT1(S32A) plasmid (0.5μg/well). Forty-eight hours following transfection, neurons were preconditioned with 3mM KCN and subsequently exposed to 100μM NMDA/10μM glycine (60min). Luciferase activity (viability; mean ± s.e.m.) was measured 24 hours following NMDA exposure from 6 independent experiments performed in triplicate ($^{\Delta}p<0.05$ repeated measures ANOVA-Bonferroni Multiple Comparisons Test).

2.5 DISCUSSION

Zn^{2+} has been implicated as a causative trigger in many forms of neuronal cell death (Choi and Koh, 1998; Weiss et al., 2000; Frederickson et al., 2005). Here, we report a different, neuroprotective role for intracellular Zn^{2+}. A sub-lethal preconditioning stimulus elicited an immediate increase in neuronal free Zn^{2+}, which attenuated a subsequent excitotoxicity-induced increase in this metal. Chelating Zn^{2+} during preconditioning restored the excitotoxic increase in neuronal free Zn^{2+} and blocked excitotoxic tolerance. We examined the molecular signaling mechanism involved in excitotoxic tolerance and found that PKC activity was required for the preconditioning-induced increase in free Zn^{2+}, activation of Zn^{2+}-regulated gene expression, and neuroprotection. Finally, we identified a PKC phosphorylation site on MT that can modulate Zn^{2+}-regulated gene expression and neuroprotection presumably by facilitating Zn^{2+}-release from MT. Taken together, these results implicate intracellular Zn^{2+} in a neuroprotective pathway critical for excitotoxic tolerance. A very similar role for Zn^{2+}-mediated neuroprotection was recently described (Lee et al., 2008).

A preconditioning-induced, sub-lethal increase in neuronal free Zn^{2+} prevents a subsequent, NMDA-induced lethal increase in Zn^{2+}, likely by triggering the expression of Zn^{2+}-regulating processes. Evidence suggesting a role for endogenous Zn^{2+}-regulated proteins in neuroprotection comes from studies that used transgenic mice to examine the role of MT in ischemic cell death. MT overexpressing mice showed an average of 42% smaller infarct volumes and better motor performance compared to control mice following focal cerebral ischemia (van Lookeren Campagne et al., 1999). In contrast, MT 1/2-knock out mice develop approximately three-fold larger infarcts than wild-type mice (Trendelenburg et al., 2002).

Endogenous proteins involved in Zn^{2+} homeostasis, including MT1/2 and Zn^{2+} transporters are transcriptionally regulated by the Zn^{2+}/MTF-1/MRE pathway (Andrews, 2001). Since delayed-onset neuronal tolerance requires *de novo* protein synthesis (Gidday, 2006), a potential survival pathway in preconditioning may involve the transcriptional upregulation of Zn^{2+}-regulated proteins. Indeed, we found that preconditioning sufficiently activates a neuronal Zn^{2+}-specific MRE reporter construct containing the conserved response element located on the promoter regions of the Zn^{2+}-regulated genes. Together, these data provide strong evidence for Zn^{2+}-triggered processes mediating neuronal survival pathways critical for preconditioning-induced tolerance.

While the preconditioning-induced upregulation of endogenous Zn^{2+}-regulated proteins may ultimately confer neuroprotection, here we focus on neuronal MT3 as a source of free intracellular Zn^{2+}, which can act as an upstream signaling agent to trigger a neuronal survival pathway. First, using an extracellular chelator of Zn^{2+} and an inhibitor of Ca-A/K channels to block the primary entry route for synaptically-released Zn^{2+}, we found the preconditioning-induced Zn^{2+} rise was maintained, suggesting that the major source of preconditioning-induced Zn^{2+} is intracellular. While the use of a higher affinity extracellular Zn^{2+} chelator (CaEDTA) substantially blocked the preconditioning-induced Zn^{2+} rise (data not shown), CaEDTA also abolished baseline intracellular free Zn^{2+}, consistent with previous reports suggesting that CaEDTA eliminates intracellular Zn^{2+} signals (Lee et al., 2000; Frederickson et al., 2002). Thus, while possible, extracellular sources of preconditioning-induced free Zn^{2+} and enhanced Zn^{2+} uptake during preconditioning are not likely. Second, using a highly Zn^{2+}-sensitive molecular assay, we found that altering the expression of MT can modulate the levels of labile Zn^{2+}

released during metal stimulation. This suggests that MT is the major intracellular source of free Zn^{2+} in neurons. Third, and most importantly, when endogenous MT3 is replaced with mutant forms of MT1, in which the putative PKC phosphorylation site on MT, serine 32, is converted to a non-phosphorylatable residue (S32A), we observed decreased excitotoxic tolerance conferred by KCN preconditioning. Thus, modulation of intracellular Zn^{2+} homeostasis, possibly by the altering the ability of MT to bind free Zn^{2+}, has a profound impact on neuronal survival. These data show that MT3 is the major source of labile Zn^{2+} in neurons, and that MT-bound Zn^{2+} is the likely the critical source of the preconditioning-induced Zn^{2+} rise.

Several signal transduction pathways central to the neuroprotective response following preconditioning have also been implicated in Zn^{2+}-mediated signaling including p38 MAPK, extracellular signal regulated protein kinase (ERK), Akt, and PKC (Noh et al., 1999; Kim et al., 2000; McLaughlin et al., 2001; Du et al., 2002; Gidday, 2006). Of these, PKC has been shown to be required for both short-lasting and delayed tolerance in several models of cardiac and neuronal preconditioning (Raval et al., 2003; Bright and Mochly-Rosen, 2005; Perez-Pinzon et al., 2005; Dave et al., 2008). Here, we found that inhibition of PKC significantly reduced neuroprotection in our model. The mechanisms involved in PKC-mediated neuroprotection remain unclear and have been suggested to involve MAPK signaling, regulation of mitochondrial ATP-dependent potassium channels (K_{ATP}), and synaptic mitochondrial proteins (Bright and Mochly-Rosen, 2005; Dave et al., 2008). We found that PKC is required for the KCN-induced Zn^{2+} rise and can modulate Zn^{2+}-regulated gene expression, providing an additional, somewhat surprising upstream role of PKC in promoting neuronal survival. In the exogenous Zn^{2+}-induced preconditioning model, PKC activity was not required for excitotoxic tolerance, indicating that

Zn^{2+} is downstream of PKC in the neuroprotective cascade. The precise mechanism underlying the activation of PKC in conferring neuronal tolerance is still unclear. Several models of ischemic preconditioning have implicated a role for adenosine in triggering a PKC-dependent survival cascade (Bright and Mochly-Rosen, 2005). Others have shown that reactive oxidative and nitrative species, which are required in delayed neuronal tolerance, can modulate the activity of phospholipases, leading to the activation of downstream kinases, such as PKC (Das and Maulik, 2003). Alternatively, Knapp and Klann (2000) reported that mild-oxidant-induced Zn^{2+}-release from the cysteine-rich region of PKC can directly trigger the activation of the kinase. This hypothesis is supported by studies in cardiac preconditioning models, where a ROS-dependent activation of PKC is critical in cardiac tolerance (Zhang et al., 2002; Novalija et al., 2003).

Although PKC has been previously suggested to influence Zn^{2+}-regulated gene expression in non-neuronal cell lines (LaRochelle et al., 2001b; Saydam et al., 2002), its mechanism of action remains unclear. Much of the literature surrounding this issue focuses on MTF-1 as a target of PKC phosphorylation. MTF-1 is a 72.5kDa, ubiquitous, Zn^{2+}-finger transcription factor in the Cys_2His_2 family that, in the presence of Zn^{2+}, can bind to MREs at the consensus site TGCRCNC (Stuart et al., 1984). MTF-1 has been shown to be phosphorylated at multiple sites in unstimulated cells, and can undergo an increase in phosphorylation following metal exposure by a mechanism involving PKC (LaRochelle et al., 2001b; Adams et al., 2002; Saydam et al., 2002). However, when immunopurified endogenous MTF-1 protein from mouse hepatoma (Hepa) cells was used rather than overexpressed MTF-1 protein, Jiang and colleagues found that while MTF-1 can be phosphorylated in unstimulated cells, metal exposure does not

alter the phosphorylation pattern of MTF-1 (Jiang et al., 2004). Further, kinase inhibition does not affect metal-induced MTF-1 nuclear translocation, MTF-1 DNA binding, or the formation of a stable MTF-1-chromatin complex (Larochelle et al., 2001a; Jiang et al., 2004). Therefore, it is certainly possible that modulation of Zn^{2+}-regulated gene expression by signaling kinases may not be mediated by post-translational modification of MTF-1. Instead, signaling kinases, including PKC, may directly target unknown factors that interact with, or regulate MTF-1 (Jiang et al. 2004).

Based on a report showing a direct interaction of the PKC kinase domain with MT2A in a yeast two-hybrid screen (Rao et al., 2003), we turned our attention to MT as a potential target of PKC phosphorylation in neurons. First, we found that PKC activity was necessary for the preconditioning-induced increase in neuronal Zn^{2+}, suggesting that PKC may target an intracellular source of labile Zn^{2+}. Second, neurons expressing constitutively active forms of PKC had enhanced Zn^{2+}-regulated gene expression, similar to MT3-depleted neurons, suggesting that PKC activity may alter the MT/Zn^{2+} interaction. Third, MT3-depleted neurons expressing mutant forms of MT1, consisting of either a non-phosphorylatable or a phospho-mimicking point mutation at a putative PKC phosphorylation site (S32) had, respectively, either diminished or enhanced Zn^{2+}-induced MRE activation, similar to neurons in which either PKC activity or MT3 expression was modulated. Fourth, a cell-free kinase assay revealed increased serine phosphorylation in immunopurified wild-type MT, but not in mutant MT(S32A), when incubated with catalytically active PKC. Fifth, preconditioning of MT3-depleted neurons that expressed MT1(S32A) conferred less neuroprotection compared to MT3-depleted neurons expressing wild-type MT1. Collectively, these data provide evidence for a role of PKC phosphorylation in

modulating Zn^{2+}-regulated gene expression by possibly altering the MT/Zn^{2+} interaction. In conditions that promote an increase in neuronal Zn^{2+}, such as preconditioning, PKC activity could facilitate the release of Zn^{2+} from the metal-binding protein, which, in turn, would promote MTF-1/MRE activation and upregulate Zn^{2+}-regulating processes. This is the first study, to our knowledge, that directly demonstrates MT phosphorylation by PKC. Thus, modulation of Zn^{2+}-regulated gene expression by direct phosphorylation of MT by PKC may resolve the conflicting interpretations in the literature.

In summary, our results provide evidence for a central role of intracellular Zn^{2+} in a neuroprotective signaling cascade. Preconditioning induces a transient, sub-lethal intracellular Zn^{2+} rise that is critical for not only attenuating a subsequent, lethal elevation in excitotoxic Zn^{2+}, but also for conferring neurons excitotoxic tolerance. This preconditioning-induced increase in neuronal Zn^{2+} is sufficient for triggering Zn^{2+}-regulated gene expression via a PKC-dependent pathway.

3.0 ZINC REGULATES KV2.1 VOLTAGE-DEPENDENT GATING AND LOCALIZATION FOLLOWING ISCHEMIA

3.1 ABSTRACT

The delayed rectifier K^+ channel Kv2.1 exists in highly phosphorylated somatodendritic clusters. Ischemia induces rapid Kv2.1 dephosphorylation and a dispersal of these clusters, accompanied by a hyperpolarizing shift in their voltage-dependent activation kinetics. Transient modulation of Kv2.1 activity and localization following ischemia is dependent on a rise in intracellular Ca^{2+} and the protein phosphatase calcineurin. Here, we show that neuronal free Zn^{2+} also plays a critical role in the ischemic modulation of Kv2.1. We found that sub-lethal ischemia in cultured rat cortical neurons led to characteristic hyperpolarizing shifts in K^+ current voltage dependency and pronounced dephosphorylation of Kv2.1. Zn^{2+} chelation, similar to calcineurin inhibition, attenuated ischemic induced changes in K^+ channel activation kinetics. Zn^{2+} chelation during ischemia also blocked Kv2.1 declustering. Surprisingly, we found that the Zn^{2+} rise following ischemia occurred in spite of calcineurin inhibition. Therefore, a calcineurin-independent rise in neuronal free Zn^{2+} is critical in altering Kv2.1 channel activity and localization following ischemia. The identification of Zn^{2+} in mediating ischemic modulation of Kv2.1 may lead to a better understanding of cellular adaptive responses to injury.

3.2 INTRODUCTION

Ischemia triggers accumulation of extracellular glutamate, rise in intracellular Ca^{2+}, and occurrence of repetitive waves of depolarization, leading to profound changes in neuronal excitability (Lee et al., 1999; Dietz et al., 2009). Delayed rectifier voltage-dependent potassium (Kv) channels are important in regulating neuronal excitability (Du et al., 2000). Of these, Kv2.1 is a major component of delayed-rectifier potassium currents (I_K) in cortical neurons (Murakoshi and Trimmer, 1999; Du et al., 2000; Malin and Nerbonne, 2002; Pal et al., 2003) and exists in large, highly phosphorylated clusters on the surface of soma and proximal dendrites (Scannevin et al., 1996). Mild ischemic injury is associated with dephosphorylation of Kv2.1, dispersal of somatodendritic Kv2.1 clusters, and hyperpolarizing shifts in voltage-dependency (Misonou et al., 2005). The latter has been proposed as a mechanism to limit neuronal excitability and thus prevent or limit widespread excitotoxic cell death (Surmeier and Foehring, 2004). Such changes in Kv2.1 following ischemia are transient, returning to baseline conditions within hours of stimulus cessation, and are mediated by a rise in intracellular Ca^{2+} and protein phosphatase 2B activity (PP2B or calcineurin; Misonou et al., 2005).

In addition to a rise in neuronal Ca^{2+}, ischemic injury also leads to an accumulation of free Zn^{2+} in neurons (Galasso and Dyck, 2007). Recent evidence suggests that the Zn^{2+} rise following ischemia may actually precede the rise in intracellular Ca^{2+}, serving as a very early signal in the ischemic cascade (Medvedeva et al., 2009). This rise in neuronal Zn^{2+} following lethal ischemic insults has been associated with irreversible neuronal injury mediated by mitochondrial dysfunction (Medvedeva et al., 2009), nicotinamide adenine dinucleotide phosphate (NADPH) oxidase activation (Suh et al., 2008; Brennan et al., 2009), generation of

reactive oxygen species (Dineley et al., 2008), and activation of a $p75^{NTR}$-mediated death executer (Park et al., 2000). In contrast to lethal injury, preconditioning with sub-lethal ischemia can activate endogenous signaling pathways that confer neuronal tolerance to irreversible ischemic damage (Kitagawa et al., 1990; Gidday, 2006). Recent evidence suggests that a transient, early rise in neuronal free Zn^{2+} may also be important in preconditioning-induced neuroprotection (Lee et al., 2008; Aras et al., 2009). Preconditioning with chemical ischemia triggers a transient rise in neuronal free Zn^{2+}, which is necessary and sufficient for excitotoxic tolerance (Aras et al., 2009).

In the present study, we find a critical role for Zn^{2+} in the modulation of Kv2.1 following preconditioning. We first confirmed that sub-lethal chemical ischemia leads to the transient modulation of Kv2.1 voltage dependency and phosphorylation state. The altered K^+ channel activation kinetics, which have been shown to be a cellular adaptive process mediating neuroprotection, are dependent on a rise in neuronal free Zn^{2+}. Moreover, the ischemia-induced dispersal of Kv2.1 clusters is also Zn^{2+}-dependent. We find that both altered kinetics and localization of Kv2.1 following chemical ischemia are dependent on calcineurin, but that the Zn^{2+} rise occurs independently of this phosphatase. Thus, Zn^{2+} may represent a novel early signal in the modulation of Kv2.1 channel activity and localization following sub-lethal chemical ischemia.

3.3 MATERIALS AND METHODS

Rat primary neuronal cultures and preconditioning. All experiments were performed in primary cortical cultures prepared from embryonic day 16 Sprague-Dawley rats (Charles River Laboratories, Wilmington, MA) as previously described (Hartnett et al., 1997). Briefly, cortices were dissociated, and the resultant cell suspension was adjusted to 670,000 cells/well (six-well tissue culture plates containing five, 12-mm poly-L-ornithine-treated coverslips per well). Cultures were maintained at 37°C, 5% CO_2 in a growth medium composed of a volume-to-volume mixture of 80% Dulbecco's modified minimal essential medium, 10% Ham's F12-nutrients, 10% bovine calf serum (heat-inactivated, iron-supplemented) with 25mM HEPES, 24U/mL penicillin, and 24μg/mL streptomycin. Non-neuronal cell proliferation was inhibited after 2 weeks in culture with 1–2μM cytosine arabinoside, after which the cultures were maintained in growth medium containing 2% serum and without F12-nutrients. Cultures were utilized at 18–22 days in vitro. An *in vitro* model of ischemic preconditioning was previously developed in our laboratory (McLaughlin et al., 2003; Aras et al., 2009). Briefly, cortical cultures were treated with 3mM potassium cyanide (KCN) in a glucose-free balanced salt solution (150mM NaCl, 2.8mM KCl, 1mM $CaCl_2$, 10mM HEPES, pH 7.2) for 90min at 37°C. Preconditioning with KCN attenuates subsequent excitotoxic cell death by ~50% (McLaughlin *et al.*, 2003; Aras *et al.*, 2009).

Electrophysiology. All recordings were made using the whole-cell configuration of the patch-clamp technique as described previously (McLaughlin et al., 2001). The extracellular solution contained (in mM): 115 NaCl, 2.5 KCl, 2.0 $MgCl_2$, 10 HEPES, 10 D-glucose; pH was

adjusted to 7.2 with concentrated KOH; 0.250 mM TTX was added to inhibit voltage gated sodium channels. The intracellular (electrode) solution contained (in mM): 100 K-Gluconate, 11 EGTA, 10 KCl, 1 $MgCl_2$, 1 $CaCl_2$ x $2H_2O$, 10 HEPES; pH was adjusted to 7.2 with concentrated KOH; 0.22 mM ATP was added and osmolarity was adjusted to 280 mOsm with sucrose. All measurements were obtained under voltage clamp with an Axopatch 1C amplifier (Molecular Devices, Sunnyvale, CA) and pClamp software (Molecular Devices) using 2-3 MOhm electrodes. Partial compensation (80%) for series resistance was provided in all instances. Currents were filtered at 2 kHz and digitized at 10 kHz (Digidata; Axon Instruments). K^+ currents were evoked with a series of 200 msec voltage steps from a holding potential of –50mV to +80mV in 10mV increments. Before the start of the depolarization, a single pre-pulse to −10mV was given for 30 ms. Peak conductance (G) was calculated from peak steady-state current amplitudes (I) using the equation $G = I/(V-E_K)$, where E_K is the Nerst K^+ equilibrium potential. The conductance was plotted against the potential (V) and fitted to a single Boltzmann function $G = G_{max}/(1 + \exp[-(V - V_{1/2})/k])$, where G_{max} is the maximum conductance, $V_{1/2}$ is the potential at which the channel has half-maximal conductance, and k is the parameter that represents the slope of the activation curve.

Immunofluorescence. Kv2.1 labeling was performed essentially as described by Misonou and colleagues (2004). Immediately following chemical ischemia, neurons were washed three times in ice-cold PBS and fixed with 4% paraformaldehyde for 15 minutes. Following three washes with PBS, neurons were permeabilized for 5 min in PBS containing 0.3% Triton X-100. Neurons were washed three times in PBS and then incubated in PBS containing 1% bovine serum albumin (BSA) for 5 min. Following overnight incubation with

anti-Kv2.1 rabbit polyclonal (1:500; Alomone Labs, Jerusalem, Israel) and anti-microtubule-associated protein-2 mouse monoclonal (MAP2; 1:500; Sigma-Aldrich, St. Louis, MO; #M9942) antibodies, neurons were incubated in FITC anti-mouse (1:1000; Sigma-Aldrich, St. Louis MO) and Cy5 anti-rabbit (1:1000; Jackson Immunoresearch, West Grove, PA) secondary antibodies at room temperature for 1 hr. Coverslips containing neurons were then mounted onto glass slides and allowed to air-dry before imaging. Imaging of neurons was performed on an Olympus Fluoview FV1000 confocal unit fitted to an Olympus BX61 microscope at 60X (PlanApo, NA 1.4 oil) using Fluoview software (Olympus Fluoview, USA). Laser and detector settings were retained for all images collected. Multiple (5-10) optical sections (0.5μm) were acquired to generate a collapsed image file. Control and treatment groups were always run in parallel within the same immunocytochemical procedure. Collapsed, raw images were transferred to NIH image processing software (ImageJ; http://rsbweb.nih.gov/ij/) for analysis. Following background subtraction, neuronal somas were selected and a plot displaying a 3-dimensional graph of pixel intensity over a region of interest was used to display Kv2.1 localization (Figure 10). Clusters on the plots appeared as orange-red peaks in pixel intensity, which corresponded to >70% of maximal intensity (Figure 10). A clustered cell was scored as such when its associated surface map revealed greater than ten orange-red peaks. Using these plots, 75-100 cells from 3-4 independent experiments were classified as either having clusters or not. Although infrequent (<10% of total), neurons containing regions of both clustered and diffuse staining patterns were scored according to the predominant (>50% of cell surface) staining pattern.

Immunoblotting. Samples for biochemical analysis were prepared from neuronal cultures immediately following chemical ischemia. Neurons were washed three times with PBS

and then incubated in lysis buffer [50mM Tris-HCl, pH 7.4, 150mM NaCl, 0.25% deoxycholic acid, 1% nonyl phenoxylpolyethoxylethanol (NP-40), 1mM EDTA] supplemented with protease inhibitor mixture (Roche Diagnostics, Indianapolis, IN), 1mM phenylmethylsulphonyl fluoride (PMSF), and 100μM vanadate for 5min on ice. Cell lystates were harvested and centrifuged at 10,000 X g for 10min at 4^{o}C. Cell lysate samples were combined in a 1:1 ratio with sample prep buffer [62.5mM Tris-HCl, pH 6.8, 2% SDS, 25% glycerol, 0.01% Bromophenol Blue] and incubated for 5 min at 100°C to denature proteins before gel electrophoresis. SDS/PAGE was carried out by standard procedures using the Mini Protean 3 System (Bio-Rad, Hercules, CA). Equal amounts of cell lysate (15 μg) were separated on 7.5% SDS/PAGE gels and transferred onto a 0.2 μm nitrocellulose membrane. The membranes were blocked with 1% bovine serum albumin (BSA) in PBS with 0.05% Tween 20 before probing with either an anti-Kv2.1 mouse monoclonal (clone K89/34, NeuroMab, Davis, CA) or an anti-GAPDH mouse monoclonal (Novus Biologicals, Littleton, CO). Blots were incubated with a goat anti-mouse secondary antibody conjugated to HRP and were visualized with a SuperSignal CL-HRP Substrate System (Pierce Biotechnology, Rockford, IL).

Neuronal Zn^{2+} imaging. To assess the relative magnitude of intracellular free Zn^{2+} in neurons, we utilized the Zn^{2+}-sensitive fluorescent probe FluoZin-3 AM (Molecular Probes, Eugene, OR). FluoZin-3 AM is a cell-permeant, non-ratiometric fluorescent dye that responds robustly to physiological changes in cellular free Zn^{2+} (K_D for Zn^{2+} 10-20nM) and is highly selective for this metal (Devinney et al., 2005). The small-molecule probe fluoresces upon binding Zn^{2+} and is best suited for assessing the presence of free Zn^{2+} in cells rather than determining its precise intracellular concentration (Thompson et al., 2002; Kay, 2003).

Following treatment with chemical ischemia, neurons were loaded with FluoZin-3 (30min; 5μM prepared in buffered solution containing 144mM NaCl, 3mM KCl, 10mM HEPES, 5.5mM glucose, 5mg/mL bovine serum albumin; pH 7.3). The culture-containing glass coverslips were then immediately transferred to a recording chamber (Warner, Hamden, CT) mounted on an inverted epifluorescence microscope superfused with phenol red-free minimal essential medium, supplemented with 25mM HEPES and 0.01% bovine serum albumin. Images were acquired by exciting the fluorescent dye with 490 nm light every 10 seconds for 5 minutes using a computer controlled monochromator (Polychrome II, TILL photonics, Martinsried, Germany) and CCD camera (IMAGO, TILL photonics). Following acquisition of baseline metal levels (for approximately 100s), any neuronal free Zn^{2+} was chelated by superfusing cells with the membrane-permeant Zn^{2+} chelator *N,N,N',N'*-tetrakis (2-pyridalmethyl) ethylenediamine (TPEN, 20μM). The magnitude of the Zn^{2+} fluorescence for all neuronal cell bodies in a single field (n = 5–20 neurons) was determined by subtracting the fluorescence signal after TPEN perfusion from the initial baseline signal (ΔF_{TPEN}), as described earlier (Knoch et al., 2008; Aras et al., 2009). With this method, larger ΔF_{TPEN} values correspond to higher amounts of pre-existing free intracellular Zn^{2+} in neurons (Knoch et al., 2008; Aras et al., 2009).

Statistical analysis. Data are expressed as mean ± SEM. Statistical analysis was performed using an ANOVA with post hoc comparisons, as indicated in figure legends. An α of $p<0.05$ was considered statistically significant.

3.4 RESULTS

3.4.1 Sub-lethal ischemia alters potassium channel activity and Kv2.1 phosphorylation

Transient hyperpolarizing shifts in the voltage-dependence of activation of neuronal I_k dramatically limit neuronal excitability and are thus thought to be an adaptive cell response to ischemia (Surmeier and Foehring, 2004). Sub-lethal chemical ischemia, using potassium cyanide (KCN) coupled with glucose-free conditions, reliably induces Zn^{2+}-dependent excitotoxic tolerance in cortical neurons (Aras et al., 2009). To first determine whether sub-lethal ischemia could alter K^+ channel activation in cortical neurons, whole-cell K^+ currents were measured from control and KCN preconditioned (3mM, 90 min) neurons immediately following treatment. We found that sub-lethal ischemia indeed led to a hyperpolarizing shift in the voltage-dependency of K^+ channel activation (Figure 8a), similar to those reported in hippocampal neurons (Misonou et al., 2005). These hyperpolarizing shifts were transient and partially returned to baseline conditions 24 hours following the ischemic stimulus (Figure 8a).

Hyperpolarizing shifts in the voltage-dependent activation of neuronal I_k are associated with a dephosphorylation of the Kv2.1 channel (Misonou et al., 2004; Misonou et al., 2005). To determine whether sub-lethal ischemia could dephosphorylate Kv2.1, we performed immunoblot experiments on cortical neurons exposed to either KCN or control conditions (Figure 8b). The major forms of Kv2.1 in control-treated rat brain cultured neurons were found to exhibit a higher range of molecular weight bands (~95-105 kDa; Figure 8b) than predicted from the deduced Kv2.1 primary sequence (95.3 kDa), reflecting its constitutively multi-phosphorylated state (Misonou et al., 2004). KCN led to a dramatic reduction in the molecular weight of Kv2.1,

representing a dephosphorylation of the channel (Figure 8b; Misonou et al., 2004). Changes in the phosphorylation state of Kv2.1 are reversible and are restored to control conditions hours after the stimulus (Misonou et al., 2004; Misonou et al., 2005). Indeed, twenty-four hours following KCN exposure, we found that Kv2.1 partially returned to its multi-phosphorylated state (Figure 8b). Thus, reminiscent to the response following ischemia in hippocampal neurons (Misonou et al., 2005), sub-lethal ischemia led to a transient dephosphorylation of Kv2.1 in cortical neurons, accompanied by hyperpolarizing shifts in the voltage-dependence of neuronal I_k.

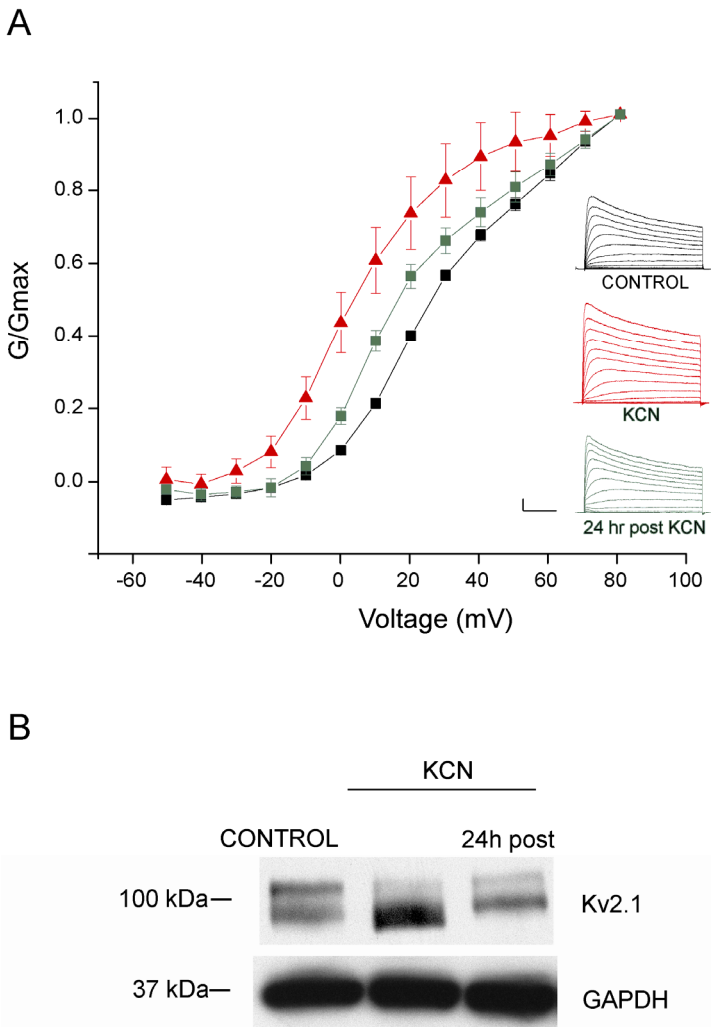

Figure 8 - Chemical ischemia alters K+ channel activation properties and phosphorylation state

Figure 8. (A) Inset, representative I_k currents in cortical neurons evoked with a series of 200ms depolarizing steps from -50mV to +80mV recorded under whole-cell voltage clamp. A single 30ms pre-pulse depolarization to -10mV was given before each recording to minimize rapidly-inactivating K^+ current. Whole-cell K^+ currents were measured immediately following either control (black traces) or 3mM KCN (red traces) exposure, or 24 hours following 3mM KCN (green traces). Calibration: 2nA, 50ms. Main plot shows the conductance-voltage (G-V) relationship of peak potassium current recorded from neurons in each treatment group. Data points represent the mean ± s.e.m from 6-18 neurons. (B) Neurons were exposed to either vehicle or 3mM KCN. In KCN treated groups, cell lysates were harvested immediately or 24 hours following stimulus. Lysates were separated and transferred to nitrocellulose membranes, which were probed with either an anti-Kv2.1 mouse monoclonal (1:1000) or an anti-GAPDH mouse monoclonal (1:1000) antibody. Representative blot of 4 independent experiments is shown.

3.4.2 Modulation of K^+ channel activity is Zn^{2+}- and calcineurin-dependent

The hyperpolarizing shifts in K^+ channel activation have been shown to be dependent on a rise in intracellular Ca^{2+} and the activation of calcineurin (Misonou et al., 2005). Recent evidence suggests that Zn^{2+} is both necessary and sufficient for mediating neuronal tolerance triggered by ischemic preconditioning (Lee et al., 2008; Aras et al., 2009). Thus, the ischemia-induced modulation of K^+ channel activation may also be Zn^{2+}-dependent. To test this, whole-cell K^+ currents were measured from neurons preconditioned in the presence of the cell-permeant Zn^{2+}-chelator, TPEN (*N,N,N',N'*-tetrakis (2-pyridalmethyl)ethylenediamine; 1μM). It is noteworthy that under these conditions the neuroprotective effects of preconditioning are severely attenuated (Aras et al., 2009). We found that TPEN almost completely blocked the hyperpolarizing shift in the voltage-dependence of activation (Figure 9). However, when neurons were treated with exogenous Zn^{2+} and pyrithione acutely (30 and 100 μM $ZnCl_2$ with 1 μM pyrithione; 2-5 min), the voltage-dependence of activation of Kv2.1 channels was not shifted (not shown), suggesting that Zn^{2+} may be necessary but not sufficient for the ischemic-induced modification of neuronal I_k. In order to verify the role of calcineurin in this process, whole-cell K^+ currents were measured from preconditioned neurons treated in the presence of the calcineurin inhibitor, FK520 (5μM; IC_{50} 49nM). We found that, like TPEN, FK520 attenuated the preconditioning-induced hyperpolarizing shift in the voltage-dependence of K^+ channel activation (Figure 9). Thus, both Zn^{2+} and calcineurin play a role in the modulation of the voltage-dependence of activation of neuronal I_k following chemical ischemia.

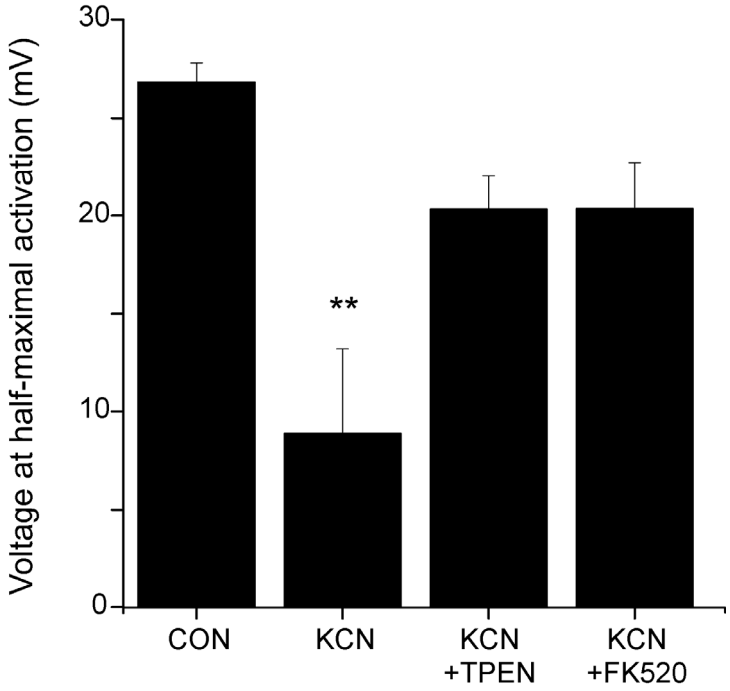

Figure 9 - Altered K+ channel activation properties are zinc- and calcineurin-dependent

Figure 9. Whole-cell K^+ currents were measured immediately following control, 3mM KCN, or 3mM KCN in the presence of 1μM TPEN or 5μM FK520. Peak current for each neuron was converted to conductance and the conductance was plotted against each potential and fit to a Boltzmann distribution. Data points represent mean ± s.e.m. half-maximal activation voltage (mV) for K^+ currents obtained from 8-18 neurons (**p<0.01 compared to control; One-way ANOVA-Dunnett).

3.4.3 Chemical ischemia induces Zn^{2+} and calcineurin-dependent Kv2.1 declustering

Hyperpolarizing shifts in K^+ channel activation and dephosphorylation of Kv2.1 are accompanied by a dispersal of surface Kv2.1 clusters to a more uniform localization (Misonou et al., 2005). To determine whether the ischemic dispersal of Kv2.1 clusters is also dependent on a rise in free Zn^{2+}, cortical neurons were exposed to KCN in the absence and presence of TPEN. Immediately following exposure, neurons were fixed and immunostained using antibodies specific for Kv2.1 and the neuronal marker, microtubule-associated protein-2 (MAP2). Maps plotting the distribution of Kv2.1 within individual neuronal somata were used to determine whether a cell contained clusters (Figure 10a). We found that sub-lethal ischemia led to a dispersal of somatic Kv2.1 clusters (Figure 10a, b). Kv2.1 dispersal partially returned to a clustered localization 24 hours following ischemia (Figure 10b). When neurons were exposed to KCN in the presence of TPEN, declustering of Kv2.1 was blocked (Figure 10a, b). As controls, we verified that ischemia- and NMDA-mediated declustering was dependent on calcineurin by using FK520 (Figure 10a, b; Misonou et al., 2005; Mulholland et al., 2008). Thus, in addition to calcineurin, ischemic declustering of Kv2.1 requires an increase in neuronal free Zn^{2+}.

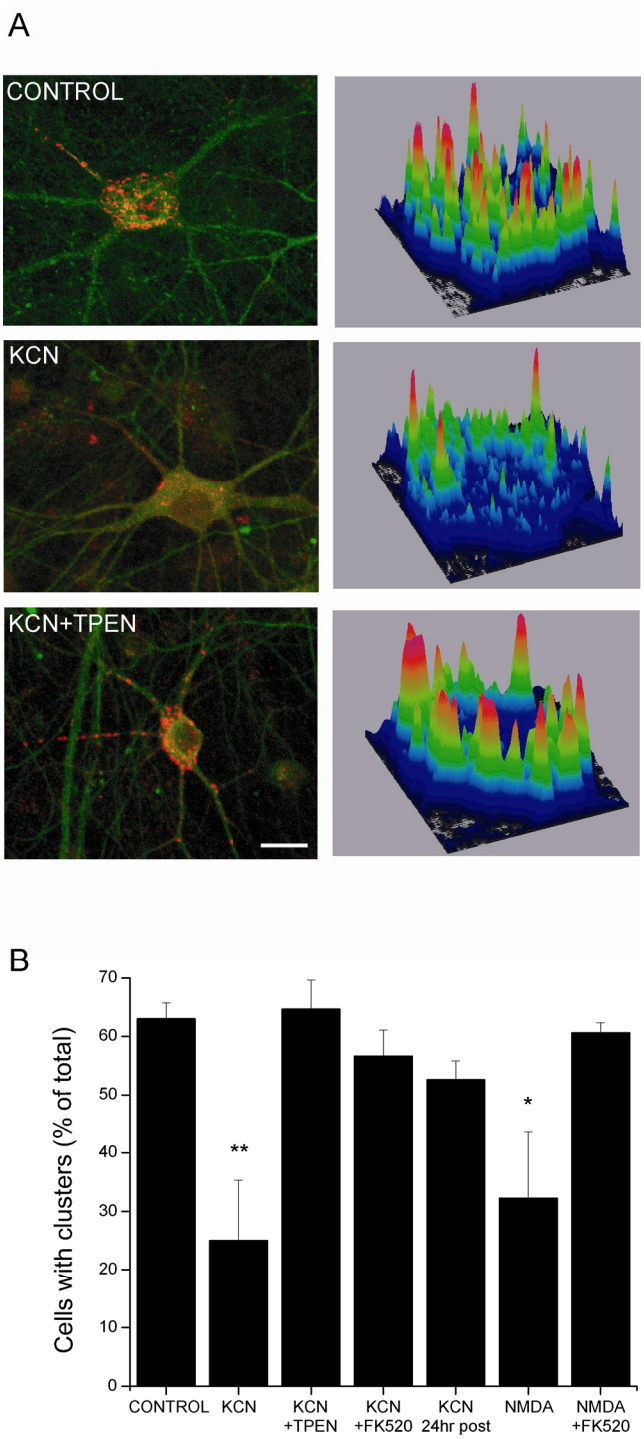

Figure 10 - Zinc is required for the calcineurin-dependent ischemic declustering of Kv2.1 in neurons

Figure 10. (A) Neurons exposed to control or 3mM KCN were fixed and immunostained with anti-Kv2.1 (1:500 red) and anti-MAP2 (1:500 green) antibodies. In KCN treated groups, neurons were fixed immediately or 24 hours following stimulus. Representative neurons and their associated surface maps from each treatment group from 3-4 independent experiments are shown. Background-subtracted neuronal surface maps show relative Kv2.1 staining intensity values plotted along the area of the cell body. Scale bar: 10μm. (B) Neurons were exposed to control, 3mM KCN (90 min), KCN in the presence of 1μM TPEN or 5μM FK520 (90 min), 100μM NMDA with 10μM glycine (10 min), or NMDA/glycine in the presence of 5μM FK520 (10min). Neurons were fixed and immunostained as in A. Fluorescent images were background subtracted and cell surface maps were created to plot Kv2.1 staining intensity over the neuronal soma. Clusters on surface maps appeared as orange-red peaks in pixel intensity. Using these plots, 75-100 cells from 3-4 independent experiments were classified as either clustered or not. Data points represent percentage of cells with clusters compared to total cell counts (mean ± s.e.m.) (*p<0.05; **p<0.01 compared to control; One-way ANOVA-Dunnett).

3.4.4 Zn^{2+} accumulation is not calcineurin-dependent

Both a rise in neuronal free Zn^{2+} and activation of calcineurin are required for the modulation of Kv2.1 following sub-lethal ischemia (Figures 9, 10). To determine the interdependence of these two signaling events, we measured the preconditioning-induced Zn^{2+} rise in the absence and presence of the calcineurin inhibitor. Cortical neurons were loaded with the Zn^{2+}-selective indicator, FluoZin-3 (5μM, 30 min) and imaged using live-cell wide-field microscopy. Intracellular TPEN-sensitive Zn^{2+} fluorescence rose significantly in neurons exposed to sub-lethal chemical ischemia (Figure 11), as previously reported (Aras et al., 2009). This KCN-induced increase in neuronal Zn^{2+} remained relatively unchanged in the presence of the calcineurin inhibitor, FK520 (5μM; Figure 11). These data suggest that the rise in neuronal Zn^{2+} occurs independently of, or is upstream of, calcineurin activity following preconditioning.

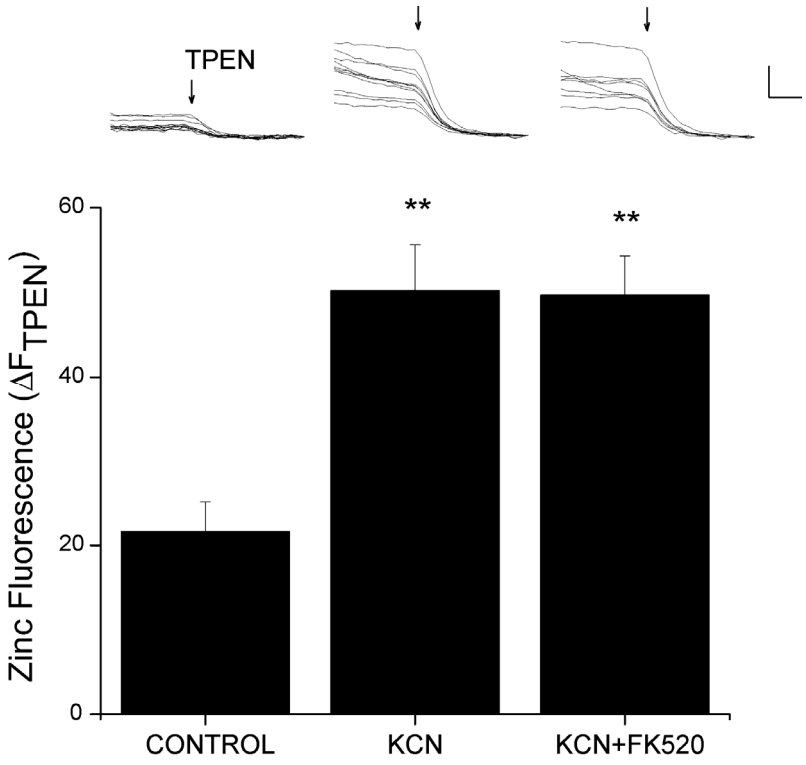

Figure 11 - Chemical ischemia induces a calcineurin-independent zinc rise

Figure 11. Cortical neurons were exposed to control or 3mM KCN in the absence or presence of 5μM FK520. Representative fluorescence traces of several neurons in a single coverslip from each treatment groups are shown above corresponding bar from bar graph. Arrow depicts the beginning of superfusion with 20μM TPEN to chelate Zn^{2+} and quench fluorescence. Calibration: 50 arbitrary fluorescence units, 50 s. Bar graph represents mean (± s.e.m.) ΔF_{TPEN} measurements from 8-15 coverslips, each containing 10-25 neurons (**p<0.01 compared to control; One-way ANOVA-Dunnett).

3.5 DISCUSSION

Previous reports have shown ischemic modulation of Kv2.1 critically depends on a rise in intracellular Ca^{2+} and on the protein serine/threonine phosphatase calcineurin (Misonou *et al.*, 2005). In the present study, we found a novel role for Zn^{2+} in mediating the modulation of Kv2.1 channel activity following sub-lethal ischemic injury. We first confirmed that sub-lethal chemical ischemia in cortical neurons leads to a hyperpolarizing shift in the voltage-dependent activation of neuronal I_k and associated reduction in molecular weight of total Kv2.1 protein, reflecting a dephosphorylation of the channel. Changes in the voltage-dependency and phosphorylation state of Kv2.1 following sub-lethal ischemia in hippocampal neurons are transient, and recover shortly following stimulus cessation (Misonou et al., 2005). In cortical neurons, we found that the ischemia-induced changes only partially recovered to baseline conditions 24 hours following KCN cessation. The difference in recovery between the two studies may simply be due to the differences in cellular model system (hippocampal neurons versus mixed cortical culture) or stimulus duration (15 min versus 90 min chemical ischemia). Importantly, however, KCN induced sub-lethal ischemia led to characteristic changes in Kv2.1 activity and phosphorylation previously described following ischemia (Misonou et al., 2005).

A rise in neuronal Zn^{2+}, likely mediated by a combination of Zn^{2+} translocation from presynaptic vesicles (Koh et al., 1996) and Zn^{2+} liberation from intracellular stores (Aizenman et al., 2000b), can trigger neurodegenerative signaling following ischemia (Frederickson et al., 2005). However, early rises in neuronal Zn^{2+} have also been reported to be required for neuroprotection following sub-lethal ischemia in both *in vivo* and *in vitro* models (Lee et al., 2008; Aras et al., 2009). Sub-lethal ischemic insults can precondition neurons by activating

endogenous protective mechanisms that render cells tolerant to subsequent lethal ischemic injury (Kitagawa et al., 1990; Gidday, 2006). Neuronal Zn^{2+} accumulation following sub-lethal ischemia was necessary and sufficient for inducing tolerance in multiple preconditioning models (Lee et al., 2008; Aras et al., 2009). Thus, in contrast to Zn^{2+} accumulation in the acute phase of lethal ischemia, an early Zn^{2+} rise following sub-lethal ischemia triggers cell survival cascades. One such adaptive survival cascade may involve the modulation of K^+ channel kinetics: transient increases in overall K^+ current can hyperpolarize neurons limiting neuronal excitability following ischemia. The delayed rectifier Kv2.1 channel, similar to other K^+ channels that are modulated in response to changes in the metabolic state (K_{ATP} channels) or $[Ca]_i$ (Ca^{2+}-activated BK channels), can play an important role in limiting excitability following ischemia (Du et al., 2000; Misonou et al., 2005). In light of the critical role of Zn^{2+} in mediating neuroprotection, we hypothesized that the ischemic change in K^+ channel activation kinetics may also be Zn^{2+} dependent. While a role for Ca^{2+} and calcineurin in the modulation of Kv2.1 channel activation following ischemia has been described (Misonou et al., 2005), recent evidence has shown that a Zn^{2+} rise occurs immediately upon onset of ischemia and even precedes, and may contribute to, Ca^{2+} deregulation (Stork and Li, 2006; Medvedeva et al., 2009). Indeed, we found that the cell-permeable Zn^{2+} chelator, TPEN, significantly attenuated the hyperpolarizing shift in the voltage-dependent activation of I_k to the same extent as calcineurin inhibition. Further, we found that the Zn^{2+} rise was not altered by calcineurin inhibition, suggesting that the early Zn^{2+} rise may precede Ca^{2+}-dependent calcineurin activation or perhaps occur concurrently. Thus, Zn^{2+} plays a critical early role in the modulation of K^+ channel kinetics following ischemia.

Kv2.1 channels are localized to large clusters found over the soma and proximal dendrites of cortical neurons (Trimmer, 1991). The assembly of Kv2.1 into large surface clusters restricted to the cell body and proximal dendrites of neurons is likely mediated by a proximal restriction and clustering (PRC) domain located within the last 318 amino acids of the intracellular C terminus (Lim et al., 2000; Mohapatra and Trimmer, 2006). The cellular components involved in cluster maintenance are currently an intense line of investigation. For example, an actin cytoskeleton-based dynamic perimeter fence may regulate cluster size and localization (O'Connell et al., 2006). Remarkably, although clusters themselves exhibit little lateral mobility, single Kv2.1 channels are mobile within and even between clusters (Tamkun et al., 2007), arguing against the presence of a sustained physical association between Kv2.1 and a scaffolding protein. Tamkun and co-workers propose a model in which retention proteins interact with the Kv2.1 C terminus, perhaps in a phospho-dependent manner, to maintain individual channels from crossing the perimeter fence (O'Connell et al., 2006). While the role of Zn^{2+} in individual Kv2.1 channel mobility is not clear, the liberation of neuronal Zn^{2+} from intracellular stores has been shown to be an important upstream signaling event in the phospho-dependent surface delivery of new Kv2.1 channels in apoptosis (McLaughlin et al., 2001; Pal et al., 2003; Redman et al., 2007). The results presented here suggest that neuronal Zn^{2+} may also regulate existing Kv2.1 cluster activity and localization following ischemia. The functional significance of maintaining Kv2.1 channels in clusters also remains unclear. A recent report by Misonou and colleagues suggest that Kv2.1 clusters are strategically situated at junctions between astrocytic and neuronal membranes to achieve rapid modulation following ischemia (Misonou et al., 2008). The authors speculate that glutamate accumulation in the extracellular space following ischemia may activate ionotropic glutamate receptors, leading to elevated

$[Ca^{2+}]_i$, calcineurin activation, and modulation of Kv2.1 (Misonou et al., 2008). Here, we provide evidence for an additional signaling event, the calcineurin-independent transient rise in neuronal Zn^{2+}, in mediating the dispersal of channel clusters following ischemia. Thus, a rise in Zn^{2+}, along with Ca^{2+} may be necessary for modulation of Kv2.1 following ischemia.

Finally, although both altered kinetics and localization of Kv2.1 following chemical ischemia were dependent on calcineurin, we observed that the Zn^{2+} rise occurred even in the presence of calcineurin inhibition. Calcineurin is a protein serine/threonine phosphatase that is regulated by Ca^{2+}- and calmodulin-binding (King and Huang, 1984). In addition, calcineurin is a Fe^{2+}- and Zn^{2+}- metalloenzyme containing both metals in its catalytic domain, which are required for full phosphatase activity (Goldberg et al., 1995). Along these lines, Zn^{2+} chelation by TPEN may prevent full calcineurin activation following ischemia, preventing Kv2.1 modulation. It should be noted that, like many phosphatases, calcineurin activity can be inhibited with excess exogenous Zn^{2+} in *in vitro* assays (Takahashi et al., 2003; Huang et al., 2008a). In light of this, direct modulation of calcineurin by Zn^{2+} is not likely. Instead, Zn^{2+} may either be necessary for full calcineurin activation following ischemic injury or may mediate a parallel signaling pathway leading to Kv2.1 modulation.

The data presented here strongly implicate a rise in free neuronal Zn^{2+} in the modulation of Kv2.1 channel activity and localization following ischemia. This study represents an intersection of emerging evidence implicating Zn^{2+} in triggering neuroprotective mechanisms and Kv2.1 modulation in limiting neuronal excitability following ischemia.

4.0 GENERAL DISCUSSION

The goal of this dissertation was to investigate the role of Zn^{2+} in endogenous signaling pathways that contribute to neuronal tolerance. Until now, the intracellular accumulation of free Zn^{2+} has been largely identified as a characteristic of degenerating neurons. However, sub-lethal activation of cell death molecules can trigger important survival mechanisms that protect neurons from lethal injury mediated by those same factors. Data presented here show that sub-lethal Zn^{2+} signals are necessary and sufficient for limiting subsequent Zn^{2+}-dependent neuronal injury. Intracellular Zn^{2+} release, facilitated by PKC modulation of MT, activated Zn^{2+}-regulated gene expression and conferred long term neuronal tolerance. Additionally, Zn^{2+} was required for the modulation of Kv2.1 activity and localization following sub-lethal ischemic injury, suggesting that the metal plays a role in mediating acute cellular responses to stress. Together, these findings critically implicate Zn^{2+} signals in the adaptive neuroprotective response to cellular injury. In this final chapter, I will discuss potential mechanisms of Zn^{2+}-mediated neuroprotection and highlight important questions that remain in our understanding of neuronal tolerance.

4.1 A DUAL ROLE FOR NEURONAL MT III

Metallothioneins contain 20 sulfur-donating cysteine residues that bind seven Zn^{2+} ions in Zn_3S_9 and Zn_4S_{11} configurations on its two metal-binding domains (Maret and Vallee, 1998). In order for MTs to buffer cellular free Zn^{2+}, these high-affinity ligands for Zn^{2+} must not be saturated with metal under normal conditions. Indeed, biochemical analysis revealed that three of the Zn^{2+}-binding sites on MT bind Zn^{2+} with low or intermediate affinity, suggesting that under normal conditions MT may not be saturated with all seven Zn^{2+} ions (Krezel and Maret, 2007). In addition, differential fluorescent labeling of the MT cysteine clusters from rat kidney, liver, and brain tissue extracts showed that tissues contain almost as much of the apo-protein thionein as metal-bound metallothionein (Yang et al., 2001). Thus, the Zn^{2+} buffering capacity of MTs is very high under control conditions and is critically dependent on the amount of Zn^{2+}-lacking thionein and unsaturated species of MT in cells. To examine the Zn^{2+}-buffering capacity of neurons, I measured the change in intracellular free Zn^{2+} following exposure to Cd^{2+} using a MRE-luciferase reporter. Any free Zn^{2+} released from MT by Cd^{2+} (Zhang et al., 2003) that is not immediately buffered will trigger luciferase expression. I found that MT III-overexpressing neurons have diminished MRE activation compared to vector-expressing neurons following Cd^{2+} exposure (Figure 7). This result suggests that transfected neurons actually overexpress metal-deficient forms of MT and thus have a surplus of available binding sites for buffering the rise in free Zn^{2+} caused by Cd^{2+} exposure. Importantly, when the expression of endogenous neuronal MT III was reduced by an MT3shRNA construct, I found that intracellular free Zn^{2+} was elevated following the Cd^{2+} stimulus compared to vector-expressing neurons (Figure 7). Thus, depletion of endogenous MT III impairs the Zn^{2+}-buffering capacity of neurons and allows increased levels of free Zn^{2+} to activate MRE gene transcription. This result is significant

because it suggests that under normal conditions, the Zn^{2+} binding capacity of neurons is high due to the presence of Zn^{2+}-deficient MT III molecules. Thus, because of the presence of Zn^{2+}-lacking species along with apo-thionein, MT III serves a significant role in buffering neuronal free Zn^{2+}.

On the other hand, MT III may also be a significant source of labile Zn^{2+} in neurons. The unique coordination environment of MT, consisting of sulfur-containing cysteines that can undergo reversible redox reactions, allows the cellular availability of Zn^{2+} to be closely tied to the redox environment of the cell (Maret and Vallee, 1998). In HT-29 cells, it was found that as the intracellular redox potential became more oxidizing, the buffering capacity of MT was lowered, leading to a pronounced elevation in free Zn^{2+} (Krezel and Maret, 2006; Krezel et al., 2007). Oxidant-induced liberation of Zn^{2+} from MT has been demonstrated in cell-free systems (Maret and Vallee, 1998) and in cortical neurons (Aizenman et al., 2000b; Zhang et al., 2004). In mouse hepatoma (Hepa) cells, exposure of oxidants H_2O_2 or tert-butylhydroquinone sufficiently activated MRE-binding by MTF-1 (Andrews, 2000). Nitric oxide can also liberate Zn^{2+} from MT from neurons in vivo (Cuajungco and Lees, 1998) and in pulmonary artery endothelial cells, which effectively activates MTF-1 and transcription of MT (St Croix et al., 2002; Spahl et al., 2003; Stitt et al., 2006). Nitrosylation can occur by transnitrosation, a transfer of NO from N-nitrosothiols to the sulfur donor of Zn^{2+} ligands (Chen et al., 2002). Other redox signals including superoxide/peroxide, selenium compounds, and NADPH have also been shown to release Zn^{2+} from MT (Fliss and Menard, 1992; Maret, 1994; Jacob et al., 1999; Chen and Maret, 2001; Stoyanovsky et al., 2005; Sagher et al., 2006). Thus, because of its susceptibility to redox signaling, MT is a significant source of labile Zn^{2+}.

While oxidative- and nitrosative-stress mediated liberation of neuronal Zn^{2+} has been previously described as a characteristic of cell death (Aizenman et al., 2000; Bossy-Wetzel et al., 2004), a similar mechanism may account for the Zn^{2+} signal in preconditioned neurons. Indeed, sub-lethal oxidative signaling has been shown to be required for tolerance in several models of preconditioning (Pain et al., 2000; Forbes et al., 2001), including KCN-induced excitotoxic tolerance used in this dissertation (McLaughlin et al., 2003). In preconditioned neurons, sub-lethal reative oxygen species generation can modify redox-sensitive protein kinases, phosphatases, or redox-sensitive transcription factors, such as nuclear factor-κB and activator protein-1, modulating gene expression and conferring neuronal tolerance (Perez-Pinzon et al., 2005). Similarly, NO generation, triggered by the influx of Ca^{2+} through NMDA receptors, has been shown to play a central role in preconditioning signal transduction by activating downstream kinases that ultimately modulate gene transcription (Gonzalez-Zulueta et al., 2000). Thus, multiple redox signals known to trigger Zn^{2+} release from MT are activated in preconditioned neurons. Evidence presented in this dissertation suggests that the predominant source of the preconditioning-induced Zn^{2+} rise is intracellular, as both tricine and the AMPA receptor blocker CNQX had little effect on KCN-induced increase in FluoZin-3 fluorescence (Figure 6). Thus, it is likely that the preconditioning-induced Zn^{2+} signal is mediated by the redox modulation of the MT/Zn^{2+} interaction.

While intracellular MTs represent a major source for labile Zn^{2+}, it is also conceivable that other Zn^{2+} bound proteins are susceptible to oxidant-induced Zn^{2+} liberation. Indeed, PKC, which contains a cysteine-rich Zn^{2+}-finger motif in the regulatory C1 region, has been shown to release Zn^{2+} in the presence of thiol oxidants, leading to auto-activation of the enzyme (Knapp

and Klann, 2000). Under these conditions, oxidant-induced Zn^{2+} release occurred prior to PKC activation. In contrast, I found that inhibiting PKC activity attenuated KCN-induced Zn^{2+} accumulation (Figure 6), suggesting that PKC is activated prior to the Zn^{2+} rise in preconditioned neurons. The PKC inhibitors used in the present studies compete with ATP at the PKC catalytic domain (Martiny-Baron et al., 1993) and thus, would not be expected to block potential Zn^{2+} release from the regulatory C1 region. The results presented here support an indirect relationship between PKC and the preconditioning-induced Zn^{2+} rise. PKC may interact with a source of labile Zn^{2+}, promoting an increase in the intracellular concentration of the metal. To this end, I found evidence for a novel role for PKC in modulating the MT/Zn^{2+} interaction to facilitate Zn^{2+} release from the metal-binding protein. I identified a highly conserved, putative PKC phosphorylation site on MT at serine 32 (S32). S32 is located in the linker region of MT between the two metal-binding domains containing the Zn^{2+}/thiolate clusters. Mutation of S32 to a non-phosphorylatable alanine (S32A) prevented the increase in PKC-dependent serine phosphorylation of MT, attenuated metal-stimulated activation of the MRE, and diminished the neuroprotective effect of preconditioning (Figure 7). However, in fluorescence resonance energy transfer (FRET)-based cell-free biochemical studies, the mutation of S32 to a cysteine residue or a fluorophore did not alter the overall structure of the protein, or its ability to bind Cd^{2+} (Hong and Maret, 2003). The effect of mutating S32 on the Zn^{2+}-binding properties of cellular MT was not examined (Hong and Maret, 2003). In the functional assays presented here, I found that modulation of S32 to a non-phosphorylatable alanine or a phospho-mimicking aspartic acid had a significant impact on neuronal free Zn^{2+} and Zn^{2+}-regualated gene expression. Thus, phosphorylation of MT on residue S32 by PKC may prevent efficient binding of Zn^{2+}, allowing for enhanced Zn^{2+} regulated gene expression and neuroprotection. Together, these data strongly

suggest that MT III plays a dual role in regulating neuronal free Zn^{2+} homeostasis. Depending on the availability of unoccupied Zn^{2+} binding sites as well as the intracellular redox environment, MT III can serve as an important buffer for, and source of, neuronal free Zn^{2+}. Another major implication of these studies is that signaling kinases can serve as regulating factors in neuronal Zn^{2+} homeostasis. Thus, other protein kinases, besides PKC, or protein phosphatases may interact with MT, ultimately regulating neuronal free Zn^{2+} and cell viability.

4.2 ZINC AND CALCIUM SIGNALS IN PRECONDITIONED NEURONS

Preconditioning triggers a transient increase in neuronal free Zn^{2+}, which is both necessary and sufficient to confer tolerance against subsequent Zn^{2+}-mediated injury (Figures 2, 3; Lee et al., 2008). Like the Zn^{2+} rise described here, an accumulation of Ca^{2+} has also been shown to play an important role in the initiation of survival pathways in preconditioned neurons. In models of cerebral tolerance, removing extracellular and cytoplasmic Ca^{2+} or preventing its influx through NMDA receptors by MK-801 [(+)-5-methyl-10,11-dihydro-5H-dibenzo [a,d] cyclohepten-5,10-imine maleate] severely attenuated neuroprotection (Kato et al., 1992; Kasischke et al., 1996; Grabb and Choi, 1999; Raval et al., 2003). The neuroprotective signal transduction pathway has been shown to stimulate Ca^{2+}-dependent enzymes, including PKC (Raval et al., 2003) and nitic oxide synthase (NOS; Nandagopal et al., 2001). While PKC and NOS activation in preconditioned neurons required NMDA receptor-dependent Ca^{2+} influx, downstream targets for these enzymes may ultimately regulate intracellular [Zn^{2+}]. Here, I show that PKC can directly interact with MT and may play a significant role in promoting Zn^{2+} release from the metal binding protein (Figure 7). Furthermore, NO, produced by the activation of NOS, can readily

trigger the release of Zn^{2+} from MT (Cuajungco and Lees, 1998). Thus, the influx of Ca^{2+} may actually contribute to the accumulation of free Zn^{2+} in preconditioned neurons, mediated by the activation of Ca^{2+}-dependent enzymes.

Another Ca^{2+}-dependent enzyme that has been implicated in mediating neuroprotection following ischemic injury is protein phosphatase 2B (PP2B or calcineurin). Rather than mediating delayed neuronal tolerance via activation of protein synthesis, calcineurin may play a central role in the acute cellular response to injury. Following sub-lethal ischemic injury, an increase in $[Ca^{2+}]_i$, mediated by release from intracellular stores, led to the activation of calcineurin and the modulation of the delayed rectifier potassium channel Kv2.1 (Misonou et al., 2005). Specifically, sub-lethal ischemia led to calcineurin-dependent dephosphorylation of Kv2.1, which was accompanied by dispersal of surface clusters and a shift in the voltage-dependent activation of neuronal potassium current (Misonou et al., 2005). In turn, these altered Kv2.1 channel properties are thought to protect neurons against sustained hyperexcitability, limiting ischemic cell death (Surmeier and Foehring, 2004). While stimulation of calcineurin activity may require Ca^{2+}, I found that chelation of Zn^{2+} during sub-lethal ischemia partially blocked the hyperpolarizing shifts in the activation kinetics as well as prevented Kv2.1 declustering (Figures 9, 10). Ischemia-induced Zn^{2+} accumulation was not prevented by a calcineurin inhibitor (Figure 11), suggesting that the Zn^{2+} rise may be upstream of, or independent of, calcineurin activity. Alternatively, Zn^{2+} chelation with TPEN may have sequestered the metal from the catalytic domain of calcineurin (Goldberg et al., 1995), preventing full enzymatic activity. The exact role of Zn^{2+} in modulating calcineurin activity,

whether direct or indirect, remains unclear. Regardless, these data provide another example of the convergence of Zn^{2+} and Ca^{2+} mediated signaling pathways in neuroprotection.

While it is clear that both Zn^{2+} and Ca^{2+} can accumulate in preconditioned neurons and trigger converging neuroprotective signaling cascades, the exact roles of the two cations in neuronal tolerance needs to be delineated. Indeed, determination of the contribution of Zn^{2+} versus Ca^{2+} signaling has been an area of intense investigation in models of neuronal injury. Careful examination of indicators traditionally used to detect changes in cellular [Ca^{2+}] revealed that they actually respond with higher affinity to Zn^{2+} (Stork and Li, 2006). Live cell detection of free Zn^{2+} has only become feasible through recent developments of Zn^{2+} sensitive and selective fluorophores (Gee et al., 2002; Thompson et al., 2002). By loading neurons with a low-affinity ratiometric Ca^{2+}-sensitive indicator (e.g., Fura-2FF) and a high-affinity Zn^{2+}-sensitive indicator (e.g., FluoZin-3), Devinney and colleagues (2005) provided a novel method for simultaneous detection of both divalent cations in living cells. Using this approach, Dineley and colleagues (2008) examined changes in free Zn^{2+} following extracellular glutamate stimulation in cortical neurons in culture. They found that the glutamate-induced release of intracellular Zn^{2+} was dependent on an influx of extracellular Ca^{2+} and subsequent production of reactive oxygen species (Dineley et al., 2008). On the other hand, in acute hippocampal slices loaded with both Zn^{2+} and Ca^{2+} indicators, oxygen-glucose deprivation (OGD) led to a progressive increase in neuronal Zn^{2+} (5-10 min following OGD onset), which preceded and may have contributed to Ca^{2+} deregulation (Medvedeva et al., 2009). As brief exposure to OGD is a prototypical preconditioning stimulus (Grabb and Choi, 1999), a similar temporal profile between Zn^{2+} and Ca^{2+} accumulation may exist in KCN preconditioned neurons. A Zn^{2+} rise

prior to Ca^{2+} deregulation was also observed in a model of spreading depression in hippocampal slices (Dietz et al., 2008). This Zn^{2+} rise was largely attributed to extracellular Zn^{2+} entry through L-type Ca^{2+} channels (Dietz et al., 2008). Thus, simultaneous detection of $[Zn^{2+}]$ and $[Ca^{2+}]$ using the dual dye approach provides great insight into how these two divalent cations respond to cellular changes. Similar to injury paradigms, neuroprotective pathways also involve critical contributions from, and intersection of, Zn^{2+} and Ca^{2+} signals.

4.3 ZINC-REGULATED GENE ACTIVATION IN NEURONAL TOLERANCE

One of the hallmark characteristics of delayed neuronal tolerance is its dependence on *de novo* protein synthesis elicited by the preconditioning stimulus (Barone et al., 1998). However, the genomic response to preconditioning may not simply involve an immediate activation of quiescent survival genes. Instead, DNA oligonucleotide microarray analysis has shown that a large number of genes may be repressed following preconditioning (Stenzel-Poore et al., 2003). Nevertheless, protein synthesis inhibition by cyclohexamide prior to, or during preconditioning blocks neuronal tolerance *in vivo* and *in vitro* (Barone et al., 1998; McLaughlin et al., 2003), suggesting a major role for gene activation and protein synthesis in neuroprotection. Changes in gene expression/repression may occur along several temporal profiles. Some genes are altered within minutes or hours (e.g., adenosine A_{2a} receptor, vascular endothelial growth factor), whereas others are affected days following the preconditioning stimulus (e.g., calbindin, serine/threonine protein kinases; Bernaudin et al., 2002a; Tang et al., 2006). Thus, the highly regulated modulation of gene expression in preconditioned neurons is an important cellular response that may ultimately confer neuronal tolerance.

In this dissertation, I found evidence suggesting that a preconditioning-induced Zn^{2+} rise triggers the activation of processes that can prevent subsequent toxic Zn^{2+} accumulations (Figure 3). Interestingly, Matsushita and colleagues (1996) reported that exogenous $ZnCl_2$ pretreatment reduced neuronal death following *in vivo* global ischemia when Zn^{2+} was administered 24 and 48 hours, but not one hour, prior to ischemia. In light of the requirement of new protein synthesis in neuronal tolerance, and that proteins involved in buffering free Zn^{2+} are regulated at the level of transcription, it is likely that preconditioning triggers the upregulation of proteins involved in maintaining cellular Zn^{2+} homeostasis. To this end, I found that KCN preconditioning sufficiently activates the MRE in transfected cortical neurons (Figure 5), suggesting that Zn^{2+} regulated gene expression can be stimulated in preconditioned cells. Thus, the Zn^{2+}-induced upregulation of Zn^{2+}-regulated proteins, such as MT I/II and ZnT1, may play a role in neuronal tolerance.

Indeed, upregulation of MT I and II have been shown in multiple models of preconditioning (Bernaudin et al., 2002a; Carmel et al., 2004; Dhodda et al., 2004; Tang et al., 2006). A two-fold induction of MT I/II mRNA can be detected as early as three hours following preconditioning, peaking at 12 hours with a 6-fold change in expression, and returning to baseline levels 24 hours following preconditioning (Carmel et al., 2004; Dhodda et al., 2004). The upregulation of MT I/II expression as a general mechanism mediating neuroprotection from lethal injury has received some attention. The induction of MT by application of transition metals protects the heart against oxidative damage (Satoh et al., 1988) and cortical cells against irradiation damage (Cai et al., 2000). Mice overexpressing MT I have reduced lesion volume and sensorimotor deficits following in vivo ischemia compared to wild-type mice (van Lookeren

Campagne et al., 1999). On the other hand, mice lacking MT I/II suffer worse outcomes compared to wild-type mice following a range of CNS injuries, including focal cryolesion (Penkowa et al., 1999), experimental autoimmune encephalomyelitis (an experimental model of multiple sclerosis; Penkowa and Hidalgo, 2001), motor neuron disease, (Puttaparthi et al., 2002), and stroke (Trendelenburg et al., 2002). MT I/II double knockout mice had approximately three-fold larger infarcts and significantly worse neurological outcome than wild-type mice following transient ischemia (Trendelenburg et al., 2002). Along these lines, I found that neurons overexpressing MT III were more resistant to NMDA excitotoxicity compared to vector-expressing neurons (Figure 2). Thus, MT plays an important neuroprotective role in response to cellular injury.

Despite the abundance of data describing the upregulation of MTs in limiting neuronal injury, the inducible isoforms MT I and II are predominantly expressed in astrocytes (Hidalgo et al., 1994; Kramer et al., 1996b; Kramer et al., 1996a; Suzuki et al., 2000). Thus, if MT I/II buffer lethal neuronal free Zn^{2+} in models of neuronal tolerance, then brain astrocytes must respond to preconditioning by upregulating MT I/II and secreting it into the extracellular space. In fact, accumulating evidence has supported the injury-induced secretion of astrocytic MT (Chung et al., 2008), the presence of MT in the extracellular space (Chung and West, 2004), and a potential receptor that may mediate MT uptake in neurons (Ambjorn et al., 2008). However, in response to brain injury, extracellular MT has been only shown to promote axonal regeneration and neurite outgrowth (Chung et al., 2008). It is conceivable that, in addition to its effects on neuronal proliferation, secreted MT could also chelate Zn^{2+} released into the extracellular space from injured neurons. By chelating extracellular Zn^{2+}, MT may be able to indirectly reduce

$[Zn^{2+}]_i$. In addition, the internalization of astrocytic MT by neurons (Chung et al., 2008) may directly buffer lethal Zn^{2+} accumulations. Thus, the recently described extracellular actions of MT I/II may provide exciting new potential neuroprotective mechanisms.

A more likely target of preconditioning-induced Zn^{2+}-regulated gene expression may be neuronal ZnT1. ZnT1 expression has been found in neurons (Tsuda et al., 1997) and can be induced by Zn^{2+} in an MTF-1 dependent pathway (Andrews, 2000; Langmade et al., 2000). ZnT1 facilitates Zn^{2+} efflux (Palmiter and Findley, 1995, but also see Ohana et al., 2006), and may actually be more efficient than MTs in regulating intracellular accumulation of Zn^{2+} (Palmiter, 2004). Using in situ hybridization, ZnT1 mRNA expression has been shown to be upregulated in gerbil CA1 pyramidal neurons 12 hours following transient forebrain ischemia (Tsuda et al., 1997). However, not all changes in ZnT1 mRNA have been realized as proportional changes in protein levels (Tsuda et al., 1997; McMahon and Cousins, 1998), indicating possible post-translational regulation of ZnT1 protein expression. It is also unclear whether blocking ZnT1-mediated Zn^{2+} efflux following ischemia exacerbates neuronal injury. Unlike MT, changes in ZnT1 mRNA and protein expression in preconditioned neurons have not been extensively investigated. However, a conceptually similar investigation has been performed in astrocytes (Nolte et al., 2004). In a pure astrocytic culture, sub-lethal exogenous Zn^{2+} exposure induced ZnT1 protein expression and conferred resistance to subsequent lethal Zn^{2+} toxicity (Nolte et al., 2004). Further, in non-preconditioned astrocytes, heterologous expression of ZnT1 reduced toxic intracellular Zn^{2+} accumulations and induced Zn^{2+}-tolerance (Nolte et al., 2004). ZnT1 may play a similar role in neurons. Data presented here show that preconditioning can activate Zn^{2+}-regulated gene expression in neurons and implicate the

upregulation of proteins involved in limiting toxic Zn^{2+} accumulations in tolerant cells. The upregulation of ZnT1 represents an attractive mechanism for mediating Zn^{2+}-induced neuroprotection in preconditioned neurons.

4.4 CONCLUDING REMARKS

Currently, the most effective therapy for ischemic stroke is timely reperfusion. Intravenous administration of human recombinant tissue plasminogen activator (tPA) within three hours of ischemic stroke onset can restore blood flow before major brain damage has occurred (Albers, 2001; Wardlaw et al., 2003). However, thrombolytic drugs must be used with caution, as lethal intracranial bleeding may result. In light of the serious side effects and limited time window of efficacy, it is imperative that alternative therapeutic strategies for ischemic stroke be developed. Over a decade of experimental evidence has described a central role for a toxic accumulation of intracellular Zn^{2+} in ischemic neuronal death. However, the results presented in this dissertation suggest that an increase in neuronal free Zn^{2+} may also trigger pathways that limit cell injury following injury and confer long-term tolerance. I found that the source of the Zn^{2+} rise was largely intracellular, and may be critically influenced by the activity of signaling kinases. Data presented here also suggest that sub-lethal Zn^{2+} signals may have diverse cellular effects, including the activation of gene transcription and the modulation of cellular excitability. Together, the identification of the source of the Zn^{2+} rise and potential downstream targets mediating neuroprotection may provide novel therapeutic targets for regulating intracellular Zn^{2+} signals, and ultimately cell survival. These results provide a new, neuroprotective role for increases in free Zn^{2+} that could aid in the development of future therapies for ischemic stroke.

Appendix A

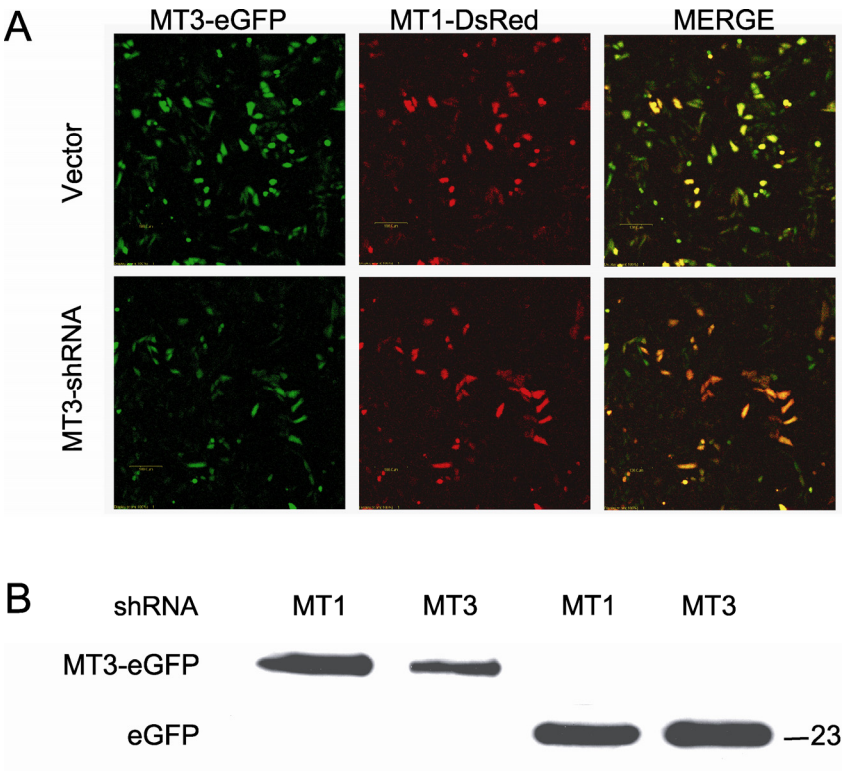

Supplementary Figure 1 – Verification of MT3shRNA construct

Supplementary Figure 1. Verification of MT3shRNA construct. Experiments performed by Hirokazu Hara, Ph.D. (A) CHO cells were plated at a density of 5.6 X 104 cells/well on coverslips in 24-well plates. Twenty-four hours later, CHO cells were transfected with either the parent pSuppressorNeo (vector; top row) or MT3-shRNA targeting plasmid (0.2 μg/well; bottom row), together with both pEGFP-MT3 (0.04 μg/well) and pDsRed-MT1 (0.04 μg/well) for 4 hours in serum-free medium (F12 nutrient medium with 10mM HEPES) with a total of 1.2 μL of Lipofectamine (Invitrogen) and 0.28 μg of DNA per well. Forty-eight hours later, cells were fixed and visualized for EGFP (green) and DsRed (red) fluorescence. Note the suppression of green fluorescence by MT3-shRNA. (B) CHO cells were plated at density of 280,000 cells/well on 6-well plates. Twenty-four hours later, cells were transfected with either MT1-shRNA or MT3-shRNA targeting vectors (1.36 μg/well) together with either pEGFP-MT3 or a plasmid encoding EGFP only (0.04 μg/well). Cell lysate samples were harvested 24 hours post-transfection in lysis buffer [1% Triton X-100, 0.1% SDS, 0.25% Na deoxycholate, 50mM HEPES, 150mM NaCl, protease inhibitor mixture (Roche Diagnostics, Indianapolis, IN), pH 7.5] after two washes with PBS. Cell lysate samples were combined in a 1:1 ratio with reducing sample prep buffer and incubated for 5 min at 100°C to denature proteins before gel electrophoresis. SDS/PAGE was carried out by standard procedures using the Mini Protean 3 System (Bio-Rad, Hercules, CA). Equal amounts of cell lysate (10 μg) were separated by reducing 15% SDS/PAGE gels. Separated protein bands were transferred onto a 0.2 μm nitrocellulose membrane. The membranes were then blocked with 1% BSA in PBS with 0.05% Tween 20 at room temperature for 1 h and probed with a GFP monoclonal primary antibody (Sigma). Blots were then incubated with goat secondary antibody conjugated to HRP (1h, room

temperature) and were visualized with a SuperSignal CL-HRP Substrate System (Pierce Biotechnology, Rockford, IL). Note the decrease in MT3-eGFP signal induced by MT3-shRNA.

Appendix B

OBLIGATORY ROLE OF ASK1 IN THE APOPTOTIC SURGE OF K^+ CURRENTS

Mandar A. Aras and Elias Aizenman

Department of Neurobiology, University of Pittsburgh School of Medicine,

Pittsburgh, PA 15261.

ABSTRACT

Apoptosis signal-regulating kinase 1 (ASK1) is a critical component of mitogen-activated protein kinase signaling pathways leading to cell death in response to cytokines and cellular stress. We use a dominant-negative (DN) form of ASK1 to show that this enzyme is necessary for the delayed surge in neuronal K^+ channel activity, a required step in apoptosis. Furthermore, expression of ASK1 DN also suppresses the apoptotic increase in Kv2.1 currents transiently expressed in Chinese hamster ovary cells. Finally, over-expression of thioredoxin, an inhibitory binding partner of ASK1, is sufficient to halt the apoptotic current surge in neurons. Thus, ASK1 is an obligatory component of the pro-apoptotic modulation of K^+ channels.

INTRODUCTION

Apoptosis signal-regulating kinase 1 (ASK1) is a ubiquitously expressed mammalian mitogen-activated protein (MAP) kinase kinase kinase (MAPKKK) that activates both the p38 and c-JUN NH_2-terminal kinase (JNK) by directly phosphorylating their respective MAPKKs (MKK3/6 for p38 and MKK4/7 for JNK; Matsukawa et al., 2004). ASK1 has been shown to be an important signaling kinase in apoptotic cell death in response to various stimuli, including oxidative stress, tumor necrosis factor, endoplasmic reticulum stress, low-potassium, and amyloid β (Ichijo et al., 1997; Liu et al., 2000; Nishitoh et al., 2002; Tobiume et al., 2002; Yamagishi et al., 2003; Kadowaki et al., 2005). Although ASK1 activation has been repeatedly linked to neuronal apoptosis (Nishitoh et al., 2002; Sarker et al., 2003; Yamagishi et al., 2003; Kadowaki et al., 2005), the specific downstream molecular cascades leading to cell death in these systems have yet to be fully characterized.

Cellular potassium efflux is a common, required feature in many apoptotic programs (Hughes and Cidlowski, 1999; Yu, 2003). In cortical neurons, the loss of intracellular potassium occurs through a delayed surge in voltage-dependent K^+ currents (Yu et al., 1997b) that is mediated by Kv2.1-encoded ion channels (Pal et al., 2003). This increase in K^+ currents can be triggered by classical apoptogens, such as staurosporine, serum deprivation, and amyloid β (Yu et al., 1997b; Yu et al., 1998), as well as by oxidants like 2,2'-dithiodipyridine (DTDP; Aizenman et al., 2000b; McLaughlin et al., 2001) and peroxynitrite (Bossy-Wetzel et al., 2004; Pal et al., 2004). We have previously observed that the apoptotic K^+ current surge is protein synthesis independent and precedes caspase activation (McLaughlin et al., 2001). Importantly,

activation of the MAPK p38 is required for this process as both chemical inhibitors of this enzyme (McLaughlin et al., 2001) and expression of p38 dominant negative (DN) vectors (Bossy-Wetzel et al., 2004; Pal et al., 2004) can completely abolish the increase in K^+ currents.

In addition to ASK1, p38 activation can be induced by other MAPKKK, including transforming growth factor-β-activated kinase 1 (TAK1), mixed-lineage protein kinase 3 (MLK3) and mitogen-activated protein three kinase 1 (MTK1; Zarubin and Han, 2005). Furthermore, it has been reported that p38 can also be activated via a MAPKKK-independent mechanism (Ge et al., 2002). We report here that ASK1 represents the principal, if not the only, upstream signaling MAP kinase linking oxidative injury to the apoptotic increase in Kv2.1-mediated currents in neurons.

MATERIALS AND METHODS

Experiments were performed on cultures of embryonic rat cerebral cortex and on Chinese hamster ovary cells. Cortical cultures were prepared from embryonic day 16 Sprague-Dawley rats and grown on 12 mm glass coverslips as previously described (Hartnett et al., 1997). Pregnant rats were sacrificed with the approval of the University of Pittsburgh School of Medicine and in accordance with National Institutes of Health protocols. Enhanced green fluorescent protein (eGFP) (pCMVIE-eGFP; Clontech, Palo Alto, CA) was used as a marker for positively transfected neurons and was combined with the ASK1 DN or Trx cDNAs (gifts from H. Ichijo, Tokyo, Japan), or vector, at a 1:1 ratio. At DIV19-23, cortical cultures were transfected using Lipofectamine 2000 (Invitrogen, Carlsbad, CA; Pal et al., 2003). Briefly, 1.5 μg of cDNA

was diluted in 50 µl Opti-Mem I medium and combined with 50 µl of Opti-Mem I medium containing 2 µl Lipofectamine 2000. Complexes were allowed to form for 30 min before addition to the cultures. Cortical cells were maintained for 48 hours at 37°C, 5% CO_2 before electrophysiological recordings. Chinese hamster ovary (CHO) cells were seeded at 2.8 x 10^5 cells per well into six well plates 24 hours before transfection. Cells were transfected with a Kv2.1eGFP-myc tagged cDNA plasmid (a gift from E. Levitan, Pittsburgh, PA) and ASK1 DN, or vector, at a 1:1 ratio in serum-free medium with 6 µl of Lipofectamine reagent (Invitrogen), and a total of 1.4 µg of DNA per well. Electrophysiological recordings from eGFP-positive CHO cells were performed 24 hours after transfection. All recordings were performed using the whole-cell configuration of the patch-clamp technique as described previously (McLaughlin et al., 2001). The extracellular solution contained (in mM): 115 NaCl, 2.5 KCl, 2.0 $MgCl_2$, 10 HEPES, 10 D-glucose; pH was adjusted to 7.2 with concentrated KOH; 0.25 µM TTX was added to inhibit voltage gated sodium channels. The intracellular (electrode) solution contained (in mM): 100 K-gluconate, 11 EGTA, 10 KCl, 1 $MgCl_2$, 1 $CaCl_2$ x $2H_2O$, 10 HEPES; pH was adjusted to 7.2 with concentrated KOH; 0.22 mM ATP was added and osmolarity was adjusted to 280 mOsm with sucrose. All measurements were obtained under voltage clamp with an Axopatch 1C amplifier (Axon Instruments, Foster City, CA) and pClamp software (Axon Instruments) using 2 MOhm electrodes. Partial compensation (80%) for series resistance was performed in all instances. Currents were filtered at 2 kHz and digitized at 10 kHz (Digidata; Axon Instruments). Potassium currents were evoked with a series of 80 ms voltage steps from a holding potential of –70mV to 35mV, in 15mV increments. Steady-state amplitudes were measured relative to baseline and normalized to cell capacitance.

Neurons were treated with DTDP (100 μM) for 10 min at 37°C, 5% CO_2, a condition that induces a well-characterized p38-dependent increase in K^+ currents approximately 3 hours later, followed by caspase activation at 5-7 hours and subsequent cell death (McLaughlin et al., 2001; Pal et al., 2003). Kv2.1-expressing CHO cells were co-treated with DTDP (25 μM) and Boc-aspartate-fmk (BAF, 10 μM), a broad-spectrum cysteine protease inhibitor, for 5 min in 37°C, 5% CO_2. Subsequently, CHO cells were maintained in BAF (10 μM) for three hours. We have previously reported that BAF prevents Kv2.1-expressing CHO cells from dying following DTDP exposure (Pal et al., 2003), and here we found the caspase inhibitor necessary to maintain cells sufficiently healthy for successful electrophysiological recordings. All data are expressed as mean ± s.e.m. Current densities were analyzed using one-way ANOVA followed by a Bonferoni Multiple Comparisons Test. P-values less than 0.05 were considered significant.

RESULTS AND DISCUSSION

We expressed an ASK1 DN vector in cortical neurons to investigate the role of this MAPKKK in the delayed apoptotic K^+ current surge. The ASK1 DN vector (ASK1 K709M) is rendered catalytically inactive by a lysine to arginine mutation and has been well characterized in prior studies (Ichijo et al., 1997; Jibiki et al., 2003; Machino et al., 2003; Yamagishi et al., 2003). Control and ASK1 DN-transfected cultures were treated with either vehicle or with 100 μM DTDP for 10 min to induce apoptosis (Aizenman et al., 2000a; McLaughlin et al., 2001; Pal et al., 2003). Electrophysiological recordings were performed from these neurons approximately three hours later, the time it normally takes to observe a pronounced K^+ current surge (McLaughlin et al., 2001). DTDP-treated control neurons had very pronounced K^+ currents,

when compared to vehicle-treated cells (Figs. 1A and 1C), reflecting the dramatic increase in channel activity that accompanies the apoptotic process (Yu et al., 1997b; McLaughlin et al., 2001). In contrast, K^+ currents in ASK1 DN-expressing neurons were essentially identical between the vehicle and DTDP treatment groups (Figs. 1B and 1C), suggesting that this MAPKKK was critical for the apoptotic K^+ current surge. As a positive control, electrophysiological recordings were also performed on DTDP-treated, untransfected neurons from the same coverslip where recordings from ASK1 DN-expressing cells had been obtained. In these untransfected cells, a clear K^+ current enhancement was measured (Figure 1C), confirming that the DTDP treatment had been effective in triggering the apoptotic program in those cultures, and reinforcing the notion that ASK1 was a critical component of the current surge process.

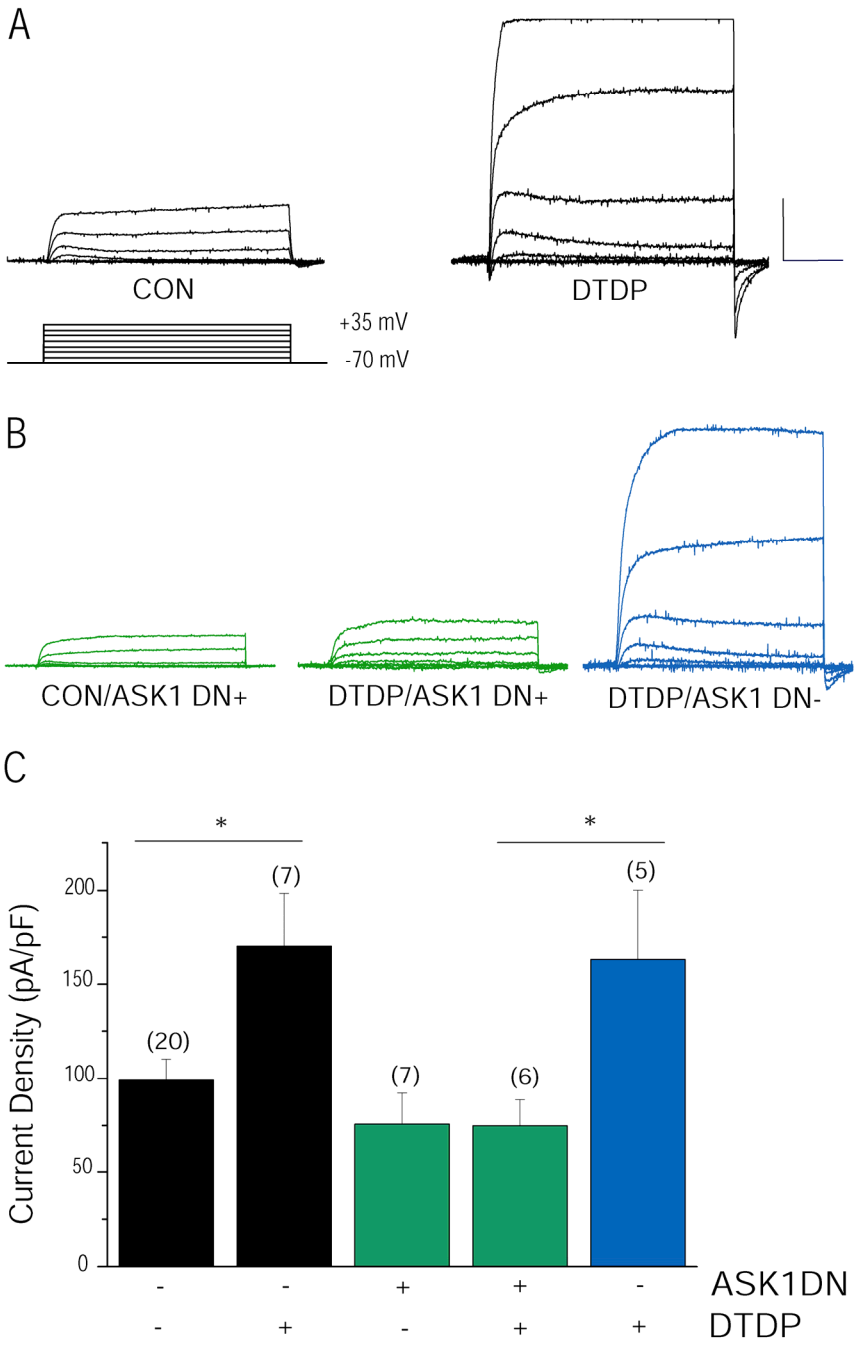
A
CON
DTDP
+35 mV
-70 mV
B
CON/ASK1 DN+
DTDP/ASK1 DN+
DTDP/ASK1 DN-
C
Current Density (pA/pF)
200
150
100
50
0
(20)
(7)
(7)
(6)
(5)
*
*
- - + + -
ASK1DN
- + - + +
DTDP

Figure 1. ASK1 is required for the apoptotic K^+ current surge in cortical neurons. (A) Whole-cell K^+ currents were evoked by a series of voltage steps from –70 mV to +35 mV in 15 mV increments in two representative control neurons exposed to either vehicle (VEH, left) or 2,2'-dithio-dipyridine (DTDP; right, 100 μM for 10 min). Note the substantial difference in current amplitudes between the two treatment groups. Also note that the current evoked by the last voltage step (+35 mV) in the DTDP-treated neuron was beyond the ability of our amplifier to appropriately hold under voltage clamp. Scale bars 5 nA, 20 ms. (B) Similar recordings were performed from ASK1 dominant negative (DN)-expressing neurons exposed to either vehicle (left) or DTDP (middle). Note the lack of an effect of DTDP on K^+ current amplitudes under these circumstances. As a positive control, recordings were also performed from a DTDP-treated untransfected neuron from the same coverslip where the measurement from the ASK DN-expressing cell had been performed (right). The large K^+ currents present in this type of cell confirmed that DTDP had triggered the apoptotic program in the culture dish. (C) Mean ± s.e.m. current densities from vehicle and DTDP treated control (black bars) and ASK1 DN-expressing (green bars) neurons. The blue bar represents the current densities obtained from DTDP-treated untransfected neurons in the same coverslip containing the ASK1 DN-expressing cells. Currents were evoked with a voltage step to +5 mV from a holding potential of –70 mV and normalized to cell capacitance (*p<0.05; ANOVA, Bonferoni). The voltage step to +5 mV was always under adequate voltage clamp.

Functional expression of Kv2.1 in Chinese hamster ovary (CHO) cells was used to firmly establish the role of ASK1 in mediating the apoptotic current surge via the channel known to be responsible for the increase in K^+ currents in neurons (Pal et al., 2003). CHO cells do not express native Kv channels (Yu et al., 1998), but can be rendered susceptible to DTDP-induced apoptosis following the expression of Kv2.1 (Pal et al., 2003). Electrophysiological recordings were performed from control and ASK1 DN-expressing CHO cells 3 hours after a 5 min exposure to vehicle or 25 μM DTDP. K^+ currents in control cells exposed to DTDP were substantially larger than vehicle-treated cells, without a noticeable change in the voltage-dependence of channel activation, which was determined from current-voltage relationships (Figs. 2A and 2C). In contrast, the K^+ currents in ASK1 DN-expressing CHO cells were virtually indistinguishable between the vehicle and DTDP-treated groups (Figs. 2B and 2C). These data indicate that Kv2.1 is a downstream target of the apoptotic pathway triggered by ASK1 activation, even in cells that do not normally express the channel. This strongly suggests that a fairly direct and ubiquitous pathway exists between the downstream signaling cascades activated by ASK1 and the mechanism responsible for the enhanced currents mediated by Kv2.1.

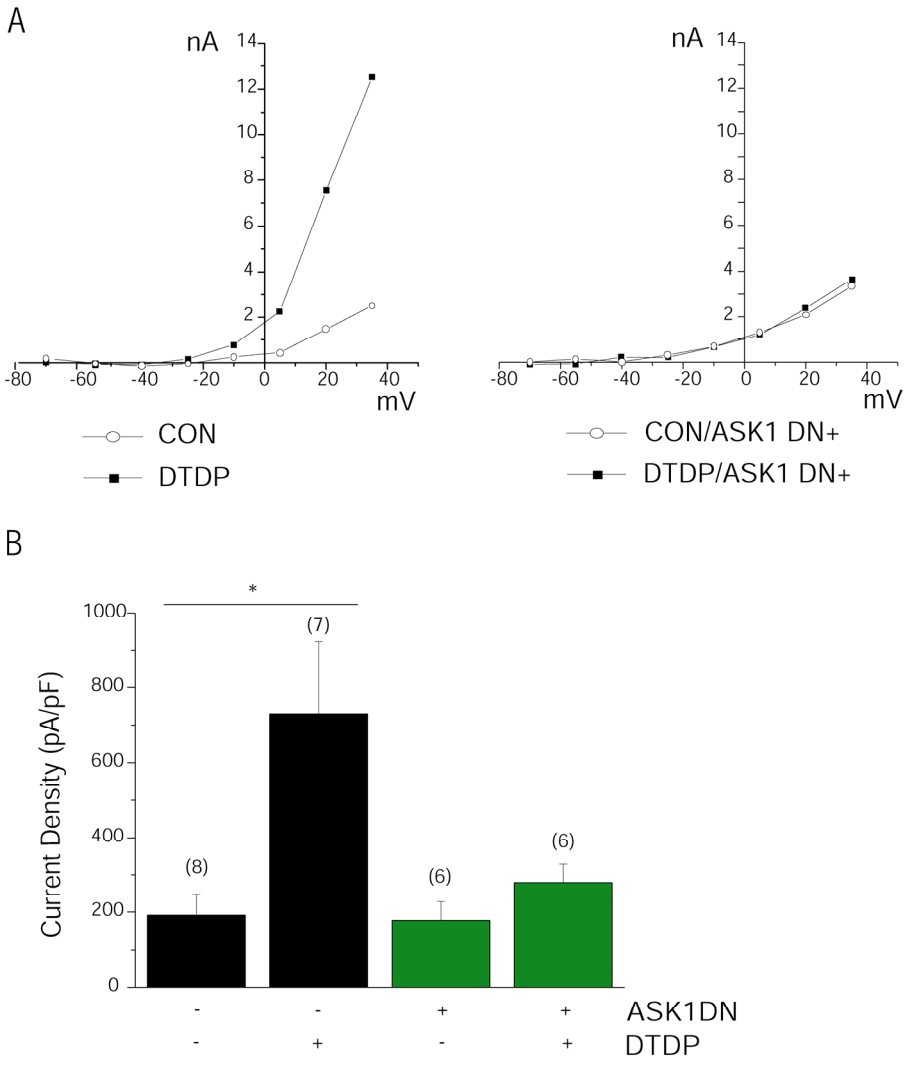
A
nA
14
12
10
8
6
4
2
-80
-60
-40
-20
0
20
40
mV
CON
DTDP
nA
14
12
10
8
6
4
2
-80
-60
-40
-20
0
20
40
mV
CON/ASK1 DN+
DTDP/ASK1 DN+
B
*
1000
800
600
400
200
0
Current Density (pA/pF)
(8)
(7)
(6)
(6)
- - + + ASK1DN
- + - + DTDP

Figure 2. Apoptotic increase in Kv2.1 currents in Chinese hamster ovary (CHO) cells requires ASK1. **(**A**)** Current-voltage (I-V) relationships of K^+ currents evoked by a series of voltage steps from –70 mV to +35 mV in 15 mV in 2 representative Kv2.1-expressing CHO cells exposed to either vehicle (circles) or DTDP (25 μM, 5 min; black squares). Note the increase in the current amplitude in the DTDP-treated cell, without a change in the voltage-dependence of activation. (B) Similar measurements were performed in ASK1 DN-expressing CHO cells exposed to either vehicle (circles) or DTDP (black squares). Note the virtually indistinguishable I-V curves between the two representative cells. (C) Mean ± s.e.m. Kv2.1-mediated current densities from vehicle and DTDP treated control (black bars) and ASK1 DN-expressing (green bars) CHO cells. Currents were evoked with a voltage step to +5 mV from a holding potential of –70 mV and normalized to cell capacitance (*p<0.05; ANOVA, Bonferoni.)

In non-stressed cells, ASK1 is bound at its N-terminal region to thioredoxin (Trx) via a protein-protein interaction, deeming the kinase inactive. Trx is a redox-regulatory protein containing two sulfhydryl groups near its catalytic center. Under cell stress, reactive oxygen species can oxidize these sulfhydryl groups, inducing the release of ASK1, which becomes activated following oligomerization and autophosphorylation (Saitoh et al., 1998; Liu and Min, 2002). We have previously observed that a free-radical spin trap can inhibit DTDP-mediated activation of p38 in neurons (McLaughlin et al., 2001), suggesting a role for reactive oxygen species in the activation of the MAPK. DTDP is known to trigger neuronal apoptosis by first liberating zinc from intracellular binding proteins (Aizenman et al., 2000b). Zinc, in turn can generate reactive oxygen species by modulating mitochondrial function (Sensi et al., 1999; Sensi et al., 2003) or activating 12-lipoxygenase (Zhang et al., 2004). We thus hypothesized that over-expression of Trx may prove sufficient to halt the DTDP-induced K^+ current surge by providing

an excess of the inhibitory binding partner of ASK1. As such, electrophysiological measurements were performed from vehicle and DTDP (100 μM, 10 min)-treated neurons previously transfected with a plasmid containing Trx. We observed virtually identical current-voltage relationships and K^+ current amplitudes (Figs. 3A and 3B) in both vehicle and DTDP-treated neurons expressing Trx. In contrast, recordings performed on DTDP-exposed cells not over-expressing Trx, but obtained from the same coverslip, revealed a pronounced K^+ current surge, indicating that the exposure to the apoptogen had been effective across the culture. These results indicate that over-expression of Trx, a suppressor of ASK1 activation, can halt the apoptotic increase in K^+ currents in neurons. It is possible, however, that over-expression of Trx may have other, non-specific effects, including a direct interaction with DTDP. The fact that DTDP activates p38 in a ROS-dependent fashion (McLaughlin et al., 2001) despite the presence of many endogenous thiol groups does suggest, however, that Trx directly suppresses ASK1 function.

Consistent with reports involving oxidative injury (Song and Lee, 2003; Takeda et al., 2003), we have found that ASK1 is a requisite upstream signaling kinase in a critical step of neuronal apoptosis; namely, an increase in voltage-dependent K^+ currents. In important recent studies, a link was established between Ca^{2+} signaling and p38 activation in neurons via the interaction of Ca^{2+}/calmodulin-dependent protein kinase II (CaMKII) and ASK1 (Sensi et al., 1999; Sagasti et al., 2001; Takeda et al., 2003). CaMKII is a well-known regulator of synaptic function (Colbran and Brown, 2004), and p38 has recently been implicated in certain forms of synaptic plasticity (Thomas and Huganir, 2004), including an NMDA (a Ca^{2+}-permeable glutamate receptor) receptor-dependent form of long-term depression that is mediated by the

internalization of glutamate receptors specific for AMPA (Zhu et al., 2002. It is thus appealing to speculate that, based on our present findings, calcium signaling may be linked in future studies to long-term changes in neuronal excitability via ASK1/p38-dependent alterations in voltage-dependent K^+ currents.

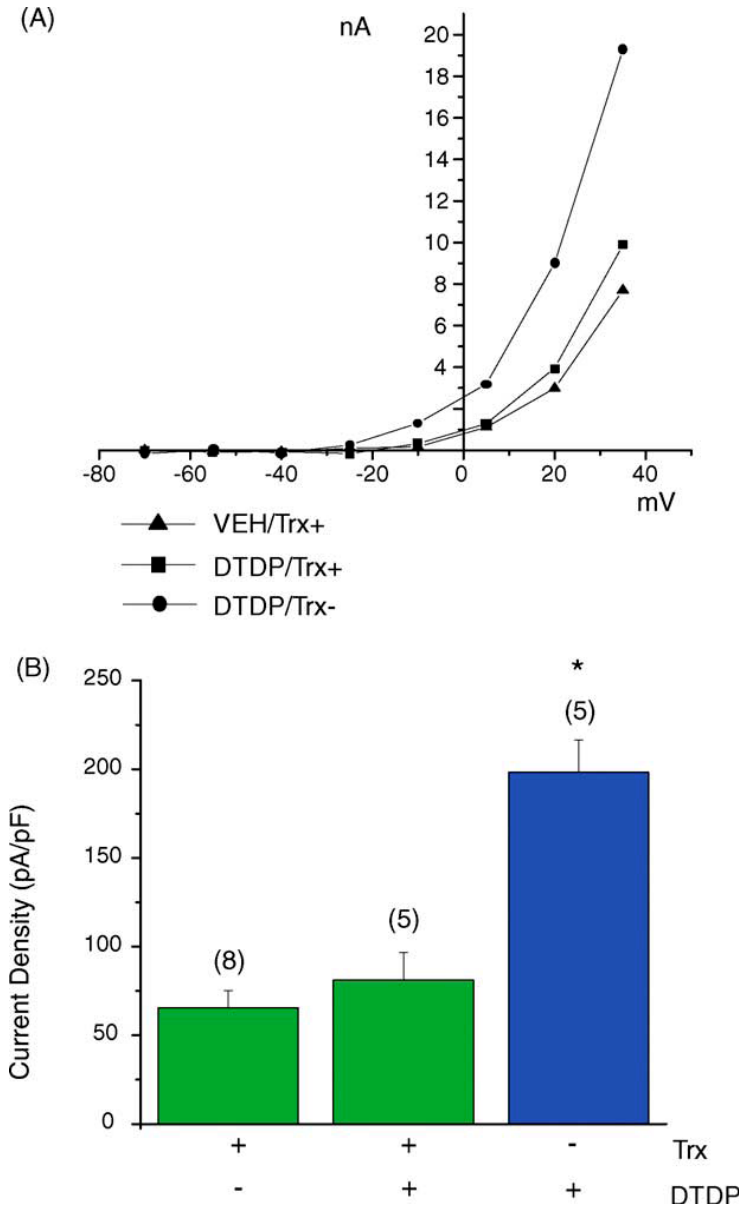
(A)
nA
20
18
16
14
12
10
8
6
4
-80
-60
-40
-20
0
20
40
mV
VEH/Trx+
DTDP/Trx+
DTDP/Trx-
(B)
Current Density (pA/pF)
250
200
150
100
50
0
*
(5)
(5)
(8)
+
+
-
Trx
-
+
+
DTDP

Figure 3. Over-expression of thioredoxin (Trx) prevents the apoptotic current surge in neurons. (A) I-V relationships of K^+ currents evoked by a series of voltage steps from –70 mV to +35 mV in 15 mV in representative Trx over-expressing neurons exposed to either vehicle (black triangles) or DTDP (100 μM, 10 min; black squares). Note the very similar I-V curves in these two cells. An I-V relationship was also established from a DTDP-treated untransfected neuron from the same coverslip where the measurements from the ASK DN-expressing cell had been performed (black circles), demonstrating the current surge. (B) Mean ± s.e.m. current densities from vehicle and DTDP-treated ASK1 DN-expressing neurons (green bars). The blue bar represents the current densities obtained from DTDP-treated untransfected neurons in the same coverslip containing the ASK1 DN-expressing cells. Currents were evoked with a voltage step to +5 mV from a holding potential of –70 mV and normalized to cell capacitance (statistically different from the Trx+ groups, $*p<0.05$; ANOVA, Bonferoni).

Appendix C

ASSESSMENT OF CELL VIABILITY IN PRIMARY NEURONAL CULTURES

Mandar A. Aras, Karen A. Hartnett, Elias Aizenman

Department of Neurobiology, University of Pittsburgh School of Medicine,

Pittsburgh, PA 15261.

ABSTRACT

This unit contains five protocols for assaying cell viability *in vitro* using primary neuronal cultures, including a novel method for use with transfected neurons. Three of the assays are based on the principle that cell death cascades alter membrane permeability. The lactate dehydrogenase (LDH) release assay measures the amount of the cytoplasmic enzyme released into the bathing medium, while the trypan blue and propidium iodide assays measure the ability of cells to exclude dye from their cytoplasm. The 3-(4,5-dimethylthiazol-2-yl)-2,5-diphenyltetrazolium bromide (MTT) assay measures the mitochondrial activity of viable cells by quantifying the conversion of the tetrazolium salt to its formazan product. Finally, the fifth assay details the measurement of luciferase expression as an indication of neuronal viability within a relatively small population of transfected neurons.

TOPIC INTRODUCTION

Research aimed at studying the cellular and molecular mechanisms of neuronal cell death and the development of novel neuroprotective strategies are critically important areas of modern neuroscience. Understanding the complexities of cell death processes has therapeutic implications for a variety of neurodegenerative pathologies, including stroke, trauma, epilepsy, Parkinson's disease (PD), and Alzheimer's disease (AD). As such, rapid, accurate and reproducible assays for measuring cell death *in vitro* are vital.

Historically, neurobiologists have distinguished two broad categories of cell death: apoptosis and necrosis. In 1972, John Kerr and colleagues first coined the term apoptosis to describe a set of morphological features associated with cell death in pathological as well as in normal physiological states (Kerr et al., 1972). These characteristics, also described in the central nervous system (Pender et al., 1991), include chromatin condensation, nuclear DNA fragmentation, cell shrinkage, apoptotic body formation, and ultimate phagocytosis. On the other hand, necrosis follows severe pathological insults and involves cytoplasmic swelling, loss of membrane integrity, and cell lysis. Since the initial description distinguishing apoptosis from necrosis, many forms of cell death have been described combining features of both death programs (Bredesen et al., 2006; Unit 3.8). Importantly, as mechanisms involved in cell death become elucidated, additional cellular, biochemical and molecular characteristics (altered intracellular ion homeostasis, mitochondrial protein release, and caspase activation) are more appropriately used to describe this process (Pettmann and Henderson, 1998; Bredesen et al., 2006). Neuronal cell culture models have been important tools for the elucidation of signaling

cascades relevant to cell death following a variety of insults, and have also provided important platforms for the screening of novel neuroprotective interventions. As such, rapid, reliable, and inexpensive methods to monitor cell death in these models have allowed researchers to provide key insights into the cellular and molecular basis of several neurodegenerative diseases.

Although there are many methods to measure cell viability, most assays are based on a few guiding principles (Table 7.18.1). These principles include, but are not limited to, cell morphology, membrane permeability, and mitochondrial activity. Selection of the most appropriate protocol is driven by the specific goals of the experiment and the relative advantages and disadvantages of the assay. In this unit, five protocols are described in detail; the first four are to be used in non-transfected neuronal cultures, while a fifth, novel assay is used in transfected primary neural cells.

The lactate dehydrogenase (LDH) release assay (Basic Protocol 1) is based on the principle that cell death processes *in vitro* eventually lead to an increase in membrane permeability, allowing the release of cytoplasmic enzymes into the bathing medium. This assay is simple, quick, and non-destructive, but it is not specific to neuronal cell death if the cultures contain additional cell types such as astrocytes. Alternatively, if the cells are lysed prior to assaying the medium, total cytoplasmic LDH can be measured as an indication of the number of viable cells remaining in the culture (Alternative Protocol 1). The tetrazolium salt, 3-(4,5-dimethylthiazol-2-yl)-2,5-diphenyltetrazolium bromide (MTT), is used to measure mitochondrial activity in viable cells (Basic Protocol 2). The MTT assay utilizes spectrophotometry to provide rapid and reproducible results, but provides no morphological information. The trypan blue and

propidium iodide assays (Basic Protocols 3 and 4, respectively) are based on the same membrane permeability principle as the LDH assay. However, rather than measuring the release of cytoplasmic contents, the trypan blue and propidium iodide assays quantify the extent to which cells are unable to exclude these two dyes from their cytoplasm. Although these two assays provide morphological information, they can be time-consuming due to manual cell counting. However, propidium iodide is a fluorescent biomarker and can also be quantified using a plate reader. Cell counting has the added advantage that it can measure cell death of neurons in mixed cultures when accompanied by a neuronal marker. Support Protocol 1 provides a procedure that can be used to extend the time window between staining and counting cells in the trypan blue and propidium iodide assays. Finally, Basic Protocol 5 describes a novel method that can be used to assess cell viability among positively transfected neurons. By co-transfecting neurons with a firefly luciferase reporter, this assay measures viability in cells with a manipulated genome. Although this assay selects for a relatively small population of cells that is transfected, it has the advantage of being able to use molecular probes to provide important mechanistic information about cell signaling pathways involved in the cell death process.

All assays described in this unit utilize primary rat cortical neurons obtained from embryonic day 16 Sprague-Dawley rats (Charles River laboratories, Wilmington, MA). Cortices are dissociated and the resultant cell suspension is adjusted to a density of 670,000 cells/well (six-well tissue culture plates containing 5, 12mm poly-L-ornithine-treated coverslips per well). Cultures are maintained at 37^{o}C, 5% CO_2 in 500 µl bathing medium/well composed of a volume-to-volume mixture of 80% Dulbecco's modified minimal essential media (MEM), 10% Ham's F12 nutrients, 10% bovine calf serum (heat-inactivated, iron-supplemented; Hyclone, Logan,

UT) with 25 mM HEPES, 24 U/mL penicillin, 24 μg/mL streptomycin, and 2 mM L-glutamine (Hartnett et al., 1997). Cultures are inhibited on *in vitro* day 15 with cytosine arabinoside to inhibit non-neuronal cell proliferation. Cultures are normally utilized at 21-25 days *in vitro* (DIV). All incubations are performed in a humidified 37°C, 5% CO_2 chamber, unless otherwise noted.

STRATEGIC PLANNING

To facilitate data interpretation, it is useful to divide a 24-well plate into a vehicle treated group, experimental treatments, as well as complete-kill wells (Figure 7.18.1). Cell viability is often presented in the literature as percent cell death, which can be calculated as follows:

$$\% \text{ cell death} = \frac{(e_i \text{ result} - \text{mean vehicle result})}{(\text{mean complete kill result} - \text{mean vehicle result})} \times 100$$

In the above formula, e_i refers to the result of individual experimentally treated wells. Mean vehicle result can be obtained by averaging the results from each of the vehicle-treated wells. Similarly, mean complete-kill result is obtained by averaging the results from each of the wells treated with a substance that produces 100% neuronal cell death conditions. If the complete-kill insult is selective for neurons, then the data can be expressed as percent neuronal death. For example, 24 hour exposure of cortical cultures containing neurons and glia to 300 μM N-methyl-D-aspartate (NMDA) or 1 mM kainate will cause 100% neuronal death while sparing astrocytes (Koh and Choi, 1988; Sinor et al., 2000).

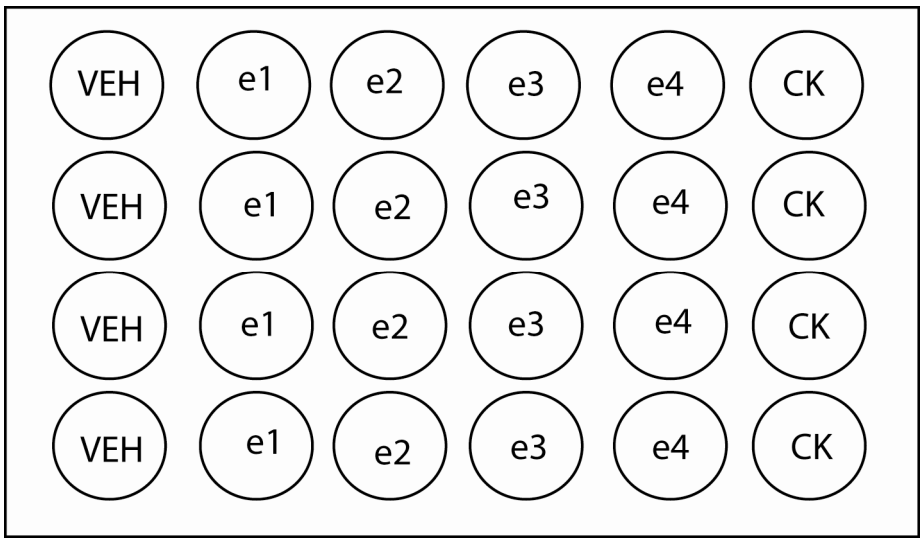

Figure 1. Experimental setup. Typically, 24-well plates are divided into vehicle (VEH) treated wells, experimental treatments (e1-4), and complete-kill (CK; 100% cell death) treated wells.

BASIC PROTOCOL 1: ASSAY OF CELL VIABILITY BY MEASUREMENT OF LACTATE DEHYDROGENASE (LDH) RELEASE

The release of lactate dehydrogenase (LDH) into the bathing medium is an indication of compromised membrane integrity (Koh and Choi, 1987). The quantification of LDH release is a rapid, reliable, and reproducible method for detecting cell toxicity without disrupting or destroying the cell in culture, which can also be assessed morphologically. In this assay, a sample of the bathing medium is combined with the assay mixture containing cofactor, substrate, and dye solutions. The Tox-7 assay kit (Sigma Chemical Company, St. Louis) is based on the conversion of the tetrazolium dye to a soluble, colored compound by nicotinamide adenine dinucleotide (NADH). The change in color can be easily quantified using a microplate spectrophotometer, with greater LDH activity indicating greater cell damage (Figure 7.18.2).

Materials

LDH-Based *In Vitro* Toxicology Assay Kit (Sigma, product# TOX7-1KT)

Minimal essential media (MEM, without phenol red; Gibco, Grand Island, NY)

Cells in 24-well culture plate, 500 μl bathing medium/well

96 well flat bottom, clear microtiter plate

Microplate spectrophotometer (e.g., Wallac 1420 Victor^2 multilabel counter; PerkinElmer, Waltham, MA)

Repeater pipette

1. Transfer duplicate (or greater) samples of 40 µl from each culture well to a well of a clear 96-well plate (Figure 7.18.3).
    a. Include 40 µl samples of MEM for blank wells, 40 µl samples from vehicle treated wells and 40 µl from complete-kill samples.
2. Prepare LDH mixture by combining equal amounts of LDH cofactor, substrate, and dye solutions (all supplied in the Tox7 kit). For example, to assay a single 24 well plate, mix 500 µl cofactor solution with 500 µl each of the substrate and dye.
3. Using a repeater pipette, add 20 µl of LDH mixture per blank, vehicle, sample, and complete-kill well.
4. Protect the 96-well plate from light and incubate at room temperature for 10-20 minutes.
5. Using the plate reader, measure the absorbance at 490 nm (0.1 second) followed by measurement of the background absorbance at 690 nm (0.1 second). Subtract the absorbance measurements at 690 nm from the primary measurements at 490 nm. Finally, subtract blank measurements from all vehicle, sample, and complete-kill measurements.
6. Background-subtracted absorbance measurements from control and treatment samples can be expressed as % cell death (see Strategic Planning) or as the ratio, $LDH_{TREATMENT}$ / $LDH_{CONTROL}$. Differences in % cell death or the LDH ratio, expressed as a mean ± S.E.M, can be compared among treatment groups for statistical significance.

ALTERNATIVE PROTOCOL 1: ASSAY OF CELL VIABILITY BY MEASUREMENT OF TOTAL CYTOPLASMIC LDH

Rather than assaying cell toxicity via the efflux of LDH into the bathing medium (Basic Protocol 1), this assay quantifies the number of viable cells left in the tissue culture plate by measuring total cytoplasmic LDH. Cells are lysed prior to sampling, allowing cytoplasmic contents to be released into the bathing medium. Here, a greater cell number will provide greater LDH activity, increasing the amount of substrate converted to colored product. This method is obviously destructive to the cells, so that no morphological information can be obtained.

Additional Materials *(also see Basic Protocol 1)*

LDH Lysis Solution (Sigma, product #L2152)

1. Add 50 µl of Lysis Solution to each well of the 24-well culture plate and incubate for 45 min at 37^{o}C.
2. Prepare samples and measure LDH activity according to Basic Protocol 1, Steps 1-5.

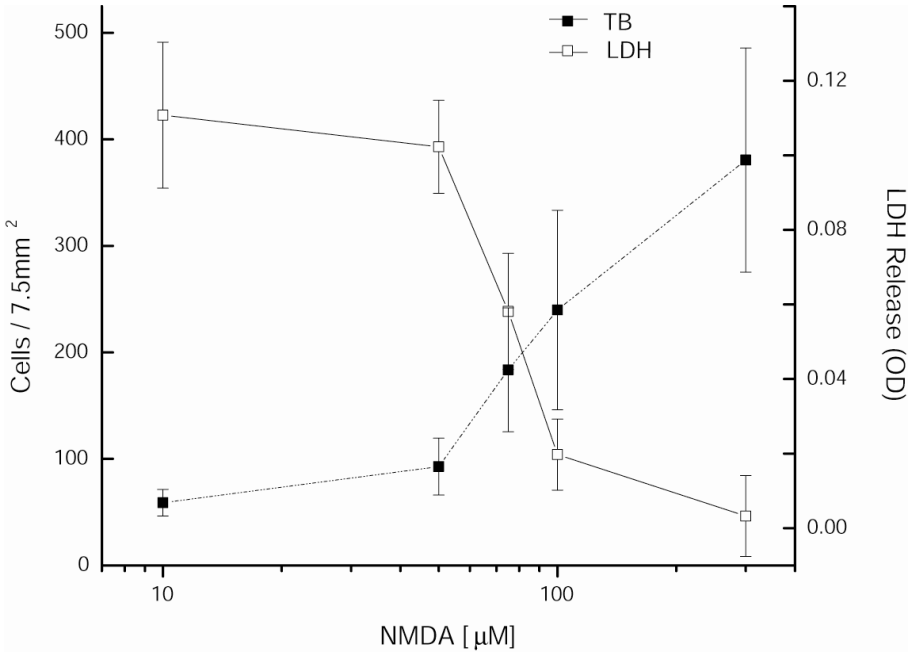

Figure 2. NMDA-mediated neuronal death characterized by trypan blue (TB) cell counts and LDH release. Cortical cultures (21-25 DIV) containing neurons resting on an astrocyte monolayer were exposed to increasing doses of NMDA for 10 min. Cell counts (EC_{50} 74.56 ± 6.15) and LDH release (EC_{50} 98.14 ± 18.84) were assayed 18-20 hours following treatment (mean ± s.e.m.; n=3 cultures).

BASIC PROTOCOL 2: ASSAY OF CELL VIABILITY BY MEASUREMENT OF MITOCHONDRIAL ACTIVITY (MTT REDUCTION)

The conversion of the yellow tetrazolium salt, 3-(4,5-dimethylthiazol-2-yl)-2,5-diphenyltetrazolium bromide (MTT) to its purple formazan product is an indication of mitochondrial activity (Mosmann, 1983). This assay provides a rapid and precise method of quantifying cell viability by measuring, via spectrophometry, the ability of living cells to reduce the MTT reagent. Following incubation of cells with the MTT reagent, lysis buffer is added to dissolve the insoluble purple formazan product to yield a colored solution, which is quantified using a microplate spectrophotometer. The relative absorbance directly correlates with cell number, that is, more purple color indicates more viable cells.

Materials

5 mg/mL 3-(4,5-dimethylthiazol-2-yl)-2,5-diphenyltetrazolium bromide (MTT; Sigma, product #M2003-1G) in phosphate buffered saline (PBS; see recipe in *Appendix 2A*)

Cells in 24-well plate, 500 µl bathing medium/well

Lysis Buffer (see recipe in *Reagents and Solutions*)

Microplate spectrophotometer (e.g., Wallac 1420 Victor^2 multilabel counter; PerkinElmer, Waltham, MA)

1. Remove the entire volume of cell culture medium by gently aspirating each well. Immediately add 50 µl /well 5mg/ml MTT solution. Incubate at 37^{o}C for 4 hours.
2. Add 500 µl lysis buffer (equal volume to original bathing medium) and incubate overnight at 37^{o}C or until the formazan precipitate is completely solubilized.
3. Measure the absorbance of the wells at 570 nm and 630 nm (reference wavelength) with microplate spectrophotometer.
4. Calculate ratio of A_{570}/A_{630}, which is directly related to the number of live cells in each well. Differences in % cell death (see Strategic Planning), expressed as a mean ± S.E.M, can be compared among treatment groups for statistical significance.

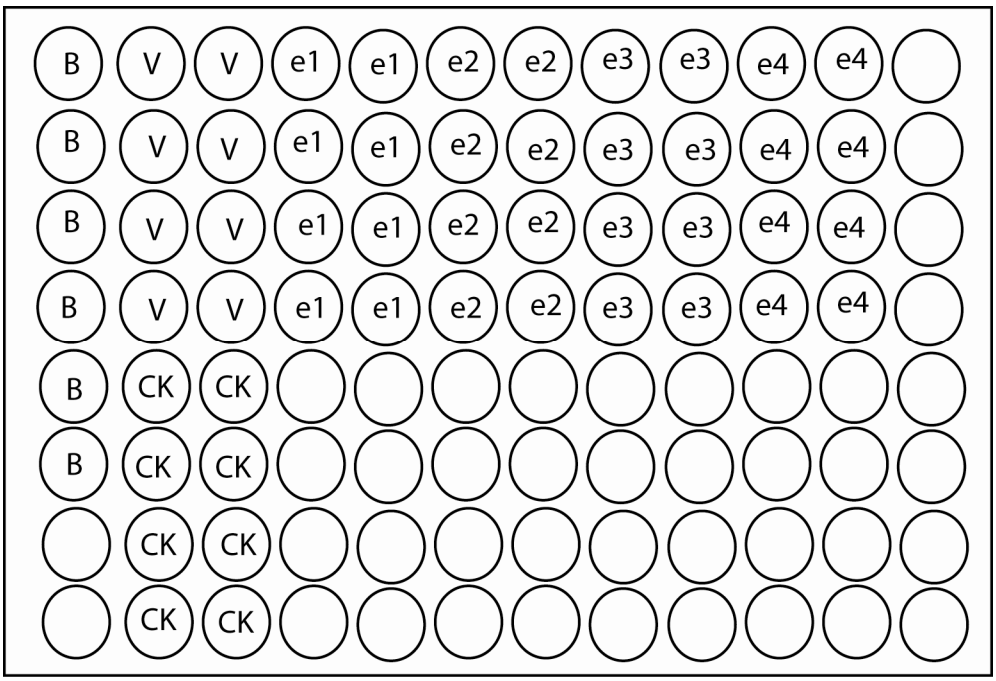

Figure 3. A typical 96-well setup for LDH Assay. Samples from vehicle (V) treated, complete kill (CK), and experimental (e1-4) wells are assayed in *duplicate*. Additionally, blank samples (B) containing MEM are used for background subtraction. Multiple 24-well plates or a greater number of replicate samples (e.g., triplicate, quadruplicate) can be assayed on a single 96-well plate.

BASIC PROTOCOL 3: ASSAY OF CELL VIABILITY BY COLLOIDAL DYE (TRYPAN BLUE) EXCLUSION

Healthy living cells contain plasma membranes that effectively exclude most large hydrophilic molecules. However, injured cells with compromised membrane integrity can allow hydrophilic molecules, such as trypan blue, into their cytoplasm. This assay is based on the simple principle that viable cells will exclude the trypan blue dye, whereas dead or dying neurons will not and thus, will appear blue. Live and/or dead cells are incubated with the dye and then counted *in situ* using bright field optics with a grid containing eye-piece. Dead cells may sometimes disintegrate or detach from the culture so most experimenters count live cells, which exclude the dye (Figure 7.18.4). In mixed cortical cultures, a neural-specific marker (e.g., mouse anti-NeuN; Chemicon, Cat# MAB377) can be coupled with standard immunocytochemistry staining methods to facilitate the identification and counting of neurons. As Figure 7.18.2 indicates, cell counts using trypan blue correlate inversely with LDH release following an NMDA insult.

Materials

HEPES-buffered salt solution (HBS, see recipe in *Reagents and Solutions*)

0.4% Trypan Blue solution (Sigma, product #T8154)

Cells plated in 24-well culture plate, 500 µl bathing medium/well

1. Rinse each well with 2 ml HBS. Add 0.5 ml 0.2% Trypan Blue solution (prepared in HBS) to each well and incubate for 2 min at room temperature.
2. Wash each well with 2 ml HBS to remove Trypan Blue solution.
3. Count cells in 10 random fields per well using the grid-containing eye piece by a person blinded to the treatment arrangement. Express the number of dead or live cells per unit area. If cells cannot be counted immediately following staining, fix cells using paraformaldehyde (Support Protocol 1).

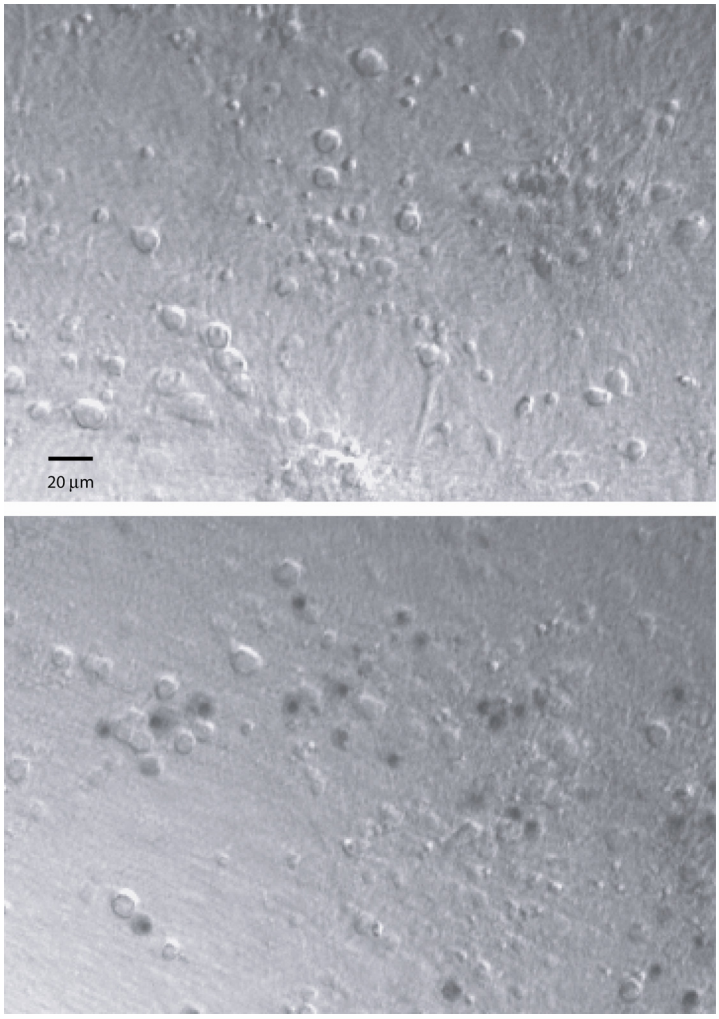

Figure 4. NMDA-mediated neuronal death characterized by Trypan blue (TB) exclusion. Phase contrast images of cortical cultures (21-25 DIV) containing neurons resting on an astrocyte monolayer exposed to vehicle (top panel) or 50µM NMDA (bottom panel) for 10 min. Cultures were fixed with phosphate-buffered 4% paraformaldehyde 24 hours following treatment. Note the uptake of TB in NMDA treated cultures and the lack of TB staining in vehicle-treated cultures.

BASIC PROTOCOL 4: ASSAY OF CELL VIABILITY USING PROPIDIUM IODIDE

Propidium iodide is a cell-impermeant fluorescent biomarker that stains DNA. This assay is similar in principle to the trypan blue assay in that healthy viable cells will be able to exclude the dye from their cytoplasm, whereas dead and dying cells will not. In this assay, cells are incubated in propidium iodide, which will fluoresce upon binding nuclear chromatin. This increase in fluorescence can be measured using a multiwell plate reader or by simply counting fluorescent (non-viable) cells. Importantly, propidium iodide is a potential mutagen, so special handling is required.

Materials

1 mg/ml propidium iodide (Molecular Probes, Eugene, OR; product #P3566)

Cells in 24-well culture plates, 500 µl bathing medium/well

Fluorescence multiwell plate reader (e.g., Wallac 1420 Victor^2 multilabel counter; PerkinElmer, Waltham, MA)

530 ± 25 nm excitation filter and a 645 ± 40 nm emission filter

1. Add 0.1 mg/ml propidium iodide (prepared in dH_2O) to culture medium for final concentration of 5 µg/ml.
2. Incubate for 1 to 2 hours, 37^o C.
3. Either a) determine fluorescence of each well using a fluorometric multiwell plate reader equipped with a 530 ± 25 nm excitation filter and a 645 ± 40 nm emission filter or b) count stained cells using a fluorescence microscope.

a. Measure initial fluorescence of each well before applying treatments. Repeat steps 1-3 as needed following treatment to monitor time dependency of cell death.

4. Express cell death as emission at 617 nm or percent cell death:

$$\% \text{ cell death} = (\# \text{ stained cells} / \# \text{ total cells}) \times 100$$

SUPPORT PROTOCOL 1: PRESERVATION OF STAINED CELLS

This protocol will extend the time that can be taken between staining and counting cells. The time window can be extended for 2-3 months, provided that the appropriate measures are taken (see below).

Materials

Stained cells (see Basic Protocols 3 & 4)

Phosphate buffered saline (PBS; see recipe in *Appendix 2A*)

Phosphate-buffered 4% Paraformaldehyde (FD NeuroTechnologies Inc., Baltimore, MD.)

1. Remove stain solution and rinse each well with 2 ml PBS.
2. Add 1 ml/well ice-cold 4% paraformaldehyde.
3. Incubate for 5 min at 4^{o}C and then at room temperature for an additional 10 min.
4. Remove the fixative solution completely and rinse each well 3 x 5 min with 2 ml PBS.
5. Store cells in the dark at 4^{o}C until ready to count. Plates should be wrapped in parafilm and/or tin foil during storage to prevent evaporation of solutions. These measures can extend the time window between staining and counting up to 2-3 months.

BASIC PROTOCOL 5: ASSAY OF TRANSFECTED CELL VIABILITY BY FIREFLY LUCIFERASE ACTIVITY

Mammalian firefly luciferase reporters, which generate enzymatic luciferase activity in transfected, surviving cells, can be used as an index of cell viability (Boeckman and Aizenman, 1996). Because, in general, transfection efficiency is low in primary neuronal cultures, the luciferase assay system offers the advantages of being highly sensitive for detecting cell viability in a small population of transfected neurons. In spite of the low transfection efficiencies observed in neuronal cultures (<10%), multiple plasmids transfected together have a 90% chance of being expressed together by the same neurons; this being true of as many as five separate plasmids introduced at the same time (Santos and Aizenman, 2002). Twenty-four to forty-eight hours following transfection of the luciferase reporter plasmid and any other plasmids of interest, cultures are treated with control and experimental conditions and assayed for luciferase-mediated luminescence. Cell viability is proportional to luciferase luminescence. This should be initially confirmed with cell counts of neurons positively transfected with a green fluorescent protein (GFP)-expressing plasmid (Figure 7.18.5), as some experimental conditions may interfere with the gene expression assay. As shown in Figure 7.18.5, luciferase activity in transfected cells correlates directly with GFP-positive cell counts and inversely with LDH release following an NMDA insult.

Materials

Minimal essential media (MEM, without phenol red; Gibco, Grand Island, NY)

SteadyLite Luciferase assay reagent (PerkinElmer, Waltham, MA; product #6016981)

Firefly luciferase (e.g., pGL2, Promega; product #E1611) transfected cells in 24-well culture plate (see *Appendix 1F* for cationic-lipid based transfection protocols), 24-48 hours post-transfection

96-well white opaque plate (Corning Life Sciences, Corning, NY)

Microplate luminometer (e.g., Wallac 1420 Victor^2 multilabel counter; PerkinElmer, Waltham, MA)

1. Bring MEM (without phenol red) and SteadyLite reagents (light sensitive) to room temperature
2. Reconstitute 1 vial of lyophilized steadylite HTS substrate solution (Perkin Elmer) with 10 ml of steadylite HTS substrate buffer solution (Perkin Elmer).

   Unused reagent can be stored at -70^{o}C for 1 month.
3. Remove the entire volume of cell culture medium by gently aspirating each well. Immediately add 100 µl /well MEM.
4. Add 100 µl /well steadylite substrate using a repeater pipette, and incubate at room temperature in the dark for 5 minutes.
5. Transfer the entire 200 µl sample volume to the well of a 96- well white opaque plate.
6. Measure luminescence (counts per second) using microplate luminometer. Differences in % cell death (see Strategic Planning), expressed as a mean ± S.E.M, can compared among treatment groups for statistical significance.

REAGENTS AND SOLUTIONS

Use deionized, distilled water in all recipes and protocol steps. For common stock solutions, see ***APPENDIX 2A****; for suppliers, see* ***SUPPLIERS APPENDIX****.*

HEPES-buffered salt solution, pH 7.4

135 mM NaCl

10 mM KCl

0.4 mM $MgCl_2$

1 mM $CaCl_2$

10 mM HEPES

Adjust pH to 7.4 with 1 N NaOH and filter sterilize. Store at 4°C for up to 6 months.

Lysis Buffer

10 g sodium dodecyl sulfate (SDS)

25 ml N,N-dimethylformamide (DMF)

25 ml H_2O

1 ml glacial acetic acid

1.25 ml 1 N HCl

Dissolve 20% w/v SDS into combined water/DMF solution. Adjust pH to 4.7 with acetic acid or 1 N HCl (Hansen et al., 1989). Store at room temperature for up to 1 month.

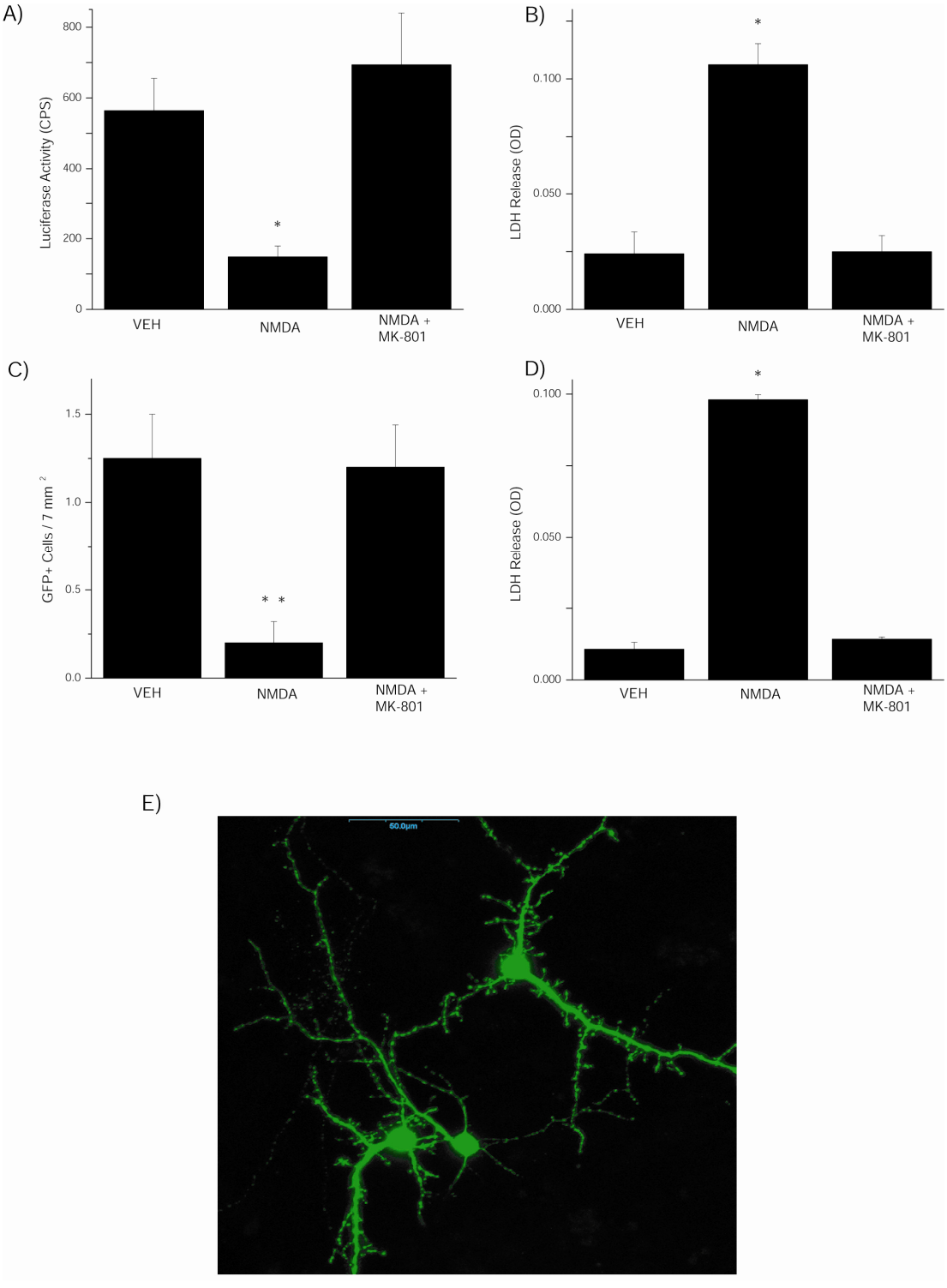
A)
Luciferase Activity (CPS)
800
600
400
200
0
*
VEH
NMDA
NMDA +
MK-801
B)
LDH Release (OD)
0.100
0.050
0.000
*
VEH
NMDA
NMDA +
MK-801
C)
GFP+ Cells / 7 mm 2
1.5
1.0
0.5
0.0
* *
VEH
NMDA
NMDA +
MK-801
D)
LDH Release (OD)
0.100
0.050
0.000
*
VEH
NMDA
NMDA +
MK-801
E)
60.0µm

Figure 5. LDH release assay verifies cell toxicity in positively transfected neurons. A&B) Cortical cultures were co-transfected with firefly luciferase (pUHC13-3) and blank vector (pBKCMV) at a ratio of 1:5. Forty-eight hours following transfection, cells were exposed to vehicle, 200 μM NMDA, or 200 μM NMDA in the presence of the non-competitive NMDA receptor antagonist, MK-801 (10 μM) for 30 minutes. Luciferase activity and LDH release were measured 24 hours following treatment (mean ± s.e.m.of 4 samples; *$p<0.001$; ANOVA, Tukey). C&D) Cortical cultures were co-transfected with firefly luciferase (pUHC13-3) and eGFP (pCMVIE-eGFP) at a ratio of 1:1. Twenty-four hours following transfection, cells were exposed to vehicle, NMDA, or NMDA + MK-801 as above. Cell counts of eGFP-positive cells and LDH release were measured 24 hours following treatment (mean ± s.e.m. of 3 samples; *$p<0.001$; ANOVA, Tukey; **$p<0.01$; ANOVA, Tukey). E) Visualization of GFP-positive transfected neurons *in situ* using fluorescence microscopy.

COMMENTARY

Background Information

LDH assay

Lactate dehydrogenase (LDH) is a ubiquitous cytoplasmic enzyme responsible for reducing pyruvate to lactate with concurrent oxidation of nicotinamide adenine dinucleotide (NADH to NAD^+). LDH has been shown to be released into the bathing medium of primary rat cortical neurons following toxic stimuli and has been correlated well to the number of lysed neurons killed by excitotoxicity (Koh and Choi, 1987). The advantages of the LDH release assay are that it is simple, rapid, and non-destructive. Since the extracellular medium is sampled, repeated measures can be assayed over time. Disadvantages include lack of specificity to neurons, LDH release dependency on cell size, and LDH degradation prior to release, or even possible uptake of LDH by healthy cells.

MTT assay

The tetrazolium salt, 3-(4,5-dimethylthiazol-2-yl)-2,5-diphenyltetrazolium bromide (MTT), is a hydrogen acceptor that is reduced to a colored formazan product. The MTT assay measures the redox activity of living cells by quantifying the formation of the dark blue formazan product at 570 nm. The reduction of the tetrazolium ring is thought to mainly occur in the mitochondria of cells through the actions of succinate dehydrogenase (Slater et al., 1963), but may also take place in other cellular and extracellular locations (Mosmann, 1983; Burdon et al., 1993). The MTT assay provides a rapid and precise method for assaying cell viability without having to manually count cells. On the other hand, the assay's disadvantages include the lack of

ability to distinguish reversible mitochondrial impairment and injury from cell death. Additionally, MTT has been shown to be inherently toxic in an adrenal pheochromocytoma (PC12) cell line (Hertel et al., 1996).

Trypan Blue assay

Trypan blue is an azo dye, which can be absorbed in the cytoplasm of dead or dying cells, staining them blue. Healthy cells, with intact cell membranes, will exclude the hydrophilic dye and will not change in color. This assay, although non-automated and time consuming, is the "gold standard" for assaying viability and is often combined with other viability assays.

Propidium Iodide assay

Propidium iodide (PI) is a DNA intercalating agent that can bind to double stranded nucleic acids of permeable, non-viable cells. The binding of PI to nuclear chromatin causes an enhancement and red shift in fluorescence (Trost and Lemasters, 1994). The PI assay is based on the same dye exclusion principle as the trypan blue assay, that is, injured cells will absorb dye and change color, whereas healthy cells will not. The advantage of using PI over trypan blue is that the colorimetric change can be automated due to its higher signal-to-noise ratio and therefore can enable rapid, repeated measures of viability over time (Trost and Lemasters, 1994). Both dyes, PI and trypan blue, can be used alone or in conjunction with counterstains that detect live cells (e.g., fluorescein diacetate). One disadvantage of using PI is that it is a potential mutagen, so special handling is required.

Luciferase assay

Luciferase is a 62 KD monomeric enzyme produced by the North American firefly (*Photinus pyralis)* and catalyzes the oxidation of its substrate, D-luciferin, to produce oxyluciferin and light. This assay system quantifies firefly luciferase expression in mammalian cells transfected with a luciferase reporter gene. Luminescence, measured by a microplate luminometer, is directly correlated with cell viability (Boeckman and Aizenman, 1996). This assay is particularly valuable when used in conjunction with other genes of interest to test molecular components of cell death pathways (Pal et al., 2003). The advantages of the luciferase assay are its reproducibility and exquisite sensitivity for measuring neuronal cell viability in a relatively low number of cells. Disadvantages of the assay include inability to perform repeated measures, dependency on transfection efficiency, and assay interference with drugs or treatments in the bathing medium.

Critical Parameters and Troubleshooting

LDH assay

Pipetting seems to be the largest source of error in this assay, causing variability among samples. To help resolve this issue, samples should be tested in at least triplicate. Additionally, since this assay depends on the amount of LDH released into the bathing medium, ensure that the bathing medium volume is consistent among wells. Low LDH values could result from expired assay solutions, whereas uncharacteristically high LDH values could result from bacterial contamination of the culture medium or the assay solutions. If the LDH signal is completely absent in samples, stain cells with trypan blue to verify cell injury.

MTT assay

Ensure that the MTT stock solution is filtered (0.22 μm) to remove insoluble debris and stored in a light protective container at 4^{o}C. Also, be sure to set up spectrophotometer to read absorbance at 570 nm. If lack of signal is a problem, stain cells with trypan blue to verify cell injury. Uncharacteristically large signals may be due to reducing activity of certain treatments, leading to cell injury-independent formazan product formation. Again, high variability in this assay could result from inconsistent bathing medium volume among wells.

Trypan Blue assay

Complete lack of staining could be due to presence of serum in media or insufficient incubation time with the dye. To resolve these issues, be sure to wash out serum with buffered medium prior to staining or increase trypan concentration and/or duration of incubation. If staining results in high background, decrease duration and/or concentration of trypan blue and be sure to thoroughly remove dye before fixing. If too few cells are stained blue, consider staining at an earlier time point, as the dead cells may be detached or degraded. Alternatively, if many healthy-looking cells appear blue, decrease incubation time and/or dye concentration. It is very important that the experimenter counting cells is blinded to the treatment conditions, as this assay depends on the unbiased counting of cells. We recommend counting cells from 10 random fields per well at 200X magnification using a 10 x 10 grid-containing eyepiece.

Propidium Iodide assay

For this assay, ensure that the excitation and emission filters are appropriately set in the plate reader. Optimization of the dye concentration and incubation time may be required to achieve conclusive results. If fluorescence continues to be lower than expected, stain cells with trypan blue to verify cell death and/or extend incubation time to allow for complete dye absorption. Be sure to prevent dye bleaching by protecting dye stocks from light.

Luciferase assay

Ensure that the culture medium is free of phenol red or any other colored compounds, as these may absorb some of the emitted light. Also, be sure to work under dim light conditions and avoid direct sunlight and bright fluorescent light. Optimal room and instrument temperature is 22^{o}C. Low luminescence values may be due to inefficient transfection of reporter gene, interference of treatment with luciferase activity, inefficient mixing of culture medium and assay reagents, and/or use of old assay reagents. It is often useful to measure LDH release activity prior to performing the luciferase assay to verify assay results (Figure 7.18.5). Additionally, parallel experiments with enhanced green fluorescent protein (eGFP; pCMVIE-eGFP, Clontech, Palo Alto, CA) -expressing neurons and cell counts can be used to initially verify results (Figure 7.18.5).

Anticipated Results

LDH assay

Depending on plating density, after subtracting the absorbance at 690 nm, the LDH release values of dead or dying cultures should be at least 5 times greater than those of vehicle-treated cultures.

MTT assay

Healthy cultures yield absorbance values of 0.5 to 0.6 units at 570 nm, again, depending on plating density.

Trypan Blue assay

Healthy cells should exclude the dye, whereas the soma of dead cells should be stained blue (Figure 7.18.4). Optimization of signal to background may require adjusting the time and concentration of trypan blue dye exposure. This assay is often used in parallel to verify cell death and assay results in non-transfected neurons.

Propidium Iodide assay

In general, fluorescence values of dead cultures should be at least twice those of vehicle-treated cultures.

Luciferase assay

We have found that luminescence values of injured cells are less than half those of vehicle-treated cultures and correlate well to cell counts of GFP-positive transfected cells, as well as LDH assay results (Figure 7.18.5).

Time Considerations

LDH assay

The LDH assay can be completed in a very short amount of time. Set up, sampling, and clean-up can be performed in 20 minutes.

MTT assay

Although overnight incubation in lysis buffer ensures the complete solubilization of the formazan product, shorter lysis buffer incubation times are possible with thorough mixing or vortexing the sample.

Trypan Blue assay

The counting of stained cells is a time consuming process. If cells cannot be counted immediately following staining, fix cells using paraformaldehyde (Support Protocol 1).

Propidium Iodide assay

By using a fluorometric plate reader, the time required to complete this assay is significantly reduced. Nevertheless, manual cell counts can also be performed. If cells cannot be counted immediately following staining, fix cells using paraformaldehyde (Support Protocol 1).

Luciferase assay

Twenty-four or forty-eight hours following transfection with the luciferase reporter gene, cells are exposed to various control and experimental conditions. Cells can be assayed for luciferase expression following experimental conditions based on time-course of treatment toxicity.

Table 1 – Methods for assessing neuronal cell viability [a]

GUIDING PRINCIPLE	ASSAY	MEASURED QUANTITY	FORMAT	SAMPLE REFERENCES
Morphology				
	Light,Electron Microscopy	Cell morphology	Microscopy	Vincent and Maiese, 1999
Membrane Permeability				
	Propidium iodide, Ethidium homodimer	Staining of nucleic acids	Fluorometry or Microscopy	Garner et al., 1994
	Trypan blue	Cell morphology	Microscopy	Perry et al., 1997
	^{51}Cr	Radiolabeled Cr	Radioactivity	Kingsbury et al., 1985
	LDH	LDH activity	Colorimetry	Koh and Choi, 1987
Electrophysiology				
	Membrane potential, action potential generation, synaptic potentials	Electrophysiological response profile of cells	Electrophysiology	Pal et al., 2003
Ionic homeostasis				
	Fura-2, Indo-1, Fluo-3	Intracellular free calcium	Fluorometry	Mattson et al., 1993
	Neutral red	Lysosomal pH	Fluorometry	Verdaguer et al., 2002
Metabolism				
	Luciferase expression, eGFP expression	Protein synthesis	Luminometry or Microscopy	Pal et al., 2003
	Glucose utilization, lactate production	Substrate utilization	Biochemistry	Mills et al., 1995
	Fluorescein diacetate, calcein-AM	Esterase activity	Fluorometry	Bozyczko-Coyne et al., 1993
Mitochondrial function				
	MTT, XTT	Succinate dehydrogenase	Colorimetry	Slater et al., 1963
	Rhodamine 123	Mitochondrial membrane potential	Fluorometry	Mattson et al., 1993
DNA damage				
	TUNEL	Cleaved DNA	Microscopy	Perry et al., 1997
	Gel electrophoresis	Cleaved DNA	Electrophoresis	Ormerod et al., 1992
	Hoechst staining	Staining of DNA	Microscopy	Ormerod et al., 1992
Signal Transduction				
	Caspase Assays	Caspase activity	Fluorometry or colorimetry	McLaughlin et al., 2001

	Annexin V	Extracellular Phosphatidylserine	Flow cytometry	Vincent and Maiese, 1999

[a] Assays indicated in **bold** are detailed in this document.

BIBLIOGRAPHY

Adam-Vizi V (2005) Production of reactive oxygen species in brain mitochondria: contribution by electron transport chain and non-electron transport chain sources. Antioxid Redox Signal 7:1140-1149.

Adams TK, Saydam N, Steiner F, Schaffner W, Freedman JH (2002) Activation of gene expression by metal-responsive signal transduction pathways. Environ Health Perspect 110 Suppl 5:813-817.

Ahn YH, Kim YH, Hong SH, Koh JY (1998) Depletion of intracellular zinc induces protein synthesis-dependent neuronal apoptosis in mouse cortical culture. Exp Neurol 154:47-56.

Aizenman E, Sinor JD, Brimecombe JC, Herin GA (2000a) Alterations of N-methyl-D-aspartate receptor properties after chemical ischemia. J Pharmacol Exp Ther 295:572-577.

Aizenman E, Stout AK, Hartnett KA, Dineley KE, McLaughlin B, Reynolds IJ (2000b) Induction of neuronal apoptosis by thiol oxidation: putative role of intracellular zinc release. J Neurochem 75:1878-1888.

Albers GW (2001) Advances in intravenous thrombolytic therapy for treatment of acute stroke. Neurology 57:S77-81.

Alonso A, Sasin J, Bottini N, Friedberg I, Osterman A, Godzik A, Hunter T, Dixon J, Mustelin T (2004) Protein tyrosine phosphatases in the human genome. Cell 117:699-711.

Ambjorn M, Asmussen JW, Lindstam M, Gotfryd K, Jacobsen C, Kiselyov VV, Moestrup SK, Penkowa M, Bock E, Berezin V (2008) Metallothionein and a peptide modeled after metallothionein, EmtinB, induce neuronal differentiation and survival through binding to receptors of the low-density lipoprotein receptor family. J Neurochem 104:21-37.

Andrews GK (2000) Regulation of metallothionein gene expression by oxidative stress and metal ions. Biochem Pharmacol 59:95-104.

Andrews GK (2001) Cellular zinc sensors: MTF-1 regulation of gene expression. Biometals 14:223-237.

Aras MA, Aizenman E (2005) Obligatory role of ASK1 in the apoptotic surge of K+ currents. Neurosci Lett 387:136-140.

Aras MA, Hartnett KA, Aizenman E (2008) Assessment of cell viability in primary neuronal cultures. Curr Protoc Neurosci Chapter 7:Unit 7 18.

Aras MA, Hara H, Hartnett KA, Kandler K, Aizenman E (2009) Protein kinase C regulation of neuronal zinc signaling mediates survival during preconditioning. J Neurochem.

Asahi M, Hoshimaru M, Uemura Y, Tokime T, Kojima M, Ohtsuka T, Matsuura N, Aoki T, Shibahara K, Kikuchi H (1997) Expression of interleukin-1 beta converting enzyme gene family and bcl-2 gene family in the rat brain following permanent occlusion of the middle cerebral artery. J Cereb Blood Flow Metab 17:11-18.

Ascher P, Nowak L (1988) The role of divalent cations in the N-methyl-D-aspartate responses of mouse central neurones in culture. J Physiol 399:247-266.

Aschner M (1996) The functional significance of brain metallothioneins. FASEB J 10:1129-1136.

Aschner M, Cherian MG, Klaassen CD, Palmiter RD, Erickson JC, Bush AI (1997) Metallothioneins in brain--the role in physiology and pathology. Toxicol Appl Pharmacol 142:229-242.

Ballanyi K (2004) Protective role of neuronal KATP channels in brain hypoxia. J Exp Biol 207:3201-3212.

Barone FC, White RF, Spera PA, Ellison J, Currie RW, Wang X, Feuerstein GZ (1998) Ischemic preconditioning and brain tolerance: temporal histological and functional outcomes, protein synthesis requirement, and interleukin-1 receptor antagonist and early gene expression. Stroke 29:1937-1950; discussion 1950-1931.

Belloni-Olivi L, Marshall C, Laal B, Andrews GK, Bressler J (2009) Localization of zip1 and zip4 mRNA in the adult rat brain. J Neurosci Res.

Berg JM, Shi Y (1996) The galvanization of biology: a growing appreciation for the roles of zinc. Science 271:1081-1085.

Bergeron M, Gidday JM, Yu AY, Semenza GL, Ferriero DM, Sharp FR (2000) Role of hypoxia-inducible factor-1 in hypoxia-induced ischemic tolerance in neonatal rat brain. Ann Neurol 48:285-296.

Bernaudin M, Tang Y, Reilly M, Petit E, Sharp FR (2002a) Brain genomic response following hypoxia and re-oxygenation in the neonatal rat. Identification of genes that might contribute to hypoxia-induced ischemic tolerance. J Biol Chem 277:39728-39738.

Bernaudin M, Nedelec AS, Divoux D, MacKenzie ET, Petit E, Schumann-Bard P (2002b) Normobaric hypoxia induces tolerance to focal permanent cerebral ischemia in association with an increased expression of hypoxia-inducible factor-1 and its target genes, erythropoietin and VEGF, in the adult mouse brain. J Cereb Blood Flow Metab 22:393-403.

Besser L, Chorin E, Sekler I, Silverman WF, Atkin S, Russell JT, Hershfinkel M (2009) Synaptically released zinc triggers metabotropic signaling via a zinc-sensing receptor in the hippocampus. J Neurosci 29:2890-2901.

Bittel D, Dalton T, Samson SL, Gedamu L, Andrews GK (1998) The DNA binding activity of metal response element-binding transcription factor-1 is activated in vivo and in vitro by zinc, but not by other transition metals. J Biol Chem 273:7127-7133.

Blondeau N, Widmann C, Lazdunski M, Heurteaux C (2001) Activation of the nuclear factor-kappaB is a key event in brain tolerance. J Neurosci 21:4668-4677.

Bloomenthal AB, Goldwater E, Pritchett DB, Harrison NL (1994) Biphasic modulation of the strychnine-sensitive glycine receptor by Zn2+. Mol Pharmacol 46:1156-1159.

Boeckman FA, Aizenman E (1996) Pharmacological properties of acquired excitotoxicity in Chinese hamster ovary cells transfected with N-methyl-D-aspartate receptor subunits. J Pharmacol Exp Ther 279:515-523.

Bonanni L, Chachar M, Jover-Mengual T, Li H, Jones A, Yokota H, Ofengeim D, Flannery RJ, Miyawaki T, Cho CH, Polster BM, Pypaert M, Hardwick JM, Sensi SL, Zukin RS, Jonas EA (2006) Zinc-dependent multi-conductance channel activity in mitochondria isolated from ischemic brain. J Neurosci 26:6851-6862.

Bortner CD, Cidlowski JA (1999) Caspase independent/dependent regulation of K(+), cell shrinkage, and mitochondrial membrane potential during lymphocyte apoptosis. J Biol Chem 274:21953-21962.

Bortner CD, Cidlowski JA (2007) Cell shrinkage and monovalent cation fluxes: role in apoptosis. Arch Biochem Biophys 462:176-188.

Bossy-Wetzel E, Talantova MV, Lee WD, Scholzke MN, Harrop A, Mathews E, Gotz T, Han J, Ellisman MH, Perkins GA, Lipton SA (2004) Crosstalk between nitric oxide and zinc pathways to neuronal cell death involving mitochondrial dysfunction and p38-activated K+ channels. Neuron 41:351-365.

Bozyczko-Coyne D, McKenna BW, Connors TJ, Neff NT (1993) A rapid fluorometric assay to measure neuronal survival in vitro. J Neurosci Methods 50:205-216.

Bredesen DE, Rao RV, Mehlen P (2006) Cell death in the nervous system. Nature 443:796-802.

Bremner I, Mehra RK, Sato M (1987) Metallothionein in blood, bile and urine. Experientia Suppl 52:507-517.

Brennan AM, Won Suh S, Joon Won S, Narasimhan P, Kauppinen TM, Lee H, Edling Y, Chan PH, Swanson RA (2009) NADPH oxidase is the primary source of superoxide induced by NMDA receptor activation. Nat Neurosci 12:857-863.

Bright R, Mochly-Rosen D (2005) The role of protein kinase C in cerebral ischemic and reperfusion injury. Stroke 36:2781-2790.

Brodie C, Blumberg PM (2003) Regulation of cell apoptosis by protein kinase c delta. Apoptosis 8:19-27.

Brusa R, Zimmermann F, Koh DS, Feldmeyer D, Gass P, Seeburg PH, Sprengel R (1995) Early-onset epilepsy and postnatal lethality associated with an editing-deficient GluR-B allele in mice. Science 270:1677-1680.

Burdon RH, Gill V, Rice-Evans C (1993) Reduction of a tetrazolium salt and superoxide generation in human tumor cells (HeLa). Free Radic Res Commun 18:369-380.

Burnashev N, Monyer H, Seeburg PH, Sakmann B (1992) Divalent ion permeability of AMPA receptor channels is dominated by the edited form of a single subunit. Neuron 8:189-198.

Cai L, Cherian MG, Iskander S, Leblanc M, Hammond RR (2000) Metallothionein induction in human CNS in vitro: neuroprotection from ionizing radiation. Int J Radiat Biol 76:1009-1017.

Calderone A, Jover T, Mashiko T, Noh KM, Tanaka H, Bennett MV, Zukin RS (2004) Late calcium EDTA rescues hippocampal CA1 neurons from global ischemia-induced death. J Neurosci 24:9903-9913.

Calderone A, Jover T, Noh KM, Tanaka H, Yokota H, Lin Y, Grooms SY, Regis R, Bennett MV, Zukin RS (2003) Ischemic insults derepress the gene silencer REST in neurons destined to die. J Neurosci 23:2112-2121.

Carmel JB, Kakinohana O, Mestril R, Young W, Marsala M, Hart RP (2004) Mediators of ischemic preconditioning identified by microarray analysis of rat spinal cord. Exp Neurol 185:81-96.

Carrasco J, Adlard P, Cotman C, Quintana A, Penkowa M, Xu F, Van Nostrand WE, Hidalgo J (2006) Metallothionein-I and -III expression in animal models of Alzheimer disease. Neuroscience 143:911-922.

Chapman GA, Kay J, Kille P (1999) Structural and functional analysis of the rat metallothionein III genomic locus. Biochim Biophys Acta 1445:321-329.

Chen JH, Huang CH, Lin LY (2001) Rottlerin stimulates metallothionein gene expression but inhibits metal transport in Chinese hamster ovary cells. Toxicol Appl Pharmacol 177:256-263.
Chen X, Zhang B, Harmon PM, Schaffner W, Peterson DO, Giedroc DP (2004) A novel cysteine cluster in human metal-responsive transcription factor 1 is required for heavy metal-induced transcriptional activation in vivo. J Biol Chem 279:4515-4522.
Chen Y, Maret W (2001) Catalytic oxidation of zinc/sulfur coordination sites in proteins by selenium compounds. Antioxid Redox Signal 3:651-656.
Chen Y, Irie Y, Keung WM, Maret W (2002) S-nitrosothiols react preferentially with zinc thiolate clusters of metallothionein III through transnitrosation. Biochemistry 41:8360-8367.
Choi DW (1987) Ionic dependence of glutamate neurotoxicity. J Neurosci 7:369-379.
Choi DW (1988) Glutamate neurotoxicity and diseases of the nervous system. Neuron 1:623-634.
Choi DW (1990) Limitations of in vitro models of ischemia. Prog Clin Biol Res 361:291-299.
Choi DW, Koh JY (1998) Zinc and brain injury. Annu Rev Neurosci 21:347-375.
Choi DW, Yokoyama M, Koh J (1988) Zinc neurotoxicity in cortical cell culture. Neuroscience 24:67-79.
Chung RS, West AK (2004) A role for extracellular metallothioneins in CNS injury and repair. Neuroscience 123:595-599.
Chung RS, Penkowa M, Dittmann J, King CE, Bartlett C, Asmussen JW, Hidalgo J, Carrasco J, Leung YK, Walker AK, Fung SJ, Dunlop SA, Fitzgerald M, Beazley LD, Chuah MI, Vickers JC, West AK (2008) Redefining the role of metallothionein within the injured brain: extracellular metallothioneins play an important role in the astrocyte-neuron response to injury. J Biol Chem 283:15349-15358.
Colbran RJ, Brown AM (2004) Calcium/calmodulin-dependent protein kinase II and synaptic plasticity. Curr Opin Neurobiol 14:318-327.
Cole TB, Martyanova A, Palmiter RD (2001) Removing zinc from synaptic vesicles does not impair spatial learning, memory, or sensorimotor functions in the mouse. Brain Res 891:253-265.
Cole TB, Wenzel HJ, Kafer KE, Schwartzkroin PA, Palmiter RD (1999) Elimination of zinc from synaptic vesicles in the intact mouse brain by disruption of the ZnT3 gene. Proc Natl Acad Sci U S A 96:1716-1721.
Csermely P, Szamel M, Resch K, Somogyi J (1988a) Zinc increases the affinity of phorbol ester receptor in T lymphocytes. Biochem Biophys Res Commun 154:578-583.
Csermely P, Szamel M, Resch K, Somogyi J (1988b) Zinc can increase the activity of protein kinase C and contributes to its binding to plasma membranes in T lymphocytes. J Biol Chem 263:6487-6490.
Cuajungco MP, Lees GJ (1998) Nitric oxide generators produce accumulation of chelatable zinc in hippocampal neuronal perikarya. Brain Res 799:118-129.
D'Amours D, Desnoyers S, D'Silva I, Poirier GG (1999) Poly(ADP-ribosyl)ation reactions in the regulation of nuclear functions. Biochem J 342 (Pt 2):249-268.
Dalton T, Palmiter RD, Andrews GK (1994) Transcriptional induction of the mouse metallothionein-I gene in hydrogen peroxide-treated Hepa cells involves a composite major late transcription factor/antioxidant response element and metal response promoter elements. Nucleic Acids Res 22:5016-5023.

Dalton TP, Bittel D, Andrews GK (1997) Reversible activation of mouse metal response element-binding transcription factor 1 DNA binding involves zinc interaction with the zinc finger domain. Mol Cell Biol 17:2781-2789.

Dalton TP, Li Q, Bittel D, Liang L, Andrews GK (1996) Oxidative stress activates metal-responsive transcription factor-1 binding activity. Occupancy in vivo of metal response elements in the metallothionein-I gene promoter. J Biol Chem 271:26233-26241.

Danscher G (1984) Autometallography. A new technique for light and electron microscopic visualization of metals in biological tissues (gold, silver, metal sulphides and metal selenides). Histochemistry 81:331-335.

Danscher G, Juhl S, Stoltenberg M, Krunderup B, Schroder HD, Andreasen A (1997) Autometallographic silver enhancement of zinc sulfide crystals created in cryostat sections from human brain biopsies: a new technique that makes it feasible to demonstrate zinc ions in tissue sections from biopsies and early autopsy material. J Histochem Cytochem 45:1503-1510.

Das DK, Maulik N (2003) Preconditioning potentiates redox signaling and converts death signal into survival signal. Arch Biochem Biophys 420:305-311.

Dave KR, DeFazio RA, Raval AP, Torraco A, Saul I, Barrientos A, Perez-Pinzon MA (2008) Ischemic preconditioning targets the respiration of synaptic mitochondria via protein kinase C epsilon. J Neurosci 28:4172-4182.

Devinney MJ, 2nd, Reynolds IJ, Dineley KE (2005) Simultaneous detection of intracellular free calcium and zinc using fura-2FF and FluoZin-3. Cell Calcium 37:225-232.

Dhodda VK, Sailor KA, Bowen KK, Vemuganti R (2004) Putative endogenous mediators of preconditioning-induced ischemic tolerance in rat brain identified by genomic and proteomic analysis. J Neurochem 89:73-89.

Dietz RM, Weiss JH, Shuttleworth CW (2008) Zn2+ influx is critical for some forms of spreading depression in brain slices. J Neurosci 28:8014-8024.

Dietz RM, Weiss JH, Shuttleworth CW (2009) Contributions of Ca2+ and Zn2+ to spreading depression-like events and neuronal injury. J Neurochem 109 Suppl 1:145-152.

Dineley KE, Richards LL, Votyakova TV, Reynolds IJ (2005) Zinc causes loss of membrane potential and elevates reactive oxygen species in rat brain mitochondria. Mitochondrion 5:55-65.

Dineley KE, Devinney MJ, 2nd, Zeak JA, Rintoul GL, Reynolds IJ (2008) Glutamate mobilizes [Zn2+] through Ca2+ -dependent reactive oxygen species accumulation. J Neurochem 106:2184-2193.

Dingledine R, Borges K, Bowie D, Traynelis SF (1999) The glutamate receptor ion channels. Pharmacol Rev 51:7-61.

Dirnagl U, Simon RP, Hallenbeck JM (2003) Ischemic tolerance and endogenous neuroprotection. Trends Neurosci 26:248-254.

Dirnagl U, Becker K, Meisel A (2009) Preconditioning and tolerance against cerebral ischaemia: from experimental strategies to clinical use. Lancet Neurol 8:398-412.

Du J, Haak LL, Phillips-Tansey E, Russell JT, McBain CJ (2000) Frequency-dependent regulation of rat hippocampal somato-dendritic excitability by the K+ channel subunit Kv2.1. J Physiol 522 Pt 1:19-31.

Du S, McLaughlin B, Pal S, Aizenman E (2002) In vitro neurotoxicity of methylisothiazolinone, a commonly used industrial and household biocide, proceeds via a zinc and extracellular

signal-regulated kinase mitogen-activated protein kinase-dependent pathway. J Neurosci 22:7408-7416.
Dufner-Beattie J, Kuo YM, Gitschier J, Andrews GK (2004) The adaptive response to dietary zinc in mice involves the differential cellular localization and zinc regulation of the zinc transporters ZIP4 and ZIP5. J Biol Chem 279:49082-49090.
Dufner-Beattie J, Langmade SJ, Wang F, Eide D, Andrews GK (2003) Structure, function, and regulation of a subfamily of mouse zinc transporter genes. J Biol Chem 278:50142-50150.
Dykxhoorn DM, Novina CD, Sharp PA (2003) Killing the messenger: short RNAs that silence gene expression. Nat Rev Mol Cell Biol 4:457-467.
Eide DJ (2003) Multiple regulatory mechanisms maintain zinc homeostasis in Saccharomyces cerevisiae. J Nutr 133:1532S-1535S.
Eide DJ (2004) The SLC39 family of metal ion transporters. Pflugers Arch 447:796-800.
Endres M, Namura S, Shimizu-Sasamata M, Waeber C, Zhang L, Gomez-Isla T, Hyman BT, Moskowitz MA (1998) Attenuation of delayed neuronal death after mild focal ischemia in mice by inhibition of the caspase family. J Cereb Blood Flow Metab 18:238-247.
Erickson JC, Sewell AK, Jensen LT, Winge DR, Palmiter RD (1994) Enhanced neurotrophic activity in Alzheimer's disease cortex is not associated with down-regulation of metallothionein-III (GIF). Brain Res 649:297-304.
Fink K, Zhu J, Namura S, Shimizu-Sasamata M, Endres M, Ma J, Dalkara T, Yuan J, Moskowitz MA (1998) Prolonged therapeutic window for ischemic brain damage caused by delayed caspase activation. J Cereb Blood Flow Metab 18:1071-1076.
Fliss H, Menard M (1992) Oxidant-induced mobilization of zinc from metallothionein. Arch Biochem Biophys 293:195-199.
Forbes RA, Steenbergen C, Murphy E (2001) Diazoxide-induced cardioprotection requires signaling through a redox-sensitive mechanism. Circ Res 88:802-809.
Franklin RB, Ma J, Zou J, Guan Z, Kukoyi BI, Feng P, Costello LC (2003) Human ZIP1 is a major zinc uptake transporter for the accumulation of zinc in prostate cells. J Inorg Biochem 96:435-442.
Frederickson CJ (1989) Neurobiology of zinc and zinc-containing neurons. Int Rev Neurobiol 31:145-238.
Frederickson CJ, Bush AI (2001) Synaptically released zinc: physiological functions and pathological effects. Biometals 14:353-366.
Frederickson CJ, Hernandez MD, McGinty JF (1989) Translocation of zinc may contribute to seizure-induced death of neurons. Brain Res 480:317-321.
Frederickson CJ, Koh JY, Bush AI (2005) The neurobiology of zinc in health and disease. Nat Rev Neurosci 6:449-462.
Frederickson CJ, Hernandez MD, Goik SA, Morton JD, McGinty JF (1988) Loss of zinc staining from hippocampal mossy fibers during kainic acid induced seizures: a histofluorescence study. Brain Res 446:383-386.
Frederickson CJ, Suh SW, Koh JY, Cha YK, Thompson RB, LaBuda CJ, Balaji RV, Cuajungco MP (2002) Depletion of intracellular zinc from neurons by use of an extracellular chelator in vivo and in vitro. J Histochem Cytochem 50:1659-1662.
Gaither LA, Eide DJ (2001) The human ZIP1 transporter mediates zinc uptake in human K562 erythroleukemia cells. J Biol Chem 276:22258-22264.
Galasso SL, Dyck RH (2007) The role of zinc in cerebral ischemia. Mol Med 13:380-387.

Garner DL, Johnson LA, Yue ST, Roth BL, Haugland RP (1994) Dual DNA staining assessment of bovine sperm viability using SYBR-14 and propidium iodide. J Androl 15:620-629.
Garnier P, Ying W, Swanson RA (2003) Ischemic preconditioning by caspase cleavage of poly(ADP-ribose) polymerase-1. J Neurosci 23:7967-7973.
Garrett SH, Xiong X, Arizono K, Brady FO (1992) Phorbol ester induction of rat hepatic metallothionein in vivo and in vitro. Int J Biochem 24:1669-1676.
Ge B, Gram H, Di Padova F, Huang B, New L, Ulevitch RJ, Luo Y, Han J (2002) MAPKK-independent activation of p38alpha mediated by TAB1-dependent autophosphorylation of p38alpha. Science 295:1291-1294.
Gee KR, Zhou ZL, Ton-That D, Sensi SL, Weiss JH (2002) Measuring zinc in living cells. A new generation of sensitive and selective fluorescent probes. Cell Calcium 31:245-251.
Geiger JR, Melcher T, Koh DS, Sakmann B, Seeburg PH, Jonas P, Monyer H (1995) Relative abundance of subunit mRNAs determines gating and Ca2+ permeability of AMPA receptors in principal neurons and interneurons in rat CNS. Neuron 15:193-204.
Gidday JM (2006) Cerebral preconditioning and ischaemic tolerance. Nat Rev Neurosci 7:437-448.
Goldberg J, Huang HB, Kwon YG, Greengard P, Nairn AC, Kuriyan J (1995) Three-dimensional structure of the catalytic subunit of protein serine/threonine phosphatase-1. Nature 376:745-753.
Goldberg MP, Weiss JH, Pham PC, Choi DW (1987) N-methyl-D-aspartate receptors mediate hypoxic neuronal injury in cortical culture. J Pharmacol Exp Ther 243:784-791.
Gonzalez-Zulueta M, Feldman AB, Klesse LJ, Kalb RG, Dillman JF, Parada LF, Dawson TM, Dawson VL (2000) Requirement for nitric oxide activation of p21(ras)/extracellular regulated kinase in neuronal ischemic preconditioning. Proc Natl Acad Sci U S A 97:436-441.
Gorter JA, Petrozzino JJ, Aronica EM, Rosenbaum DM, Opitz T, Bennett MV, Connor JA, Zukin RS (1997) Global ischemia induces downregulation of Glur2 mRNA and increases AMPA receptor-mediated Ca2+ influx in hippocampal CA1 neurons of gerbil. J Neurosci 17:6179-6188.
Grabb MC, Choi DW (1999) Ischemic tolerance in murine cortical cell culture: critical role for NMDA receptors. J Neurosci 19:1657-1662.
Greger IH, Khatri L, Kong X, Ziff EB (2003) AMPA receptor tetramerization is mediated by Q/R editing. Neuron 40:763-774.
Ha HC, Snyder SH (1999) Poly(ADP-ribose) polymerase is a mediator of necrotic cell death by ATP depletion. Proc Natl Acad Sci U S A 96:13978-13982.
Haase H, Maret W (2003) Intracellular zinc fluctuations modulate protein tyrosine phosphatase activity in insulin/insulin-like growth factor-1 signaling. Exp Cell Res 291:289-298.
Haase H, Maret W (2005) Fluctuations of cellular, available zinc modulate insulin signaling via inhibition of protein tyrosine phosphatases. J Trace Elem Med Biol 19:37-42.
Hansen MB, Nielsen SE, Berg K (1989) Re-examination and further development of a precise and rapid dye method for measuring cell growth/cell kill. J Immunol Methods 119:203-210.
Haq F, Mahoney M, Koropatnick J (2003) Signaling events for metallothionein induction. Mutat Res 533:211-226.
Hara H, Aizenman E (2004) A molecular technique for detecting the liberation of intracellular zinc in cultured neurons. J Neurosci Methods 137:175-180.

Hartnett KA, Stout AK, Rajdev S, Rosenberg PA, Reynolds IJ, Aizenman E (1997) NMDA receptor-mediated neurotoxicity: a paradoxical requirement for extracellular Mg2+ in Na+/Ca2+-free solutions in rat cortical neurons in vitro. J Neurochem 68:1836-1845.

Heller B, Wang ZQ, Wagner EF, Radons J, Burkle A, Fehsel K, Burkart V, Kolb H (1995) Inactivation of the poly(ADP-ribose) polymerase gene affects oxygen radical and nitric oxide toxicity in islet cells. J Biol Chem 270:11176-11180.

Hertel C, Hauser N, Schubenel R, Seilheimer B, Kemp JA (1996) Beta-amyloid-induced cell toxicity: enhancement of 3-(4,5-dimethylthiazol-2-yl)-2,5-diphenyltetrazolium bromide-dependent cell death. J Neurochem 67:272-276.

Heuchel R, Radtke F, Georgiev O, Stark G, Aguet M, Schaffner W (1994) The transcription factor MTF-1 is essential for basal and heavy metal-induced metallothionein gene expression. EMBO J 13:2870-2875.

Hidalgo J, Gasull T, Giralt M, Armario A (1994) Brain metallothionein in stress. Biol Signals 3:198-210.

Hidalgo J, Aschner M, Zatta P, Vasak M (2001) Roles of the metallothionein family of proteins in the central nervous system. Brain Res Bull 55:133-145.

Hong SH, Maret W (2003) A fluorescence resonance energy transfer sensor for the beta-domain of metallothionein. Proc Natl Acad Sci U S A 100:2255-2260.

Hosie AM, Dunne EL, Harvey RJ, Smart TG (2003) Zinc-mediated inhibition of GABA(A) receptors: discrete binding sites underlie subtype specificity. Nat Neurosci 6:362-369.

Huang J, Zhang D, Xing W, Ma X, Yin Y, Wei Q, Li G (2008a) An approach to assay calcineurin activity and the inhibitory effect of zinc ion. Anal Biochem 375:385-387.

Huang YZ, Pan E, Xiong ZQ, McNamara JO (2008b) Zinc-mediated transactivation of TrkB potentiates the hippocampal mossy fiber-CA3 pyramid synapse. Neuron 57:546-558.

Hughes FM, Jr., Cidlowski JA (1999) Potassium is a critical regulator of apoptotic enzymes in vitro and in vivo. Adv Enzyme Regul 39:157-171.

Ichijo H, Nishida E, Irie K, ten Dijke P, Saitoh M, Moriguchi T, Takagi M, Matsumoto K, Miyazono K, Gotoh Y (1997) Induction of apoptosis by ASK1, a mammalian MAPKKK that activates SAPK/JNK and p38 signaling pathways. Science 275:90-94.

Imbra RJ, Karin M (1987) Metallothionein gene expression is regulated by serum factors and activators of protein kinase C. Mol Cell Biol 7:1358-1363.

Jacob C, Maret W, Vallee BL (1998) Control of zinc transfer between thionein, metallothionein, and zinc proteins. Proc Natl Acad Sci U S A 95:3489-3494.

Jacob C, Maret W, Vallee BL (1999) Selenium redox biochemistry of zinc-sulfur coordination sites in proteins and enzymes. Proc Natl Acad Sci U S A 96:1910-1914.

Jiang D, Sullivan PG, Sensi SL, Steward O, Weiss JH (2001) Zn(2+) induces permeability transition pore opening and release of pro-apoptotic peptides from neuronal mitochondria. J Biol Chem 276:47524-47529.

Jiang H, Fu K, Andrews GK (2004) Gene- and cell-type-specific effects of signal transduction cascades on metal-regulated gene transcription appear to be independent of changes in the phosphorylation of metal-response-element-binding transcription factor-1. Biochem J 382:33-41.

Jiang LJ, Maret W, Vallee BL (1998) The glutathione redox couple modulates zinc transfer from metallothionein to zinc-depleted sorbitol dehydrogenase. Proc Natl Acad Sci U S A 95:3483-3488.

Jibiki I, Hashimoto S, Maruoka S, Gon Y, Matsuzawa A, Nishitoh H, Ichijo H, Horie T (2003) Apoptosis signal-regulating kinase 1-mediated signaling pathway regulates nitric oxide-induced activator protein-1 activation in human bronchial epithelial cells. Am J Respir Crit Care Med 167:856-861.

Kadowaki H, Nishitoh H, Urano F, Sadamitsu C, Matsuzawa A, Takeda K, Masutani H, Yodoi J, Urano Y, Nagano T, Ichijo H (2005) Amyloid beta induces neuronal cell death through ROS-mediated ASK1 activation. Cell Death Differ 12:19-24.

Kagi JH, Schaffer A (1988) Biochemistry of metallothionein. Biochemistry 27:8509-8515.

Kasischke K, Ludolph AC, Riepe MW (1996) NMDA-antagonists reverse increased hypoxic tolerance by preceding chemical hypoxia. Neurosci Lett 214:175-178.

Kato H, Liu Y, Araki T, Kogure K (1992) MK-801, but not anisomycin, inhibits the induction of tolerance to ischemia in the gerbil hippocampus. Neurosci Lett 139:118-121.

Kay AR (2003) Evidence for chelatable zinc in the extracellular space of the hippocampus, but little evidence for synaptic release of Zn. J Neurosci 23:6847-6855.

Kerr JF, Wyllie AH, Currie AR (1972) Apoptosis: a basic biological phenomenon with wide-ranging implications in tissue kinetics. Br J Cancer 26:239-257.

Kim EY, Koh JY, Kim YH, Sohn S, Joe E, Gwag BJ (1999a) Zn2+ entry produces oxidative neuronal necrosis in cortical cell cultures. Eur J Neurosci 11:327-334.

Kim S, Jung Y, Kim D, Koh H, Chung J (2000) Extracellular zinc activates p70 S6 kinase through the phosphatidylinositol 3-kinase signaling pathway. J Biol Chem 275:25979-25984.

Kim TY, Hwang JJ, Yun SH, Jung MW, Koh JY (2002) Augmentation by zinc of NMDA receptor-mediated synaptic responses in CA1 of rat hippocampal slices: mediation by Src family tyrosine kinases. Synapse 46:49-56.

Kim YH, Kim EY, Gwag BJ, Sohn S, Koh JY (1999b) Zinc-induced cortical neuronal death with features of apoptosis and necrosis: mediation by free radicals. Neuroscience 89:175-182.

Kim YM, Reed W, Wu W, Bromberg PA, Graves LM, Samet JM (2006) Zn2+-induced IL-8 expression involves AP-1, JNK, and ERK activities in human airway epithelial cells. Am J Physiol Lung Cell Mol Physiol 290:L1028-1035.

King MM, Huang CY (1984) The calmodulin-dependent activation and deactivation of the phosphoprotein phosphatase, calcineurin, and the effect of nucleotides, pyrophosphate, and divalent metal ions. Identification of calcineurin as a Zn and Fe metalloenzyme. J Biol Chem 259:8847-8856.

Kingsbury AE, Gallo V, Woodhams PL, Balazs R (1985) Survival, morphology and adhesion properties of cerebellar interneurones cultured in chemically defined and serum-supplemented medium. Brain Res 349:17-25.

Kitagawa K, Matsumoto M, Tagaya M, Hata R, Ueda H, Niinobe M, Handa N, Fukunaga R, Kimura K, Mikoshiba K, et al. (1990) 'Ischemic tolerance' phenomenon found in the brain. Brain Res 528:21-24.

Knapp LT, Klann E (2000) Superoxide-induced stimulation of protein kinase C via thiol modification and modulation of zinc content. J Biol Chem 275:24136-24145.

Knoch ME, Hartnett KA, Hara H, Kandler K, Aizenman E (2008) Microglia induce neurotoxicity via intraneuronal Zn(2+) release and a K(+) current surge. Glia 56:89-96.

Koh JY, Choi DW (1987) Quantitative determination of glutamate mediated cortical neuronal injury in cell culture by lactate dehydrogenase efflux assay. J Neurosci Methods 20:83-90.

Koh JY, Choi DW (1988) Vulnerability of cultured cortical neurons to damage by excitotoxins: differential susceptibility of neurons containing NADPH-diaphorase. J Neurosci 8:2153-2163.
Koh JY, Choi DW (1994) Zinc toxicity on cultured cortical neurons: involvement of N-methyl-D-aspartate receptors. Neuroscience 60:1049-1057.
Koh JY, Suh SW, Gwag BJ, He YY, Hsu CY, Choi DW (1996) The role of zinc in selective neuronal death after transient global cerebral ischemia. Science 272:1013-1016.
Koponen S, Goldsteins G, Keinanen R, Koistinaho J (2000) Induction of protein kinase Cdelta subspecies in neurons and microglia after transient global brain ischemia. J Cereb Blood Flow Metab 20:93-102.
Korichneva I (2005) Redox regulation of cardiac protein kinase C. Exp Clin Cardiol 10:256-261.
Kramer KK, Zoelle JT, Klaassen CD (1996a) Induction of metallothionein mRNA and protein in primary murine neuron cultures. Toxicol Appl Pharmacol 141:1-7.
Kramer KK, Liu J, Choudhuri S, Klaassen CD (1996b) Induction of metallothionein mRNA and protein in murine astrocyte cultures. Toxicol Appl Pharmacol 136:94-100.
Krezel A, Maret W (2006) Zinc-buffering capacity of a eukaryotic cell at physiological pZn. J Biol Inorg Chem 11:1049-1062.
Krezel A, Maret W (2007) Dual nanomolar and picomolar Zn(II) binding properties of metallothionein. J Am Chem Soc 129:10911-10921.
Krezel A, Hao Q, Maret W (2007) The zinc/thiolate redox biochemistry of metallothionein and the control of zinc ion fluctuations in cell signaling. Arch Biochem Biophys 463:188-200.
Kristian T, Siesjo BK (1998) Calcium in ischemic cell death. Stroke 29:705-718.
Krnjevic K (2008) Electrophysiology of cerebral ischemia. Neuropharmacology 55:319-333.
Kwak S, Weiss JH (2006) Calcium-permeable AMPA channels in neurodegenerative disease and ischemia. Curr Opin Neurobiol 16:281-287.
Langmade SJ, Ravindra R, Daniels PJ, Andrews GK (2000) The transcription factor MTF-1 mediates metal regulation of the mouse ZnT1 gene. J Biol Chem 275:34803-34809.
Larochelle O, Stewart G, Moffatt P, Tremblay V, Seguin C (2001a) Characterization of the mouse metal-regulatory-element-binding proteins, metal element protein-1 and metal regulatory transcription factor-1. Biochem J 353:591-601.
LaRochelle O, Gagne V, Charron J, Soh JW, Seguin C (2001b) Phosphorylation is involved in the activation of metal-regulatory transcription factor 1 in response to metal ions. J Biol Chem 276:41879-41888.
Laube B, Kuhse J, Rundstrom N, Kirsch J, Schmieden V, Betz H (1995) Modulation by zinc ions of native rat and recombinant human inhibitory glycine receptors. J Physiol 483 (Pt 3):613-619.
Lazebnik YA, Kaufmann SH, Desnoyers S, Poirier GG, Earnshaw WC (1994) Cleavage of poly(ADP-ribose) polymerase by a proteinase with properties like ICE. Nature 371:346-347.
Le DA, Wu Y, Huang Z, Matsushita K, Plesnila N, Augustinack JC, Hyman BT, Yuan J, Kuida K, Flavell RA, Moskowitz MA (2002) Caspase activation and neuroprotection in caspase-3- deficient mice after in vivo cerebral ischemia and in vitro oxygen glucose deprivation. Proc Natl Acad Sci U S A 99:15188-15193.
Lee JM, Zipfel GJ, Choi DW (1999) The changing landscape of ischaemic brain injury mechanisms. Nature 399:A7-14.

Lee JY, Cole TB, Palmiter RD, Koh JY (2000) Accumulation of zinc in degenerating hippocampal neurons of ZnT3-null mice after seizures: evidence against synaptic vesicle origin. J Neurosci 20:RC79.

Lee JY, Kim JH, Palmiter RD, Koh JY (2003) Zinc released from metallothionein-iii may contribute to hippocampal CA1 and thalamic neuronal death following acute brain injury. Exp Neurol 184:337-347.

Lee JY, Kim YJ, Kim TY, Koh JY, Kim YH (2008) Essential role for zinc-triggered p75NTR activation in preconditioning neuroprotection. J Neurosci 28:10919-10927.

Lerma J, Morales M, Ibarz JM, Somohano F (1994) Rectification properties and Ca2+ permeability of glutamate receptor channels in hippocampal cells. Eur J Neurosci 6:1080-1088.

Li Y, Hough CJ, Frederickson CJ, Sarvey JM (2001a) Induction of mossy fiber --> Ca3 long-term potentiation requires translocation of synaptically released Zn2+. J Neurosci 21:8015-8025.

Li Y, Hough CJ, Suh SW, Sarvey JM, Frederickson CJ (2001b) Rapid translocation of Zn(2+) from presynaptic terminals into postsynaptic hippocampal neurons after physiological stimulation. J Neurophysiol 86:2597-2604.

Lim ST, Antonucci DE, Scannevin RH, Trimmer JS (2000) A novel targeting signal for proximal clustering of the Kv2.1 K+ channel in hippocampal neurons. Neuron 25:385-397.

Liu H, Nishitoh H, Ichijo H, Kyriakis JM (2000) Activation of apoptosis signal-regulating kinase 1 (ASK1) by tumor necrosis factor receptor-associated factor 2 requires prior dissociation of the ASK1 inhibitor thioredoxin. Mol Cell Biol 20:2198-2208.

Liu Y, Min W (2002) Thioredoxin promotes ASK1 ubiquitination and degradation to inhibit ASK1-mediated apoptosis in a redox activity-independent manner. Circ Res 90:1259-1266.

Liuzzi JP, Cousins RJ (2004) Mammalian zinc transporters. Annu Rev Nutr 24:151-172.

Lo EH, Dalkara T, Moskowitz MA (2003) Mechanisms, challenges and opportunities in stroke. Nat Rev Neurosci 4:399-415.

Lobner D, Canzoniero LM, Manzerra P, Gottron F, Ying H, Knudson M, Tian M, Dugan LL, Kerchner GA, Sheline CT, Korsmeyer SJ, Choi DW (2000) Zinc-induced neuronal death in cortical neurons. Cell Mol Biol (Noisy-le-grand) 46:797-806.

Machino T, Hashimoto S, Maruoka S, Gon Y, Hayashi S, Mizumura K, Nishitoh H, Ichijo H, Horie T (2003) Apoptosis signal-regulating kinase 1-mediated signaling pathway regulates hydrogen peroxide-induced apoptosis in human pulmonary vascular endothelial cells. Crit Care Med 31:2776-2781.

Malin SA, Nerbonne JM (2002) Delayed rectifier K+ currents, IK, are encoded by Kv2 alpha-subunits and regulate tonic firing in mammalian sympathetic neurons. J Neurosci 22:10094-10105.

Manev H, Kharlamov E, Uz T, Mason RP, Cagnoli CM (1997) Characterization of zinc-induced neuronal death in primary cultures of rat cerebellar granule cells. Exp Neurol 146:171-178.

Maret W (1994) Oxidative metal release from metallothionein via zinc-thiol/disulfide interchange. Proc Natl Acad Sci U S A 91:237-241.

Maret W (1995) Metallothionein/disulfide interactions, oxidative stress, and the mobilization of cellular zinc. Neurochem Int 27:111-117.

Maret W, Vallee BL (1998) Thiolate ligands in metallothionein confer redox activity on zinc clusters. Proc Natl Acad Sci U S A 95:3478-3482.
Maret W, Jacob C, Vallee BL, Fischer EH (1999) Inhibitory sites in enzymes: zinc removal and reactivation by thionein. Proc Natl Acad Sci U S A 96:1936-1940.
Martiny-Baron G, Kazanietz MG, Mischak H, Blumberg PM, Kochs G, Hug H, Marme D, Schachtele C (1993) Selective inhibition of protein kinase C isozymes by the indolocarbazole Go 6976. J Biol Chem 268:9194-9197.
Maske H (1955) [A new method for demonstrating A and B cells in the islands of Langerhans.]. Klin Wochenschr 33:1058.
Masters BA, Quaife CJ, Erickson JC, Kelly EJ, Froelick GJ, Zambrowicz BP, Brinster RL, Palmiter RD (1994) Metallothionein III is expressed in neurons that sequester zinc in synaptic vesicles. J Neurosci 14:5844-5857.
Matsukawa J, Matsuzawa A, Takeda K, Ichijo H (2004) The ASK1-MAP kinase cascades in mammalian stress response. J Biochem 136:261-265.
Matsushita K, Kitagawa K, Matsuyama T, Ohtsuki T, Taguchi A, Mandai K, Mabuchi T, Yagita Y, Yanagihara T, Matsumoto M (1996) Effect of systemic zinc administration on delayed neuronal death in the gerbil hippocampus. Brain Res 743:362-365.
Mattson MP, Lovell MA, Ehmann WD, Markesbery WR (1993) Comparison of the effects of elevated intracellular aluminum and calcium levels on neuronal survival and tau immunoreactivity. Brain Res 602:21-31.
McDonald JW, Silverstein FS, Johnston MV (1987) MK-801 protects the neonatal brain from hypoxic-ischemic damage. Eur J Pharmacol 140:359-361.
McLaughlin B, Pal S, Tran MP, Parsons AA, Barone FC, Erhardt JA, Aizenman E (2001) p38 activation is required upstream of potassium current enhancement and caspase cleavage in thiol oxidant-induced neuronal apoptosis. J Neurosci 21:3303-3311.
McLaughlin B, Hartnett KA, Erhardt JA, Legos JJ, White RF, Barone FC, Aizenman E (2003) Caspase 3 activation is essential for neuroprotection in preconditioning. Proc Natl Acad Sci U S A 100:715-720.
McMahon RJ, Cousins RJ (1998) Regulation of the zinc transporter ZnT-1 by dietary zinc. Proc Natl Acad Sci U S A 95:4841-4846.
Medvedeva YV, Lin B, Shuttleworth CW, Weiss JH (2009) Intracellular Zn2+ accumulation contributes to synaptic failure, mitochondrial depolarization, and cell death in an acute slice oxygen-glucose deprivation model of ischemia. J Neurosci 29:1105-1114.
Meller R, Minami M, Cameron JA, Impey S, Chen D, Lan JQ, Henshall DC, Simon RP (2005) CREB-mediated Bcl-2 protein expression after ischemic preconditioning. J Cereb Blood Flow Metab 25:234-246.
Mills JC, Nelson D, Erecinska M, Pittman RN (1995) Metabolic and energetic changes during apoptosis in neural cells. J Neurochem 65:1721-1730.
Misonou H, Thompson SM, Cai X (2008) Dynamic regulation of the Kv2.1 voltage-gated potassium channel during brain ischemia through neuroglial interaction. J Neurosci 28:8529-8538.
Misonou H, Mohapatra DP, Menegola M, Trimmer JS (2005) Calcium- and metabolic state-dependent modulation of the voltage-dependent Kv2.1 channel regulates neuronal excitability in response to ischemia. J Neurosci 25:11184-11193.

Misonou H, Mohapatra DP, Park EW, Leung V, Zhen D, Misonou K, Anderson AE, Trimmer JS (2004) Regulation of ion channel localization and phosphorylation by neuronal activity. Nat Neurosci 7:711-718.

Mohapatra DP, Trimmer JS (2006) The Kv2.1 C terminus can autonomously transfer Kv2.1-like phosphorylation-dependent localization, voltage-dependent gating, and muscarinic modulation to diverse Kv channels. J Neurosci 26:685-695.

Morikawa E, Mori H, Kiyama Y, Mishina M, Asano T, Kirino T (1998) Attenuation of focal ischemic brain injury in mice deficient in the epsilon1 (NR2A) subunit of NMDA receptor. J Neurosci 18:9727-9732.

Mosmann T (1983) Rapid colorimetric assay for cellular growth and survival: application to proliferation and cytotoxicity assays. J Immunol Methods 65:55-63.

Muir KW (2006) Glutamate-based therapeutic approaches: clinical trials with NMDA antagonists. Curr Opin Pharmacol 6:53-60.

Mulholland PJ, Carpenter-Hyland EP, Hearing MC, Becker HC, Woodward JJ, Chandler LJ (2008) Glutamate transporters regulate extrasynaptic NMDA receptor modulation of Kv2.1 potassium channels. J Neurosci 28:8801-8809.

Murakoshi H, Trimmer JS (1999) Identification of the Kv2.1 K+ channel as a major component of the delayed rectifier K+ current in rat hippocampal neurons. J Neurosci 19:1728-1735.

Murata M, Gong P, Suzuki K, Koizumi S (1999) Differential metal response and regulation of human heavy metal-inducible genes. J Cell Physiol 180:105-113.

Murphy BJ, Andrews GK, Bittel D, Discher DJ, McCue J, Green CJ, Yanovsky M, Giaccia A, Sutherland RM, Laderoute KR, Webster KA (1999) Activation of metallothionein gene expression by hypoxia involves metal response elements and metal transcription factor-1. Cancer Res 59:1315-1322.

Murry CE, Jennings RB, Reimer KA (1986) Preconditioning with ischemia: a delay of lethal cell injury in ischemic myocardium. Circulation 74:1124-1136.

Namura S, Zhu J, Fink K, Endres M, Srinivasan A, Tomaselli KJ, Yuan J, Moskowitz MA (1998) Activation and cleavage of caspase-3 in apoptosis induced by experimental cerebral ischemia. J Neurosci 18:3659-3668.

Nandagopal K, Dawson TM, Dawson VL (2001) Critical role for nitric oxide signaling in cardiac and neuronal ischemic preconditioning and tolerance. J Pharmacol Exp Ther 297:474-478.

Newton AC (2001) Protein kinase C: structural and spatial regulation by phosphorylation, cofactors, and macromolecular interactions. Chem Rev 101:2353-2364.

Nishimura M, Sugino T, Nozaki K, Takagi Y, Hattori I, Hayashi J, Hashimoto N, Moriguchi T, Nishida E (2003) Activation of p38 kinase in the gerbil hippocampus showing ischemic tolerance. J Cereb Blood Flow Metab 23:1052-1059.

Nishitoh H, Matsuzawa A, Tobiume K, Saegusa K, Takeda K, Inoue K, Hori S, Kakizuka A, Ichijo H (2002) ASK1 is essential for endoplasmic reticulum stress-induced neuronal cell death triggered by expanded polyglutamine repeats. Genes Dev 16:1345-1355.

Noh KM, Koh JY (2000) Induction and activation by zinc of NADPH oxidase in cultured cortical neurons and astrocytes. J Neurosci 20:RC111.

Noh KM, Kim YH, Koh JY (1999) Mediation by membrane protein kinase C of zinc-induced oxidative neuronal injury in mouse cortical cultures. J Neurochem 72:1609-1616.

Noh KM, Yokota H, Mashiko T, Castillo PE, Zukin RS, Bennett MV (2005) Blockade of calcium-permeable AMPA receptors protects hippocampal neurons against global ischemia-induced death. Proc Natl Acad Sci U S A 102:12230-12235.

Nolte C, Gore A, Sekler I, Kresse W, Hershfinkel M, Hoffmann A, Kettenmann H, Moran A (2004) ZnT-1 expression in astroglial cells protects against zinc toxicity and slows the accumulation of intracellular zinc. Glia 48:145-155.

Novalija E, Kevin LG, Camara AK, Bosnjak ZJ, Kampine JP, Stowe DF (2003) Reactive oxygen species precede the epsilon isoform of protein kinase C in the anesthetic preconditioning signaling cascade. Anesthesiology 99:421-428.

O'Connell KM, Rolig AS, Whitesell JD, Tamkun MM (2006) Kv2.1 potassium channels are retained within dynamic cell surface microdomains that are defined by a perimeter fence. J Neurosci 26:9609-9618.

O'Duffy AE, Bordelon YM, McLaughlin B (2007) Killer proteases and little strokes--how the things that do not kill you make you stronger. J Cereb Blood Flow Metab 27:655-668.

Obenauer JC, Cantley LC, Yaffe MB (2003) Scansite 2.0: Proteome-wide prediction of cell signaling interactions using short sequence motifs. Nucleic Acids Res 31:3635-3641.

Obrenovitch TP (2008) Molecular physiology of preconditioning-induced brain tolerance to ischemia. Physiol Rev 88:211-247.

Ogoshi F, Weiss JH (2003) Heterogeneity of Ca2+-permeable AMPA/kainate channel expression in hippocampal pyramidal neurons: fluorescence imaging and immunocytochemical assessment. J Neurosci 23:10521-10530.

Ohana E, Sekler I, Kaisman T, Kahn N, Cove J, Silverman WF, Amsterdam A, Hershfinkel M (2006) Silencing of ZnT-1 expression enhances heavy metal influx and toxicity. J Mol Med 84:753-763.

Olney JW (1986) Inciting excitotoxic cytocide among central neurons. Adv Exp Med Biol 203:631-645.

Opitz T, Grooms SY, Bennett MV, Zukin RS (2000) Remodeling of alpha-amino-3-hydroxy-5-methyl-4-isoxazole-propionic acid receptor subunit composition in hippocampal neurons after global ischemia. Proc Natl Acad Sci U S A 97:13360-13365.

Ormerod MG, Collins MK, Rodriguez-Tarduchy G, Robertson D (1992) Apoptosis in interleukin-3-dependent haemopoietic cells. Quantification by two flow cytometric methods. J Immunol Methods 153:57-65.

Outten CE, O'Halloran TV (2001) Femtomolar sensitivity of metalloregulatory proteins controlling zinc homeostasis. Science 292:2488-2492.

Pain T, Yang XM, Critz SD, Yue Y, Nakano A, Liu GS, Heusch G, Cohen MV, Downey JM (2000) Opening of mitochondrial K(ATP) channels triggers the preconditioned state by generating free radicals. Circ Res 87:460-466.

Pal S, He K, Aizenman E (2004) Nitrosative stress and potassium channel-mediated neuronal apoptosis: is zinc the link? Pflugers Arch 448:296-303.

Pal S, Hartnett KA, Nerbonne JM, Levitan ES, Aizenman E (2003) Mediation of neuronal apoptosis by Kv2.1-encoded potassium channels. J Neurosci 23:4798-4802.

Pal SK, Takimoto K, Aizenman E, Levitan ES (2006) Apoptotic surface delivery of K+ channels. Cell Death Differ 13:661-667.

Palmiter RD (1994) Regulation of metallothionein genes by heavy metals appears to be mediated by a zinc-sensitive inhibitor that interacts with a constitutively active transcription factor, MTF-1. Proc Natl Acad Sci U S A 91:1219-1223.

Palmiter RD (1998) The elusive function of metallothioneins. Proc Natl Acad Sci U S A 95:8428-8430.
Palmiter RD (2004) Protection against zinc toxicity by metallothionein and zinc transporter 1. Proc Natl Acad Sci U S A 101:4918-4923.
Palmiter RD, Findley SD (1995) Cloning and functional characterization of a mammalian zinc transporter that confers resistance to zinc. EMBO J 14:639-649.
Palmiter RD, Huang L (2004) Efflux and compartmentalization of zinc by members of the SLC30 family of solute carriers. Pflugers Arch 447:744-751.
Palmiter RD, Cole TB, Quaife CJ, Findley SD (1996) ZnT-3, a putative transporter of zinc into synaptic vesicles. Proc Natl Acad Sci U S A 93:14934-14939.
Paoletti P, Vergnano AM, Barbour B, Casado M (2009) Zinc at glutamatergic synapses. Neuroscience 158:126-136.
Park JA, Koh JY (1999) Induction of an immediate early gene egr-1 by zinc through extracellular signal-regulated kinase activation in cortical culture: its role in zinc-induced neuronal death. J Neurochem 73:450-456.
Park JA, Lee JY, Sato TA, Koh JY (2000) Co-induction of p75NTR and p75NTR-associated death executor in neurons after zinc exposure in cortical culture or transient ischemia in the rat. J Neurosci 20:9096-9103.
Pellegrini-Giampietro DE, Zukin RS, Bennett MV, Cho S, Pulsinelli WA (1992) Switch in glutamate receptor subunit gene expression in CA1 subfield of hippocampus following global ischemia in rats. Proc Natl Acad Sci U S A 89:10499-10503.
Pender MP, Nguyen KB, McCombe PA, Kerr JF (1991) Apoptosis in the nervous system in experimental allergic encephalomyelitis. J Neurol Sci 104:81-87.
Peng PL, Zhong X, Tu W, Soundarapandian MM, Molner P, Zhu D, Lau L, Liu S, Liu F, Lu Y (2006) ADAR2-dependent RNA editing of AMPA receptor subunit GluR2 determines vulnerability of neurons in forebrain ischemia. Neuron 49:719-733.
Penkowa M (2006) Metallothioneins are multipurpose neuroprotectants during brain pathology. FEBS J 273:1857-1870.
Penkowa M, Hidalgo J (2001) Metallothionein treatment reduces proinflammatory cytokines IL-6 and TNF-alpha and apoptotic cell death during experimental autoimmune encephalomyelitis (EAE). Exp Neurol 170:1-14.
Penkowa M, Carrasco J, Giralt M, Moos T, Hidalgo J (1999) CNS wound healing is severely depressed in metallothionein I- and II-deficient mice. J Neurosci 19:2535-2545.
Perez-Pinzon MA, Dave KR, Raval AP (2005) Role of reactive oxygen species and protein kinase C in ischemic tolerance in the brain. Antioxid Redox Signal 7:1150-1157.
Perry SW, Epstein LG, Gelbard HA (1997) Simultaneous in situ detection of apoptosis and necrosis in monolayer cultures by TUNEL and trypan blue staining. Biotechniques 22:1102-1106.
Pettmann B, Henderson CE (1998) Neuronal cell death. Neuron 20:633-647.
Prasad AS (1995) Zinc: an overview. Nutrition 11:93-99.
Puttaparthi K, Gitomer WL, Krishnan U, Son M, Rajendran B, Elliott JL (2002) Disease progression in a transgenic model of familial amyotrophic lateral sclerosis is dependent on both neuronal and non-neuronal zinc binding proteins. J Neurosci 22:8790-8796.
Qian J, Noebels JL (2005) Visualization of transmitter release with zinc fluorescence detection at the mouse hippocampal mossy fibre synapse. J Physiol 566:747-758.

Qian J, Noebels JL (2006) Exocytosis of vesicular zinc reveals persistent depression of neurotransmitter release during metabotropic glutamate receptor long-term depression at the hippocampal CA3-CA1 synapse. J Neurosci 26:6089-6095.
Quest AF, Bloomenthal J, Bardes ES, Bell RM (1992) The regulatory domain of protein kinase C coordinates four atoms of zinc. J Biol Chem 267:10193-10197.
Radtke F, Georgiev O, Muller HP, Brugnera E, Schaffner W (1995) Functional domains of the heavy metal-responsive transcription regulator MTF-1. Nucleic Acids Res 23:2277-2286.
Rao PS, Jaggi M, Smith DJ, Hemstreet GP, Balaji KC (2003) Metallothionein 2A interacts with the kinase domain of PKCmu in prostate cancer. Biochem Biophys Res Commun 310:1032-1038.
Raval AP, Dave KR, Mochly-Rosen D, Sick TJ, Perez-Pinzon MA (2003) Epsilon PKC is required for the induction of tolerance by ischemic and NMDA-mediated preconditioning in the organotypic hippocampal slice. J Neurosci 23:384-391.
Redman PT, He K, Hartnett KA, Jefferson BS, Hu L, Rosenberg PA, Levitan ES, Aizenman E (2007) Apoptotic surge of potassium currents is mediated by p38 phosphorylation of Kv2.1. Proc Natl Acad Sci U S A 104:3568-3573.
Rothwell PM (2001) The high cost of not funding stroke research: a comparison with heart disease and cancer. Lancet 357:1612-1616.
Runden-Pran E, Haug FM, Storm JF, Ottersen OP (2002) BK channel activity determines the extent of cell degeneration after oxygen and glucose deprivation: a study in organotypical hippocampal slice cultures. Neuroscience 112:277-288.
Ryu H, Lee J, Zaman K, Kubilis J, Ferrante RJ, Ross BD, Neve R, Ratan RR (2003) Sp1 and Sp3 are oxidative stress-inducible, antideath transcription factors in cortical neurons. J Neurosci 23:3597-3606.
Sagasti A, Hisamoto N, Hyodo J, Tanaka-Hino M, Matsumoto K, Bargmann CI (2001) The CaMKII UNC-43 activates the MAPKKK NSY-1 to execute a lateral signaling decision required for asymmetric olfactory neuron fates. Cell 105:221-232.
Sagher D, Brunell D, Brot N, Vallee BL, Weissbach H (2006) Selenocompounds can serve as oxidoreductants with the methionine sulfoxide reductase enzymes. J Biol Chem 281:31184-31187.
Saitoh M, Nishitoh H, Fujii M, Takeda K, Tobiume K, Sawada Y, Kawabata M, Miyazono K, Ichijo H (1998) Mammalian thioredoxin is a direct inhibitor of apoptosis signal-regulating kinase (ASK) 1. EMBO J 17:2596-2606.
Santos S, Aizenman E (2002) Functional expression of muscle-type nicotinic acetylcholine receptors in rat forebrain neurons in vitro. Methods Find Exp Clin Pharmacol 24:63-66.
Sarker KP, Biswas KK, Yamakuchi M, Lee KY, Hahiguchi T, Kracht M, Kitajima I, Maruyama I (2003) ASK1-p38 MAPK/JNK signaling cascade mediates anandamide-induced PC12 cell death. J Neurochem 85:50-61.
Sato M, Bremner I (1993) Oxygen free radicals and metallothionein. Free Radic Biol Med 14:325-337.
Satoh M, Naganuma A, Imura N (1988) Involvement of cardiac metallothionein in prevention of adriamycin induced lipid peroxidation in the heart. Toxicology 53:231-237.
Saydam N, Adams TK, Steiner F, Schaffner W, Freedman JH (2002) Regulation of metallothionein transcription by the metal-responsive transcription factor MTF-1: identification of signal transduction cascades that control metal-inducible transcription. J Biol Chem 277:20438-20445.

Scannevin RH, Murakoshi H, Rhodes KJ, Trimmer JS (1996) Identification of a cytoplasmic domain important in the polarized expression and clustering of the Kv2.1 K+ channel. J Cell Biol 135:1619-1632.

Sekler I, Moran A, Hershfinkel M, Dori A, Margulis A, Birenzweig N, Nitzan Y, Silverman WF (2002) Distribution of the zinc transporter ZnT-1 in comparison with chelatable zinc in the mouse brain. J Comp Neurol 447:201-209.

Semenza GL (2001) HIF-1 and mechanisms of hypoxia sensing. Curr Opin Cell Biol 13:167-171.

Sensi SL, Jeng JM (2004) Rethinking the excitotoxic ionic milieu: the emerging role of Zn(2+) in ischemic neuronal injury. Curr Mol Med 4:87-111.

Sensi SL, Yin HZ, Weiss JH (2000) AMPA/kainate receptor-triggered Zn2+ entry into cortical neurons induces mitochondrial Zn2+ uptake and persistent mitochondrial dysfunction. Eur J Neurosci 12:3813-3818.

Sensi SL, Ton-That D, Weiss JH (2002) Mitochondrial sequestration and Ca(2+)-dependent release of cytosolic Zn(2+) loads in cortical neurons. Neurobiol Dis 10:100-108.

Sensi SL, Yin HZ, Carriedo SG, Rao SS, Weiss JH (1999) Preferential Zn2+ influx through Ca2+-permeable AMPA/kainate channels triggers prolonged mitochondrial superoxide production. Proc Natl Acad Sci U S A 96:2414-2419.

Sensi SL, Canzoniero LM, Yu SP, Ying HS, Koh JY, Kerchner GA, Choi DW (1997) Measurement of intracellular free zinc in living cortical neurons: routes of entry. J Neurosci 17:9554-9564.

Sensi SL, Ton-That D, Sullivan PG, Jonas EA, Gee KR, Kaczmarek LK, Weiss JH (2003) Modulation of mitochondrial function by endogenous Zn2+ pools. Proc Natl Acad Sci U S A 100:6157-6162.

Sharp FR, Bernaudin M (2004) HIF1 and oxygen sensing in the brain. Nat Rev Neurosci 5:437-448.

Sheline CT, Wang H, Cai AL, Dawson VL, Choi DW (2003) Involvement of poly ADP ribosyl polymerase-1 in acute but not chronic zinc toxicity. Eur J Neurosci 18:1402-1409.

Simon RP, Swan JH, Griffiths T, Meldrum BS (1984) Blockade of N-methyl-D-aspartate receptors may protect against ischemic damage in the brain. Science 226:850-852.

Sinor JD, Du S, Venneti S, Blitzblau RC, Leszkiewicz DN, Rosenberg PA, Aizenman E (2000) NMDA and glutamate evoke excitotoxicity at distinct cellular locations in rat cortical neurons in vitro. J Neurosci 20:8831-8837.

Slater TF, Sawyer B, Straeuli U (1963) Studies on Succinate-Tetrazolium Reductase Systems. Iii. Points of Coupling of Four Different Tetrazolium Salts. Biochim Biophys Acta 77:383-393.

Smirnova IV, Bittel DC, Ravindra R, Jiang H, Andrews GK (2000) Zinc and cadmium can promote rapid nuclear translocation of metal response element-binding transcription factor-1. J Biol Chem 275:9377-9384.

Soh JW, Lee EH, Prywes R, Weinstein IB (1999) Novel roles of specific isoforms of protein kinase C in activation of the c-fos serum response element. Mol Cell Biol 19:1313-1324.

Sommer B, Kohler M, Sprengel R, Seeburg PH (1991) RNA editing in brain controls a determinant of ion flow in glutamate-gated channels. Cell 67:11-19.

Song JJ, Lee YJ (2003) Differential role of glutaredoxin and thioredoxin in metabolic oxidative stress-induced activation of apoptosis signal-regulating kinase 1. Biochem J 373:845-853.

Spahl DU, Berendji-Grun D, Suschek CV, Kolb-Bachofen V, Kroncke KD (2003) Regulation of zinc homeostasis by inducible NO synthase-derived NO: nuclear metallothionein translocation and intranuclear Zn2+ release. Proc Natl Acad Sci U S A 100:13952-13957.

St Croix CM, Wasserloos KJ, Dineley KE, Reynolds IJ, Levitan ES, Pitt BR (2002) Nitric oxide-induced changes in intracellular zinc homeostasis are mediated by metallothionein/thionein. Am J Physiol Lung Cell Mol Physiol 282:L185-192.

Stenzel-Poore MP, Stevens SL, Simon RP (2004) Genomics of preconditioning. Stroke 35:2683-2686.

Stenzel-Poore MP, Stevens SL, Xiong Z, Lessov NS, Harrington CA, Mori M, Meller R, Rosenzweig HL, Tobar E, Shaw TE, Chu X, Simon RP (2003) Effect of ischaemic preconditioning on genomic response to cerebral ischaemia: similarity to neuroprotective strategies in hibernation and hypoxia-tolerant states. Lancet 362:1028-1037.

Stitt MS, Wasserloos KJ, Tang X, Liu X, Pitt BR, St Croix CM (2006) Nitric oxide-induced nuclear translocation of the metal responsive transcription factor, MTF-1 is mediated by zinc release from metallothionein. Vascul Pharmacol 44:149-155.

Stork CJ, Li YV (2006) Intracellular zinc elevation measured with a "calcium-specific" indicator during ischemia and reperfusion in rat hippocampus: a question on calcium overload. J Neurosci 26:10430-10437.

Stoyanovsky DA, Tyurina YY, Tyurin VA, Anand D, Mandavia DN, Gius D, Ivanova J, Pitt B, Billiar TR, Kagan VE (2005) Thioredoxin and lipoic acid catalyze the denitrosation of low molecular weight and protein S-nitrosothiols. J Am Chem Soc 127:15815-15823.

Stuart GW, Searle PF, Palmiter RD (1985) Identification of multiple metal regulatory elements in mouse metallothionein-I promoter by assaying synthetic sequences. Nature 317:828-831.

Stuart GW, Searle PF, Chen HY, Brinster RL, Palmiter RD (1984) A 12-base-pair DNA motif that is repeated several times in metallothionein gene promoters confers metal regulation to a heterologous gene. Proc Natl Acad Sci U S A 81:7318-7322.

Suh SW, Chen JW, Motamedi M, Bell B, Listiak K, Pons NF, Danscher G, Frederickson CJ (2000) Evidence that synaptically-released zinc contributes to neuronal injury after traumatic brain injury. Brain Res 852:268-273.

Suh SW, Hamby AM, Gum ET, Shin BS, Won SJ, Sheline CT, Chan PH, Swanson RA (2008) Sequential release of nitric oxide, zinc, and superoxide in hypoglycemic neuronal death. J Cereb Blood Flow Metab 28:1697-1706.

Surmeier DJ, Foehring R (2004) A mechanism for homeostatic plasticity. Nat Neurosci 7:691-692.

Suzuki Y, Apostolova MD, Cherian MG (2000) Astrocyte cultures from transgenic mice to study the role of metallothionein in cytotoxicity of tert-butyl hydroperoxide. Toxicology 145:51-62.

Szabo C, Dawson VL (1998) Role of poly(ADP-ribose) synthetase in inflammation and ischaemia-reperfusion. Trends Pharmacol Sci 19:287-298.

Takahashi K, Akaishi E, Abe Y, Ishikawa R, Tanaka S, Hosaka K, Kubohara Y (2003) Zinc inhibits calcineurin activity in vitro by competing with nickel. Biochem Biophys Res Commun 307:64-68.

Takeda K, Matsuzawa A, Nishitoh H, Ichijo H (2003) Roles of MAPKKK ASK1 in stress-induced cell death. Cell Struct Funct 28:23-29.

Tamkun MM, O'Connell K M, Rolig AS (2007) A cytoskeletal-based perimeter fence selectively corrals a sub-population of cell surface Kv2.1 channels. J Cell Sci 120:2413-2423.
Tanaka H, Yokota H, Jover T, Cappuccio I, Calderone A, Simionescu M, Bennett MV, Zukin RS (2004) Ischemic preconditioning: neuronal survival in the face of caspase-3 activation. J Neurosci 24:2750-2759.
Tang Y, Pacary E, Freret T, Divoux D, Petit E, Schumann-Bard P, Bernaudin M (2006) Effect of hypoxic preconditioning on brain genomic response before and following ischemia in the adult mouse: identification of potential neuroprotective candidates for stroke. Neurobiol Dis 21:18-28.
Taylor RC, Cullen SP, Martin SJ (2008) Apoptosis: controlled demolition at the cellular level. Nat Rev Mol Cell Biol 9:231-241.
Thomas GM, Huganir RL (2004) MAPK cascade signalling and synaptic plasticity. Nat Rev Neurosci 5:173-183.
Thompson RB, Peterson D, Mahoney W, Cramer M, Maliwal BP, Suh SW, Frederickson C, Fierke C, Herman P (2002) Fluorescent zinc indicators for neurobiology. J Neurosci Methods 118:63-75.
Timm F (1958) [Histochemistry of heavy metals; the sulfide-silver procedure.]. Dtsch Z Gesamte Gerichtl Med 46:706-711.
Tobiume K, Saitoh M, Ichijo H (2002) Activation of apoptosis signal-regulating kinase 1 by the stress-induced activating phosphorylation of pre-formed oligomer. J Cell Physiol 191:95-104.
Tonder N, Johansen FF, Frederickson CJ, Zimmer J, Diemer NH (1990) Possible role of zinc in the selective degeneration of dentate hilar neurons after cerebral ischemia in the adult rat. Neurosci Lett 109:247-252.
Trendelenburg G, Prass K, Priller J, Kapinya K, Polley A, Muselmann C, Ruscher K, Kannbley U, Schmitt AO, Castell S, Wiegand F, Meisel A, Rosenthal A, Dirnagl U (2002) Serial analysis of gene expression identifies metallothionein-II as major neuroprotective gene in mouse focal cerebral ischemia. J Neurosci 22:5879-5888.
Trimmer JS (1991) Immunological identification and characterization of a delayed rectifier K+ channel polypeptide in rat brain. Proc Natl Acad Sci U S A 88:10764-10768.
Trost LC, Lemasters JJ (1994) A cytotoxicity assay for tumor necrosis factor employing a multiwell fluorescence scanner. Anal Biochem 220:149-153.
Tsuda M, Imaizumi K, Katayama T, Kitagawa K, Wanaka A, Tohyama M, Takagi T (1997) Expression of zinc transporter gene, ZnT-1, is induced after transient forebrain ischemia in the gerbil. J Neurosci 17:6678-6684.
Uchida Y, Takio K, Titani K, Ihara Y, Tomonaga M (1991) The growth inhibitory factor that is deficient in the Alzheimer's disease brain is a 68 amino acid metallothionein-like protein. Neuron 7:337-347.
Vallee BL, Coleman JE, Auld DS (1991) Zinc fingers, zinc clusters, and zinc twists in DNA-binding protein domains. Proc Natl Acad Sci U S A 88:999-1003.
van Lookeren Campagne M, Thibodeaux H, van Bruggen N, Cairns B, Gerlai R, Palmer JT, Williams SP, Lowe DG (1999) Evidence for a protective role of metallothionein-1 in focal cerebral ischemia. Proc Natl Acad Sci U S A 96:12870-12875.
Vasak M, Hasler DW (2000) Metallothioneins: new functional and structural insights. Curr Opin Chem Biol 4:177-183.

Verdaguer E, Pubill D, Rimbau V, Jimenez A, Escubedo E, Camarasa J, Pallas M, Camins A (2002) Evaluation of neuronal cell death by laser scanning cytometry. Brain Res Brain Res Protoc 9:41-48.
Vincent AM, Maiese K (1999) Direct temporal analysis of apoptosis induction in living adherent neurons. J Histochem Cytochem 47:661-672.
Virag L, Szabo C (2002) The therapeutic potential of poly(ADP-ribose) polymerase inhibitors. Pharmacol Rev 54:375-429.
Vogt K, Mellor J, Tong G, Nicoll R (2000) The actions of synaptically released zinc at hippocampal mossy fiber synapses. Neuron 26:187-196.
Wardlaw JM, Zoppo G, Yamaguchi T, Berge E (2003) Thrombolysis for acute ischaemic stroke. Cochrane Database Syst Rev:CD000213.
Watabe M, Gross S, Lawyer C, Brewer GJ, Mashimo T, Watabe K (1997) Sequence and functional analysis of the 5'-flanking region of the mouse growth inhibitory factor gene. Cell Mol Neurobiol 17:235-243.
Weih M, Kallenberg K, Bergk A, Dirnagl U, Harms L, Wernecke KD, Einhaupl KM (1999) Attenuated stroke severity after prodromal TIA: a role for ischemic tolerance in the brain? Stroke 30:1851-1854.
Weiss JH, Sensi SL, Koh JY (2000) Zn(2+): a novel ionic mediator of neural injury in brain disease. Trends Pharmacol Sci 21:395-401.
Weiss JH, Hartley DM, Koh JY, Choi DW (1993) AMPA receptor activation potentiates zinc neurotoxicity. Neuron 10:43-49.
Wenzel HJ, Cole TB, Born DE, Schwartzkroin PA, Palmiter RD (1997) Ultrastructural localization of zinc transporter-3 (ZnT-3) to synaptic vesicle membranes within mossy fiber boutons in the hippocampus of mouse and monkey. Proc Natl Acad Sci U S A 94:12676-12681.
West AK, Hidalgo J, Eddins D, Levin ED, Aschner M (2008) Metallothionein in the central nervous system: Roles in protection, regeneration and cognition. Neurotoxicology 29:489-503.
Westbrook GL, Mayer ML (1987) Micromolar concentrations of Zn2+ antagonize NMDA and GABA responses of hippocampal neurons. Nature 328:640-643.
Westin G, Schaffner W (1988) A zinc-responsive factor interacts with a metal-regulated enhancer element (MRE) of the mouse metallothionein-I gene. EMBO J 7:3763-3770.
Yamagishi S, Yamada M, Koshimizu H, Takai S, Hatanaka H, Takeda K, Ichijo H, Shimoke K, Ikeuchi T (2003) Apoptosis-signal regulating kinase-1 is involved in the low potassium-induced activation of p38 mitogen-activated protein kinase and c-Jun in cultured cerebellar granule neurons. J Biochem 133:719-724.
Yamasaki S, Sakata-Sogawa K, Hasegawa A, Suzuki T, Kabu K, Sato E, Kurosaki T, Yamashita S, Tokunaga M, Nishida K, Hirano T (2007) Zinc is a novel intracellular second messenger. J Cell Biol 177:637-645.
Yang G, Chan PH, Chen SF, Babuna OA, Simon RP, Weinstein PR (1994) Reduction of vasogenic edema and infarction by MK-801 in rats after temporary focal cerebral ischemia. Neurosurgery 34:339-345; discussion 345.
Yang Y, Maret W, Vallee BL (2001) Differential fluorescence labeling of cysteinyl clusters uncovers high tissue levels of thionein. Proc Natl Acad Sci U S A 98:5556-5559.
Yin HZ, Weiss JH (1995) Zn(2+) permeates Ca(2+) permeable AMPA/kainate channels and triggers selective neural injury. Neuroreport 6:2553-2556.

Yin HZ, Ha DH, Carriedo SG, Weiss JH (1998) Kainate-stimulated Zn2+ uptake labels cortical neurons with Ca2+-permeable AMPA/kainate channels. Brain Res 781:45-55.

Yin HZ, Sensi SL, Carriedo SG, Weiss JH (1999) Dendritic localization of Ca(2+)-permeable AMPA/kainate channels in hippocampal pyramidal neurons. J Comp Neurol 409:250-260.

Yin HZ, Sensi SL, Ogoshi F, Weiss JH (2002) Blockade of Ca2+-permeable AMPA/kainate channels decreases oxygen-glucose deprivation-induced Zn2+ accumulation and neuronal loss in hippocampal pyramidal neurons. J Neurosci 22:1273-1279.

Yokoyama M, Koh J, Choi DW (1986) Brief exposure to zinc is toxic to cortical neurons. Neurosci Lett 71:351-355.

Yu CW, Chen JH, Lin LY (1997a) Metal-induced metallothionein gene expression can be inactivated by protein kinase C inhibitor. FEBS Lett 420:69-73.

Yu SP (2003) Regulation and critical role of potassium homeostasis in apoptosis. Prog Neurobiol 70:363-386.

Yu SP, Farhangrazi ZS, Ying HS, Yeh CH, Choi DW (1998) Enhancement of outward potassium current may participate in beta-amyloid peptide-induced cortical neuronal death. Neurobiol Dis 5:81-88.

Yu SP, Yeh CH, Gottron F, Wang X, Grabb MC, Choi DW (1999) Role of the outward delayed rectifier K+ current in ceramide-induced caspase activation and apoptosis in cultured cortical neurons. J Neurochem 73:933-941.

Yu SP, Yeh CH, Sensi SL, Gwag BJ, Canzoniero LM, Farhangrazi ZS, Ying HS, Tian M, Dugan LL, Choi DW (1997b) Mediation of neuronal apoptosis by enhancement of outward potassium current. Science 278:114-117.

Zarubin T, Han J (2005) Activation and signaling of the p38 MAP kinase pathway. Cell Res 15:11-18.

Zhang B, Egli D, Georgiev O, Schaffner W (2001) The Drosophila homolog of mammalian zinc finger factor MTF-1 activates transcription in response to heavy metals. Mol Cell Biol 21:4505-4514.

Zhang B, Georgiev O, Hagmann M, Gunes C, Cramer M, Faller P, Vasak M, Schaffner W (2003) Activity of metal-responsive transcription factor 1 by toxic heavy metals and H2O2 in vitro is modulated by metallothionein. Mol Cell Biol 23:8471-8485.

Zhang HY, McPherson BC, Liu H, Baman TS, Rock P, Yao Z (2002) H(2)O(2) opens mitochondrial K(ATP) channels and inhibits GABA receptors via protein kinase C-epsilon in cardiomyocytes. Am J Physiol Heart Circ Physiol 282:H1395-1403.

Zhang Y, Wang H, Li J, Jimenez DA, Levitan ES, Aizenman E, Rosenberg PA (2004) Peroxynitrite-induced neuronal apoptosis is mediated by intracellular zinc release and 12-lipoxygenase activation. J Neurosci 24:10616-10627.

Zhu JJ, Qin Y, Zhao M, Van Aelst L, Malinow R (2002) Ras and Rap control AMPA receptor trafficking during synaptic plasticity. Cell 110:443-455.